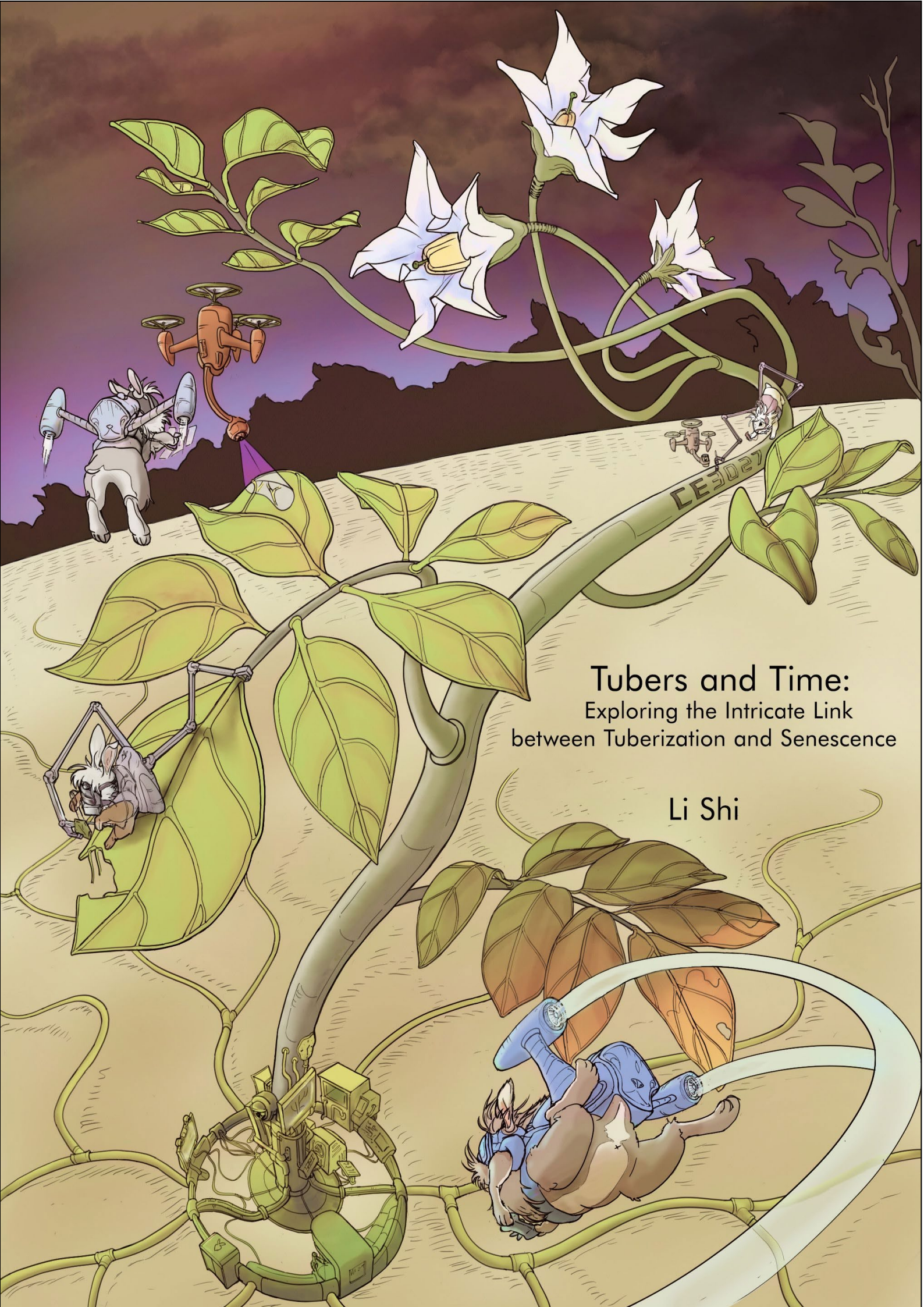

Tubers and Time:

Exploring the Intricate Link between Tuberization and Senescence

Li Shi

Propositions

1. *CYCLING DOF FACTOR1* (*StCDF1*) is a regulator that acts as a central hub throughout the potato life cycle.
(this thesis)

2. The comprehensive molecular study of central hub genes in crop plants offers valuable benefits to both academia and the industry.
(this thesis)

3. Although advanced technologies are extensively employed in the study of model plants, the applicability of their outcomes to crop plants is not straightforward.

4. Internal friction poses the most significant obstacle in performing experimental science.

5. Admitting powerlessness to change a situation is a sign not of weakness, but of a strong heart.

6. All cosmetics should be cruelty-free.

Propositions belonging to the thesis, entitled

Tubers and Time: Exploring the Intricate Link between Tuberization and Senescence

Li Shi
Wageningen, 29 November 2023

Tubers and Time: Exploring the Intricate Link between Tuberization and Senescence

Li Shi

Thesis committee

Promotor
Prof. Dr R. G. F. Visser
Professor of Plant Breeding
Wageningen University & Research

Co-promotor
Dr C. W. Bachem
Assistant professor, Plant Breeding
Wageningen University & Research

Other members
Prof. Dr R. G. H Immink, Wageningen University & Research, the Netherlands
Dr S. Sonnewald, Friedrich-Alexander University, Erlangen-Nuremberg, Germany
Dr S. Oome, HZPC, Metselawier, The Netherlands
Dr R. Heidstra, Wageningen University & Research, the Netherlands

This research was conducted under the auspices of the Graduate School Experimental Plant Sciences (EPS).

Tubers and Time: Exploring the Intricate Link between Tuberization and Senescence

Li Shi

Thesis

submitted in fulfilment of the requirements for the degree of doctor
at Wageningen University
by the authority of the Rector Magnificus,
Prof. Dr A.P.J. Mol,
in the presence of the
Thesis Committee appointed by the Academic Board
to be defended in public
on Wednesday 29 November 2023
at 1:30 p.m. in the Omnia Auditorium

Li Shi
Tubers and Time: Exploring the Intricate Link between Tuberization and Senescence
138 pages.

PhD thesis, Wageningen University, Wageningen, the Netherlands (2023)
With references, with summary in English

ISBN 978-94-6447-833-4
DOI https://doi.org/10.18174/636038

Table of contents

Chapter 1

General Introduction

General Introduction

Control of potato tuberization through day length

Potato (*Solanum tuberosum* L.) is the largest non-grain food crop and grown across diverse regions (FAO, 2019). The tuber, which is the storage organ of potato, is a great source of carbohydrates and other essential nutrients. The formation of tubers underground (tuberization) is a critical process that significantly impacts the final yield of the potato crop. As a result, tuberization is considered one of the most critical traits in potato breeding programs.

The potato originated in the Andes of South America, where it evolved to grow and form tubers under short day conditions, which is known as short day tuberization (Van der Plank, 1946; Spooner *et al.*, 2005). However, in northern latitudes, where the growing season spans across summer and has long day conditions, tuberization can be negatively impacted. This can result in low yields, as seen when the first potato plants were introduced to Europe and tuberization likely occurred after the switch to short day length. Figure. 1 shows an interesting approach to imitate short-day conditions in northern latitudes, which was developed to improve potato yields in 1956. Day length-dependent tuberization regulation is undeniably crucial to obtaining optimal yields in northern latitudes.

Cultivated varieties of potatoes are derived from Chilean landraces, only tuberize under long-day conditions (Ewing & Struik, 1992; Spooner *et al.*, 2005; Navarro *et al.*, 2011). In modern potato breeding programs, capability of tuberization under long day condition, also known as “earliness”, is still one of the first traits in selective screening.

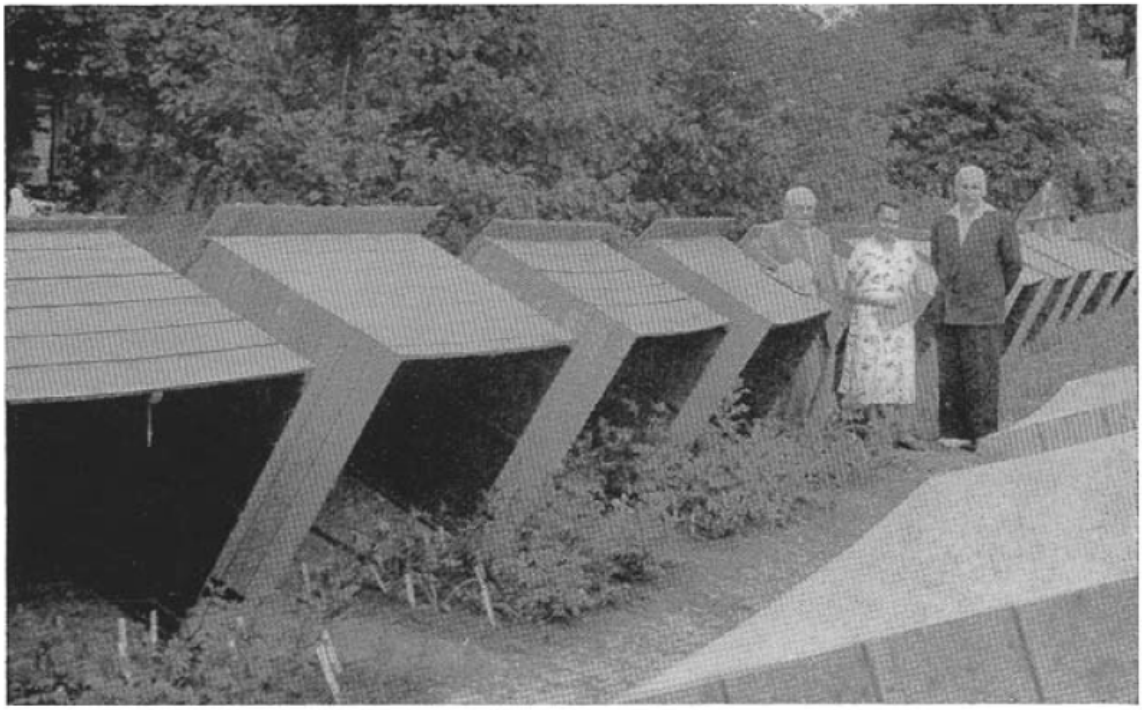

Figure 1. An interesting approach to imitate short-day conditions in northern latitudes. These specialized boxes can be used to create artificial short-day conditions in Leningrad, which is beneficial for optimizing the yield of South American potato varieties (Hawkes, 1957).

The above-ground maturity of potato

In addition to day-length dependence of tuber formation the earliness trait is closely linked to the length of canopy senescence, the trait known as maturity. Maturity is a critical factor in crop breeding programs, as it is used to estimate the optimal time for harvesting. Depending on the crop, maturity can refer to various stages of growth, such as flowering time, seed maturity, fruit ripening, or leaf senescence (TeKrony *et al.*, 1979; Maul *et al.*, 1998; Wang *et al.*, 2020). In potatoes, phenotyping underground maturity is difficult. As a result, breeding efforts tend to prioritize the evaluation of above-ground leaf maturity rather than tuber maturity. The maturity of above-ground leaves is a measure of senescence, which is an essential stage in the life cycle of potato plants. During this stage, plants initiate a coordinated process that involves remobilization of nutrients from senescing leaves to sink tissues. This process involves breaking down structures and chemical compounds within the chloroplast, which allows for the efficient recycling and reallocation of nutrients to other parts of the plant for storage or further development (Guiboileau *et al.*, 2010). The most apparent phenotype is the process is leaf yellowing. In various plant systems, numerous studies have demonstrated the significant impact of the senescence process on both yield and nutritional value (Woo *et al.*, 2018). In potato breeding programs, the leaf senescence phenotype is also used to select for improved yield.

The multi-faceted role of StCDF1 in potato plant development

Quantitative Trait Locus (QTL) mapping is a powerful technique used in breeding programs to identify the genetic loci that control complex, quantitative traits such as crop yield, disease resistance. This technique involves analyzing the genetic variation in a population of individuals and correlating it with the variation in the trait of interest, allowing breeders to identify the specific genomic regions associated with the trait. Breeders can identify markers associated with these QTLs allowing rapid selection of the desired trait in breeding programs.

The genetic control of underground earliness and above ground maturity in potato has been investigated using QTL mapping in many previous field studies, and the results suggest that both traits can be controlled by the same genetic loci (Visker, 2005; Massa *et al.*, 2018). Specifically, both traits have been mapped to a specific region of the potato genome located on the top arm of chromosome 5 (Chr05) (Visker, 2005; Kloosterman, B. *et al.*, 2013). Later, this identified genetic locus was functionally linked to a member of the DOF family (DNA-binding with one finger) coding for a transcription factor (TF) named *CYCLING DOF FACTOR 1* (*StCDF1*)(Kloosterman, B. *et al.*, 2013). During the afternoon under long day conditions, the StCDF1 (StCDF1.1) wild-type protein is subject to ubiquitin-dependent degradation that is facilitated by its interaction with two proteins, called GIGANTEA (StGI) and FLAVIN-BINDING KELCH REPEAT F-BOX PROTEIN 1 (StFKF1). Allelic variation at the 3′ end of the *StCDF1* gene can result in truncated allelic variants (*StCDF1.2* and *StCDF1.3*; Figure. 2). The proteins produced by these truncated variants exhibit impaired binding to StFKF1 and maintain a constant abundance throughout the day. The plants carrying the truncated allelic

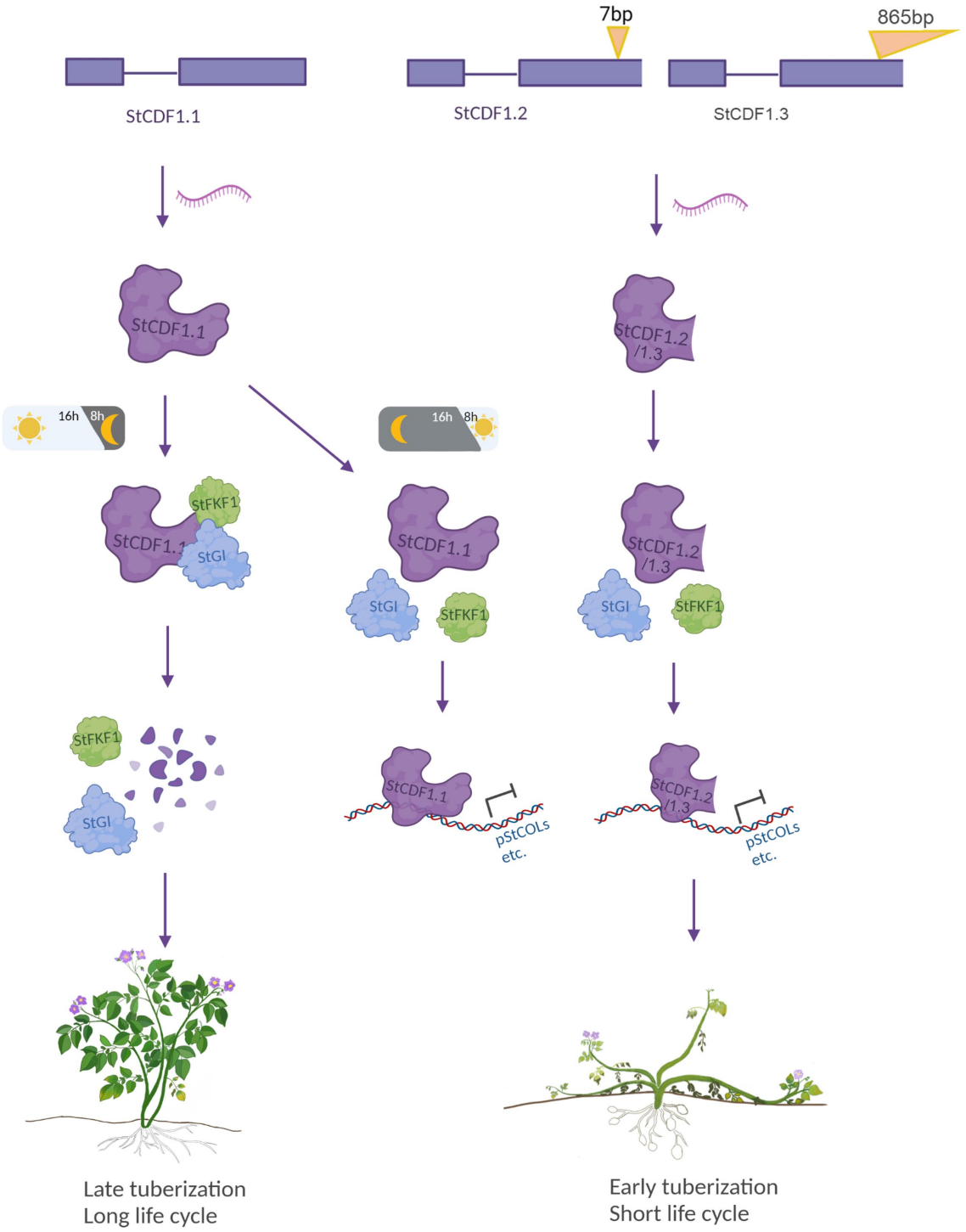

Figure. 2. The truncated allele of StCDF1 induces early tuberization and a shortened life cycle. The wild-type StCDF1 (StCDF1.1) undergoes degradation in response to long-day conditions through its interaction with StGI and StFKF1 proteins. Plants homozygous for *StCDF1.1* exhibit a prolonged life cycle and delayed tuberization. Conversely, under short-day conditions, this interaction is inhibited, allowing StCDF1.1 to repress the expression of downstream genes, such as *StCONSTANS-Like* (*StCOLs*). On the other hand, the *StCDF1.2* and *1.3* alleles which carry insertions, resulting in premature stop codons and the production of a truncated protein. The StCDF1.2/3 alleles show enhanced protein stability, as a result of which, it exhibits inhibited binding to StFKF1 protein. Plants carrying the truncated *StCDF1* alleles show early tuberization and a shortened life cycle under long day conditions (Kloosterman, B. *et al.*, 2013).

variants tuberize independent of day length and have shorter life cycles. Moreover, overexpressing of *StCDF1.2* in *S. andigenum*, a potato species that only tuberizes under short-day conditions, can induce tuberization under long-day conditions and significantly shorten the potato plant's life cycle (Kloosterman, B. *et al.*, 2013). Both genetic and molecular evidence suggest that the underground earliness and above ground maturity can be linked to the same gene, *StCDF1*.

StCDF1 is a transcription factor belonging to the DOF (DNA binding with one finger) family, which regulates gene expression by binding to a specific DNA sequence (5'-T/AAAG-3') in the promoter region of target genes(Gupta *et al.*, 2015). This binding is mediated by the DOF domain located at the N-terminal end of StCDF1, which is a conserved motif found in most DOF transcription factors. Kloosterman, B. *et al.* (2013) were the first to describe the regulatory network of StCDF1 in regulating day-length depending tuberization. Similar to the photoperiodic-dependent flowering regulatory pathway in *Arabidopsis*, StCDF1 directly binds to the promoter of potato *CONSTANS* homologues (*StCO-Like 1* and *StCO-Like 2*) and represses their expression. StCOL1&2 negatively regulate tuberization by directly upregulating the expression of a potato homologue of *FLOWERING LOCUS T* (*FT*), called *SELF-PRUNING 5G* (*StSP5G*). Furthermore, StSP5G reduces the expression of its homologue, called *StSP6A*, by a yet unknown mechanism. StSP6A serves as a vital mobile signal, known as a 'tuberigen,' that is expressed and translated into protein in the leaf (Figure 3). It is then transported to the stolon, where it initiates the process of tuberization (Abelenda *et al.*, 2014). The tuberization

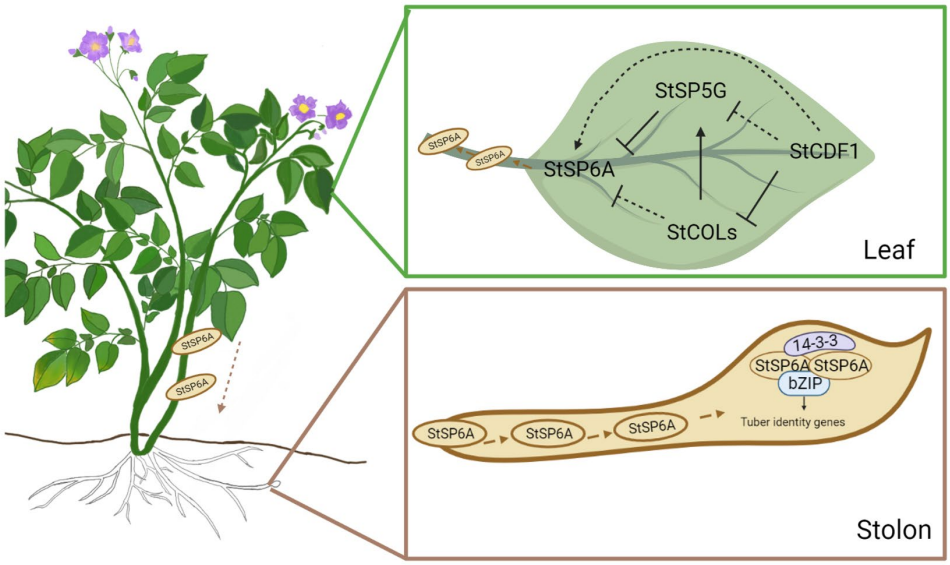

Figure. 3. Model for tuberization induction adapted from Abelenda *et al.* (2014) and Taoka *et al.* (2011). The potato leaf senses various environmental signals, including day length, which influences the stability of the StCDF1 protein. StCDF1 directly inhibits the expression of *StCOLs*, while StCOLs, in turn, negatively regulate the expression of *StSP6A*. This regulation can occur either through direct repression or indirectly by repressing the expression of *StSP5G*. Notably, *StSP6A* is expressed and translated into protein in the leaf and subsequently the protein is transported through the phloem to the stolons, where it plays a crucial role in

promoting tuberization. The arrival of StSP6A to the stolon results in the formation of TAC and further affects the expression of tuber identity genes.

initiation involves a molecular process similar to that in florigen activation in the shoot apical meristem. Upon arrival in stolons, StSP6A interacts with bZIP-type transcription factors (such as StABI5 and FD homologs in potato) and forms a tuberigen activation complex (TAC) in conjunction with 14-3-3 proteins (Teo *et al.*, 2017; Jing *et al.*, 2022b)(Figure. 3). The TAC complex plays a crucial role in inducing tuberization by triggering the local expression of tuberization-related genes (Jing *et al.*, 2022b).

Hence, StCDF1 contributes to the promotion of tuberization by indirectly activating the expression of *StSP6A*, as it curtails the expression of *StCOLs* and *StSP5G*, as illustrated in Figure 3. The increased protein stability of StCDF1.2 and StCDF1.3 enables them to continuously inhibit the expression of *StCOLs* and *StSP5G*, resulting in early tuberization under long-day conditions. While the regulatory role of StCDF1 in controlling day length-dependent tuberization has been extensively studied, it is still not clear how StCDF1 governs above-ground maturity/senescence, and how these two pathways are interconnected. In this thesis, we investigated the role of StCDF1 in regulating senescence (**Chapter 2**).

StCDF1 influences potato plant response to abiotic stresses

Potato yield is constantly threatened by environmental stresses (Dahal *et al.*, 2019; Lehretz *et al.*, 2019). Drought and heat-prone countries account for over 50% of global potato cultivation (FAOSTAT, 2021; Demirel, 2023). However, under conditions of restricted water availability, high temperatures, and elevated soil salinity, the yield of potato tubers is severely negatively affected (Levy *et al.*, 2013; Monneveux *et al.*, 2013). With rapid global climate change, the loss in total potato yield due to abiotic stress is expected to reach up to 32% by 2050 (Hijmans, 2003; Raymundo *et al.*, 2018).

In recent years, various members of the CDF protein family across different plant species have been shown to play a role in regulating responses to abiotic stress (Corrales *et al.*, 2014; Fornara *et al.*, 2015; Xu & Dai, 2016; Corrales *et al.*, 2017; Renau-Morata *et al.*, 2017). Despite the well-known cyclic diurnal regulatory network, several new stress tolerance regulatory networks of *CDFs* have been uncovered. For instance, overexpression of AtCDF3 has been found to activate the expression of genes involved in cellular osmoprotection and ROS homeostasis, including heat shock proteins, peroxidases, and catalases (Corrales *et al.*, 2017). The upregulation of these genes is associated with improved plant tolerance to drought, cold, and osmotic stress in 35S::*AtCDF3 Arabidopsis* plants (Corrales *et al.*, 2017). Therefore, CDFs have been demonstrated to respond to a wide range of environmental changes, regulating downstream genes to facilitate adaptation. Recent research has highlighted the significance of AtCDF1 as one of the six early responder transcription factors in nitrogen level responses (Varala *et al.*, 2018; Alvarez *et al.*, 2020). These intriguing findings imply that StCDF1 may not only be regulated by photoperiod but also by various other environmental signals. However, the mechanisms underlying the process of environmental sensing by CDFs remain largely unclear.

In potato, StCDF1 has been link to regulating drought response. Anithakumari *et al.* (2012) reported that the QTLs for growth and yield under drought co-localized with the QTL for maturity on chromosome 5, which was later identified as the *StCDF1* locus (Kloosterman, B. *et al.*, 2013). Recently, a molecular study by Ramírez Gonzales *et al.* (2021) showed that *StCDF1*, along with its lncRNA counterpart *StFLORE*, regulates drought tolerance in potato. The physiological evidence suggests that StCDF1 is involved in regulating stomatal morphology and the opening and closing of stomata, which affects transpiration (Ramírez Gonzales *et al.*, 2021). A similar module was previously found for *AtCDF5*/ *FLORE* in *Arabidopsis* (Henriques *et al.*, 2017). Based on the antiphasic expression pattern and other phenotypic evidence, *FLORE* was proposed to be the natural antisense transcript (NAT) for AtCDF5 and to function in regulating flowering. In potato, *StFLORE* seems to have a more obvious function in response to abiotic stress, such as drought. The mutual inhibition between *StCDF1* and *StFLORE* gives rise to a broad hypothesis suggesting that *StFLORE* may play a role in sensing environmental changes, such as in water availability. It is postulated that *StFLORE* might directly transmit this signal to *StCDF1* at the transcriptional level. However, the molecular mechanism of *StCDF1/StFLORE* in regulating specific abiotic stress response remains elusive.

Abscisic Acid (ABA) is a key phytohormone that mediates stomatal closure to reduce water loss by decreasing the transpiration rate (Muhammad Aslam *et al.*, 2022). This primary role of ABA makes it critical for plant drought response. *NCEDs* (9-cis-epoxycarotenoid dioxygenase) encode rate-limiting enzymes in the ABA biosynthesis pathway (Sussmilch *et al.*, 2017). Overexpression of NCEDs in various plant species has been shown to enhance ABA levels and improve drought tolerance (Qin & Zeevaart, 2002; Endo *et al.*, 2008). Interestingly, the expression of NCEDs follows a diurnal oscillation pattern that aligns with ABA level fluctuations throughout the day (Lee *et al.*, 2006; Pizzio, 2022). Numerous circadian rhythm regulators have been identified that regulate the expression of *NCEDs*, including PPR5, CCA1, LUX, LHY, and ELF3 (Adams *et al.*, 2018; Pizzio, 2022). CDFs are known as clock-controlled factors and are involved in regulating multiple photoperiod-dependent pathways. In fact, recent research has shown that CDF4, a member of the CDF family, directly binds to the *NCED2* and *NCED3* promoters, thereby activating their expression in *Arabidopsis*. Furthermore, DAP-seq analysis of StCDF1 (Gonzales, 2022) revealed potential binding between StCDF1 and the *StNCED3* promoter, suggesting a possible role for StCDF1 in regulating ABA biosynthesis. In **Chapter 3**, we present molecular evidence that StCDF1 negatively regulates the expression of *StNCED3* and *StNCED4* to repress ABA biosynthesis.

In addition to drought, potato is also sensitive to elevated temperatures (Ewing & Struik, 1992; Fahad *et al.*, 2017; Lehretz *et al.*, 2019). In fact, exposing potato plants to long periods of temperatures above 25 degrees Celsius can lead to reduced yields and poor-quality tubers. Previous studies suggest that heat stress negatively impacts various physiological processes in the plant, including tuberization, carbon fixation and photosynthesis (Ewing, 1981; Timlin *et al.*, 2006; Dahal *et al.*, 2019). Due to global warming, this issue is becoming more and more pressing for potato growers as rising temperatures and more frequent heatwaves pose a significant threat to potato production and food security. Lehretz *et al.* (2019) published a comprehensive study elucidating the molecular mechanism underlying the inhibition of

tuberization by heat. They discovered a novel micro-RNA called *SES* (Suppression of Expression of *SP6A*), which exhibited upregulated expression in response to heat treatment. Notably, *StSES* was found to target and reduce the transcripts of *StSP6A*. These findings shed light on the molecular basis of heat-induced inhibition of tuberization. Further exploration of the upstream regulators of *StSES* is crucial for enhancing potato heat tolerance.

Although CDFs have not yet been directly linked to heat stress response, an interesting study conducted on 50 potato varieties under heat stress revealed that early maturing cultivars tended to be less affected by heat than their late maturing counterparts (Zhang, G *et al.*, 2020). Considering that StCDF1 is the major locus for regulating potato maturity, it is reasonable to speculate that StCDF1 may also play a role in regulating potato heat stress response, given that both processes involve complex genetic and physiological mechanisms. In **Chapter 3**, we investigated the role of StCDF1 in regulating heat tolerance.

The molecular basis of StCDF1 in regulating transcription

Many important agronomic traits have been genetically linked to the StCDF1 locus (Visker, 2005; Hoopes, G *et al.*, 2022). StCDF1, as a transcription factor, was known to influence plant phenotypes by regulating transcription of downstream genes. The interactions within the gene regulatory networks downstream of StCDF1 underlie the association of different traits. Therefore, a better understanding of the molecular regulation of StCDF1 will provide insight into how different traits are coordinately regulated by this important transcription factor.

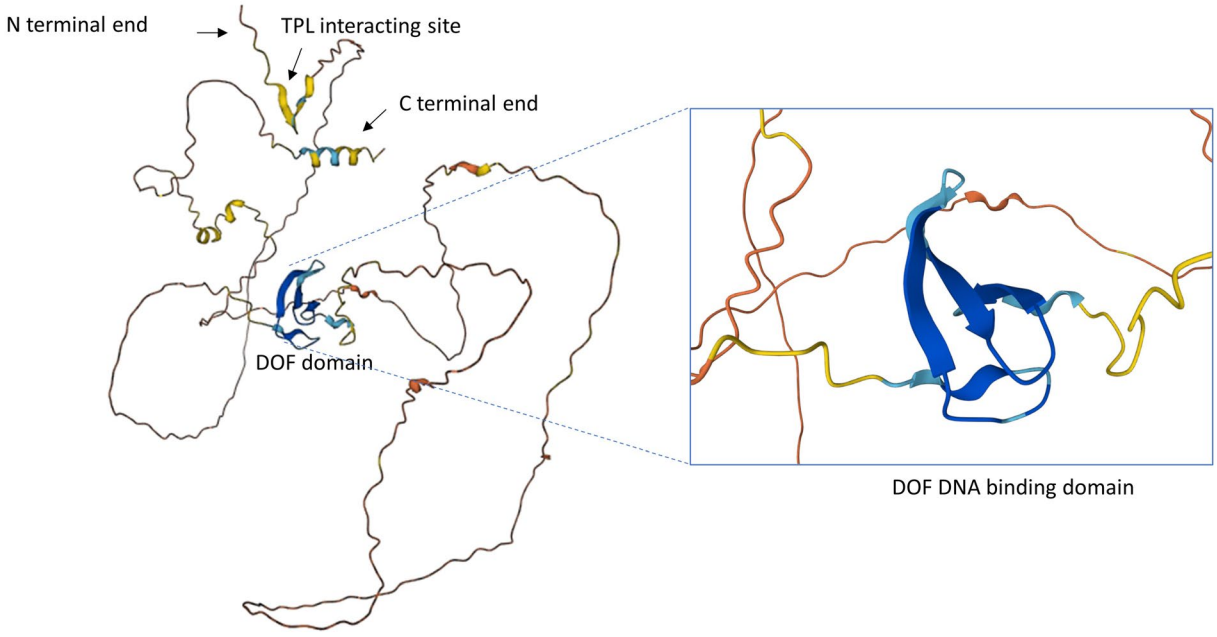

Figure. 4. Modelled structure of StCDF1.1 protein. The arrows indicate the terminal ends and interaction site for the co-repressor TPL. The box on the right shows a zoom-in of the DOF DNA binding domain. The 3D model of StCDF1.1 was predicted by AlphaFold (Jumper *et al.*, 2021; Varadi *et al.*, 2022).

StCDF1 is a transcription factor that belongs to the DOF family and contains a DOF domain, which typically includes a zinc finger motif consisting of 55 amino acid residues. As with most DOF transcription factors, the DOF domain is located at the N-terminal end of the protein (Figure 4). The DNA-binding activities of DOF family members have been studied through various *in vitro* and *in vivo* approaches (Renau-Morata *et al.*, 2020). Notably, the DNA-binding activity of StCDF1 was tested, and a 9-bp consensus sequence, YWAAAGRYC, was found to be the StCDF1 binding motif (Ramírez Gonzales *et al.*, 2021; Gonzales, 2022). Interestingly, in addition to its role in DNA binding, the DOF domain has been shown in several studies to have other functions, such as interaction with other transcription factors and cell-to-cell trafficking (Chen *et al.*, 2013; Renau-Morata *et al.*, 2020; Gao *et al.*, 2022).

It is worth noting that the transcriptional regulation function of CDF1 is not solely dependent on its DOF domain. Goralogia, Greg S *et al.* (2017) reported the existence of a conserved region in CDFs across different plant species, which is located at the N-terminal end of the protein and is required for interaction with the well-known co-repressor TOPLESS (TPL) protein. TOPLESS (TPL)/TOPLESS-RELATED (TPR) proteins belong to the Groucho (Gro)/Tup1 family and are conserved corepressors in plants (Plant *et al.*, 2021). The current understanding of their role in gene repression is that they are recruited by specific transcription factors and recruit histone deacetylases (HDACs), which remove acetyl groups from histones (Zhu *et al.*, 2010; Causier *et al.*, 2012a; Krogan *et al.*, 2012). This results in a more condensed chromatin structure, making it difficult for RNA polymerase to access the DNA and initiate transcription. In essence, TOPLESS proteins help to repress gene expression by altering the chromatin structure and preventing the transcriptional machinery from accessing the DNA (Kadosh & Struhl, 1998; Tanaka *et al.*, 2008; Causier *et al.*, 2012a). Based on current knowledge, it is hypothesized that StCDF1 is transcriptionally regulated by a mechanism involving the DOF domain, which recognizes a specific DNA motif, and subsequently recruits TPL and HDACs to induce a repressive chromatin state.

Recently, a study was conducted using a combination of DAP-seq and RNA-seq to investigate the downstream targets of StCDF1 (Gonzales, 2022). The results revealed that StCDF1 functions not only as a repressor but also as an activator in regulating gene expression. Interestingly, the study identified 330 genes that are negatively regulated by StCDF1, while over 575 genes were found to be upregulated by it (Gonzales, 2022). However, despite these findings, the precise mechanism through which StCDF1 activates gene expression remains largely unknown. The StCDF1 locus has been recognized for its profound influence on various aspects of potato plant development. Enhancing our understanding of this novel activation mechanism holds the potential to unveil important genes associated with StCDF1 in regulating potato plant development traits, thus providing valuable insights for breeding programs.

Proximity labeling: a novel tool for investigating protein-protein interaction *in vivo*

Exploring protein-protein interactions (PPIs) in crop plants, like potatoes, has always presented challenges. Our understanding of PPIs in these crops heavily relies on studies conducted in model plant systems, such as Arabidopsis. In fact, all three interactors of StCDF1 have been previously identified in *Arabidopsis* studies (Sawa *et al.*, 2007; Kloosterman, B. *et al.*, 2013;

Goralogia, Greg S *et al.*, 2017). The recently discovered activation function of StCDF1 suggests that it may recruit other transcription factors (TFs) to jointly activate downstream gene expression. However, very limited studies have been done and testing potential interactors individually is time-consuming. To investigate PPIs in plants, several methods have been used in previous studies like yeast two hybrid (Y2H), Co-immunoprecipitation (Co-IP), and immunoprecipitation or affinity purification combined with mass spectrometry (IP-MS/ AP-MS). Among these methods, Y2H has the advantages of being low in financial costs and easy to perform, but this method has a high labor cost, high false positive rate and is limited to a non-native environment. The immunoprecipitation-based approaches can be performed in the native biological environment. However, these approaches have difficulty detecting weak or instantaneous interactions.

Proximity labeling (PL) has been developed over the past decade to study PPIs in mammalian cells (Yang *et al.*, 2021). This method is based on fusing engineered ascorbate peroxidase (APEX) or the mutant biotin ligase BirAR118G (BioID) with the protein of interest (POI). A significant advantage of this PL approach is its ability to biotinylate interactors of the fused POI within their native cellular environment. However, both enzymes have disadvantages, like requiring toxic hydrogen peroxide (H_2O_2), a high optimal working temperature or having a low efficiency in labelling, and these disadvantages make them difficult to use in plant research. Lately, a new engineered biotin ligase, TurboID, was described as a better candidate for PL in plants (Branon *et al.*, 2018; Zhang, Y *et al.*, 2020). TurboID based PL protocols have been established for *N. benthamiana*, *Arabidopsis* and tomato hairy roots (Kim *et al.*, 2019; Zhang, Y *et al.*, 2019; Arora *et al.*, 2020; Zhang, Y *et al.*, 2020). Notably, when coupled with mass spectrometry (MS), TurboID based PL enables high-throughput analysis of PPIs and mapping of protein networks *in vivo* condition. Despite that, this novel method has not yet been widely applied in other crop plant studies. In **Chapter 4**, we utilized the current proximity labelling protocol for application on potato material in a transient approach. By applying this approach, we identified a novel regulatory partner of StCDF1(**Chapter 5**). These results improved our understanding of how StCDF1 cooperatively interacts with its partners in regulating downstream gene expression throughout the day.

Scope of the thesis

The main goal of this thesis is gaining knowledge of the later development stage in potato senescence and building knowledge of how developmental traits influence the final yield. This thesis presents a comprehensive investigation of StCDF1, the key gene that regulates multiple aspects of potato plant development. Our research provides valuable insights into the interconnections among various developmental processes in potatoes.

In **Chapter 2**, we analyzed the StCDF1 DAP-seq data to identify a novel direct downstream target called *StORE1S02*, coding for a NAC transcription factor associated with senescence induction in *A. thalia*na. We revealed that *StORE1S02* is involved in regulating leaf senescence in potato, especially the onset of senescence, by comparing overexpression and knockdown *StORE1SO2* transgenic plants with non-transformed controls. We provide evidence that StCDF1 controls senescence onset separately from senescence progression and the total life cycle duration. Moreover, our study demonstrated that *StORE1S02* regulates sugar transport

during senescence, contributing to dry matter accumulation in tubers. In this work, by examining the role of the *StCDF1* locus, we address the long-standing question on how potato tuberization and senescence are linked in *S. tuberosum*. We show here that StCDF1 promotes tuberization by not only inducing tuberization signals but also by regulating nutrient reallocation during senescence.

In **Chapter 3**, we delve into the role of *StCDF1* in regulating heat-induced premature senescence. Our findings reveal that *StCDF1* not only enhances heat tolerance but also promotes tuberization across varying temperature conditions. Specifically, our experiments demonstrate that plants overexpressing *StCDF1* or expressing a truncated *StCDF1* allele exhibit reduced premature leaf senescence. Furthermore, these plants show a remarkable increase in yield (from 16 to 47%) when exposed to higher temperatures. Additionally, we observed that both *StCDF1* overexpressing transgenic plants and plants carrying a truncated allele exhibited heightened transpiration rates, which were accompanied by reduced endogenous levels of ABA, under both experimental conditions.

To further enhance our understanding of the regulatory mechanism of StCDF1, our research aims to identify novel interactors of StCDF1. TurboID based proximity labelling is considered to be the most suitable approach for our purpose. In **Chapter 4**, we focused on adapting the TurboID-based proximity labeling protocol for implementation in potato material. This modification enabled us to investigate the regulatory mechanism with improved precision.

In **Chapter 5**, we present proximity labeling results of StCDF1. We successfully identified both known interactors, such as StFKF1 and StTPLs, as well as 7 novel interactors through the application of TurboID-based proximity labeling. These findings expand our understanding of the complex protein interaction network involving StCDF1.Furthermore, we provide compelling evidence that the activation regulatory mechanism of StCDF1 is dependent on the DOF DNA binding domain, rather than the TPL binding domain. Additionally, we present further evidence demonstrating that StCDF1 specifically regulates the progression of senescence without affecting its onset or the total life cycle length of the plant. Notably, we observed a delayed senescence progression and an over 50% increase in tuber mass weight in the case of overexpressing StCDF1.2 with a defective TPL binding site. These findings indicate that StCDF1 plays a multifaceted role in the regulation of senescence, highlighting its potential as a targeted modulator for selectively influencing specific aspects of this process.

In **Chapter 6**, the major findings of this thesis are summarized and placed in the broader research context of the functions of StCDF1 and the intricate link between tuberization and senescence.

Chapter 2

Aging later but faster; how *StCDF1* regulates senescence in *Solanum tuberosum*

Li Shi[1,2], Laura de Biolley[1], Maroof Ahmed Shaikh[3], Michiel E. de Vries[4], Sybille Ursula Mittmann[5], Richard G.F. Visser[1], Salome Prat[3], Christian W.B. Bachem[1]

[1]Plant Breeding, Wageningen University & Research, 6708PB, Wageningen, The Netherlands.
[2]Gradute School Experimental Plant Sciences, Wageningen University & Research, 6708PB, Wageningen, The Netherlands.
[3]Center for Research in Agriculture Genomics (CRAG), Barcelona, 08193, Spain.
[4] Solynta, Dreijenlaan 2, 6703 HA, Wageningen. The Netherlands.
[5] Aardevo B.V. Johannes Postweg 8, 8308 PB, Nagele, The Netherlands.

Summary

- In potato, maturity is assessed by leaf senescence, which in turn affects yield and tuber quality traits. Previously, we showed that the *CYCLING DOF FACTOR1* (*StCDF*1) locus controls leaf maturity in addition to the timing of tuberization. Here, we provide evidence that *StCDF1* controls senescence onset separately from senescence progression and the total life cycle duration.
- We used molecular–biological approaches (DAP-seq) to identify a direct downstream target of StCDF1, named *ORESARA1* (*StORE1S02*), which is a NAC transcription factor acting as a positive senescence regulator.
- By overexpressing *StORE1S02* in the long life-cycle genotype, early onset of senescence was shown, but the total life cycle remained long. At the same time, *StORE1S02* knockdown lines have a delayed senescence onset. Furthermore, we show that StORE1 proteins play an indirect role in sugar transport from source to sink by regulating expression of *SWEET* sugar efflux transporters during leaf senescence.
- This study clarifies the important link between tuber formation and senescence and provides insight into the molecular regulatory network of potato leaf senescence onset. We propose a complex role of *StCDF1* in the regulation of potato plant senescence.

Keywords: Senescence, *StCDF1*, *StORE1*, Tuberization, Life cycle.

Introduction

Plant senescence is the last stage of plant development. During this period, structures and chemical compounds in the chloroplast are broken down allowing nutrients to be recycled and reallocated to other parts of the plant for storage or further development (Guiboileau *et al.*, 2010). This process includes leaf senescence, which is characterized by a decrease in chlorophyll content of leaves, discontinuation of meristem development, and degradation of macromolecules such as proteins and nucleic acids (Hörtensteiner, 2009). The senescence process has been well studied in several plant systems as it is a critical trait which can influence yield and nutritional value (Woo *et al.*, 2018). Potato (*Solanum tuberosum* L.) is a member of the *Solanaceae* family and the most important non-grain food crop (Zaheer & Akhtar, 2016). Despite a long history of potato cultivation, several aspects of potato development and life-cycle regulation remain elusive.

In many other crops, maturity refers to flowering time, seed maturity, fruit ripening and leaf senescence (TeKrony *et al.*, 1979; Maul *et al.*, 1998; Wang *et al.*, 2020). In potato, phenotyping underground development is difficult. Therefore, breeders focus mainly on phenotyping the above ground leaf maturity, instead of tuber maturity. For potato, plant maturity is considered to be one of the most important genetically controlled, physiological components for phenotyping in breeding programs for predicted harvest timing and yield improvement (Wallace *et al.*, 1993; Prat, 2006). Maturity is generally scored on an ordinal scale from 1-7 with 1 being green plants and 7 being dead plants (Hurtado *et al.*, 2011). Furthermore, potato maturity is frequently evaluated by scoring only once, at a time-point where the breeder observes the greatest variation in a population. Thus, the senescence onset, senescence progression speed and other senescence related factors remain less well characterized.

Leaf maturity is affected by numerous internal and environmental cues. In potato, tuberization onset and leaf maturity are tightly linked physiologically and genetically. In fact, these two traits have often been mapped to the same genetic locus (Visker *et al.*, 2003; Kloosterman, B. *et al.*, 2013; Jing *et al.*, 2022a). A major-effect quantitative trait locus (QTL), located on chromosome 5, is responsible for foliage maturity, tuberization onset, and final potato yield (Visker *et al.*, 2003; Kloosterman, B. *et al.*, 2013; Li, J *et al.*, 2019). This QTL was shown to be functionally linked to a DOF family gene (DNA-binding with one finger) coding for a transcription factor named CYCLING DOF FACTOR1 (StCDF1) that was found to regulate tuberization and plant life cycle length. In diploid potato, the genotypes with truncated variants have earlier leaf maturity. The truncated variants of StCDF1 exhibit enhanced protein stability caused by inability to bind to GIGANTEA (StGI) and FLAVIN-BINDING, KELCH REPEAT, F-BOX (StFKF1) (Kloosterman, B. *et al.*, 2013). Overexpressing truncated *StCDF1* (*StCDF1.2*) in the late tuberizing and late leaves maturing background (homozygous *StCDF1.1*) leads to both early tuberization and a short life cycle in potato (Kloosterman, B. *et al.*, 2013). Furthermore, a study based on 6 tetraploid genomes demonstrated that the allelic variants of *StCDF1* correlate with leaf maturity in a dosage-dependent manner (Hoopes, G *et al.*, 2022). Recently, Jing *et al.* (2022a) reported that the *StABI5-like 1* gene (*StABL1*) codes for a transcription factor which also positively influences tuberization onset and leaf senescence. In these studies, early tuberization was linked to the *FLOWERING LOCUS T-like* (*FT-like*) gene *SELF-*

PRUNING 6A (*StSP6A*). StSP6A is a small globular protein that acts as a mobile tuberigen and belongs to the phosphatidylethanolamine-binding protein (PEBP) family (Navarro *et al.*, 2011; Zhang, X *et al.*, 2020). In stolon tips, StSP6A forms a tuberigen activation complex (TAC) with St14-3-3s and StFD-LIKE1 (StFDL1) to activate downstream tuberization related genes (Teo *et al.*, 2017). Tuber formation requires assimilate translocation. StSP6A is also found to be involved in leaf to stolon sugar transport, by physically interacting with the sucrose efflux transporter Sugar Will Eventually be Exported Transporter 11 (StSWEET11) to promote symplasmic sucrose transport (Abelenda *et al.*, 2019). While sugar transport is crucial for plant development throughout the life cycle, it plays a particularly important role during senescence, as it enables the mobilization of nutrients from senescing tissues to other parts of the plant for storage or further use (Wingler, 2018). A molecular link between both *StCDF1* and *StSP6A* with plant senescence has not yet been demonstrated.

To gain insight into how potato tuberization associates with leaf senescence, understanding the senescence regulatory network is important. The Arabidopsis NAC transcription factor ORESARA1 (ORE1) has been shown to act as a critical positive senescence regulator (Woo *et al.*, 2004; Rauf *et al.*, 2013; Qiu *et al.*, 2015; Kim *et al.*, 2018). ORE1 promotes senescence by directly binding to *BIFUNCTIONAL NUCLEASE1* (*BFN1*), *SENESCENCE-ASSOCIATED GENE 29* (*SAG29*) and other promoters of senescence-associated genes (Matallana-Ramirez *et al.*, 2013). *Arabidopis thaliana AtORE1* mutants display a stay-green phenotype (Kim *et al.*, 2018). In the early development stages of plants, *AtORE1* is targeted and downregulated by the microRNA *miR164* at the transcription level (Kim *et al.*, 2009; Lira, B. S. *et al.*, 2017). During leaf senescence*, miR164* expression is downregulated while *AtORE1* expression is enhanced (Pulido & Laufs, 2010). The balance between miR164 and AtORE1 transcripts is critical for leaf-stage transition. Moreover, a number of *AtORE1* orthologues affecting leaf senescence and fruit quality traits have been identified in tomatoes, termed *SlORE1S02*, *3* and *6* according to their chromosomal position (Lira, B. S. *et al.*, 2017).

Despite all previous research, knowledge about the regulation of senescence in potatoes is limited. In previous studies, *StCDF1* has been mapped as responsible for the onset of tuberization and senescence (Visker *et al.*, 2003; Kloosterman, B. *et al.*, 2013; Li, J *et al.*, 2019). In this study, we show that potato plant's senescence has several different aspects: onset of senescence, progression of senescence, and life cycle length. *StCDF1* negatively affects the onset of senescence but accelerates the progression of senescence and shortens the life cycle. In addition, we identify the direct downstream target of *StCDF1*, *StORE1S02* (named by analogy to tomato), which has been found to regulate the onset of senescence specifically in potatoes. We also found that *StORE1s* play a key role in sugar transportation throughout several leaf developmental stages. This study discovered a new connection between tuber formation and senescence and provides insight into the molecular regulatory network of potato leaf senescence onset.

Results

StCDF1 represses senescence onset and shortens growing period

Previously, we showed that overexpressing a truncated *StCDF1(StCDF1.2)* in a late tuberizing background (homozygous *StCDF1.1*), not only induced early tuberization but also shortened life cycle length (Kloosterman, B. *et al.*, 2013; Hoopes, G *et al.*, 2022). To study the function of *StCDF1* in regulating senescence, we selected two offspring plants of the C x E population described previously (Kloosterman, B. *et al.*, 2013; Ramírez Gonzales *et al.*, 2021) with different *StCDF1* allele combinations for observing senescence related traits in detail (Fig. 1A). To study the impact of StCDF1 in regulating senescence, we aimed at overexpressing StCDF1 in a late background. Due to the better protein stability, StCDF1.2 was selected as backbone (Kloosterman, B. *et al.*, 2013). Furthermore, to avoid negative regulation by the lncRNA *StFLORE* transcript (Ramírez Gonzales *et al.*, 2021) and thereby ensuring high expression throughout the day, we edited the coding usage in the 35S:*StCDF1.2* construct (Fig. S1) resulting in a construct named p35S:*StCDF1.2* ^{Coed}. Strong expression of p35S:*StCDF1.2* ^{Coed} was found in transgenic lines (Fig. S2).

Interestingly, although a longer life cycle was observed in CE3027 (homozygous *StCDF1.1*), the lowest leaves have visible yellowing (50 days after planting, DAP) earlier than those in CE3130 (early tuberizing, containing two truncated *StCDF1* variants: the *StCDF1.2* and *StCDF1.3* alleles) and OE *StCDF1.2* ^{Coed} (Fig. 1A). The visible leaf yellowing in CE3130 started at 72 DAP and it rapidly completed its life cycle within one week. The weekly measurements of chlorophyll content consistently demonstrate a gradual decline in the lower leaves of CE3027 starting from 37 DAP. In contrast, the chlorophyll content in OE *StCDF1.2* ^{Coed} and CE3130 plants appears to remain relatively stable until reaching 65 DAP (Fig. 1B). We observed a similar pattern in change of chlorophyll fluorescence (quantum yield of PSII) through the time (Fig. 1C). Together, the delayed senescence onset and shortened life cycle also were clearly visible in overexpressing *StCDF1.2* ^{Coed} transgenics (Fig. 1A-C).

These phenotypes suggest that senescence related traits, like senescence onset, speed of senescence progression and life cycle length are not positively correlated in potato. Overexpressing *StCDF1.2* ^{Coed} in a late background or carrying a truncated *StCDF1* allele (*StCDF1.2/1.3*) will shorten the life cycle, but delay senescence onset. In summary, *StCDF1* controls both senescence onset and total life cycle length separately.

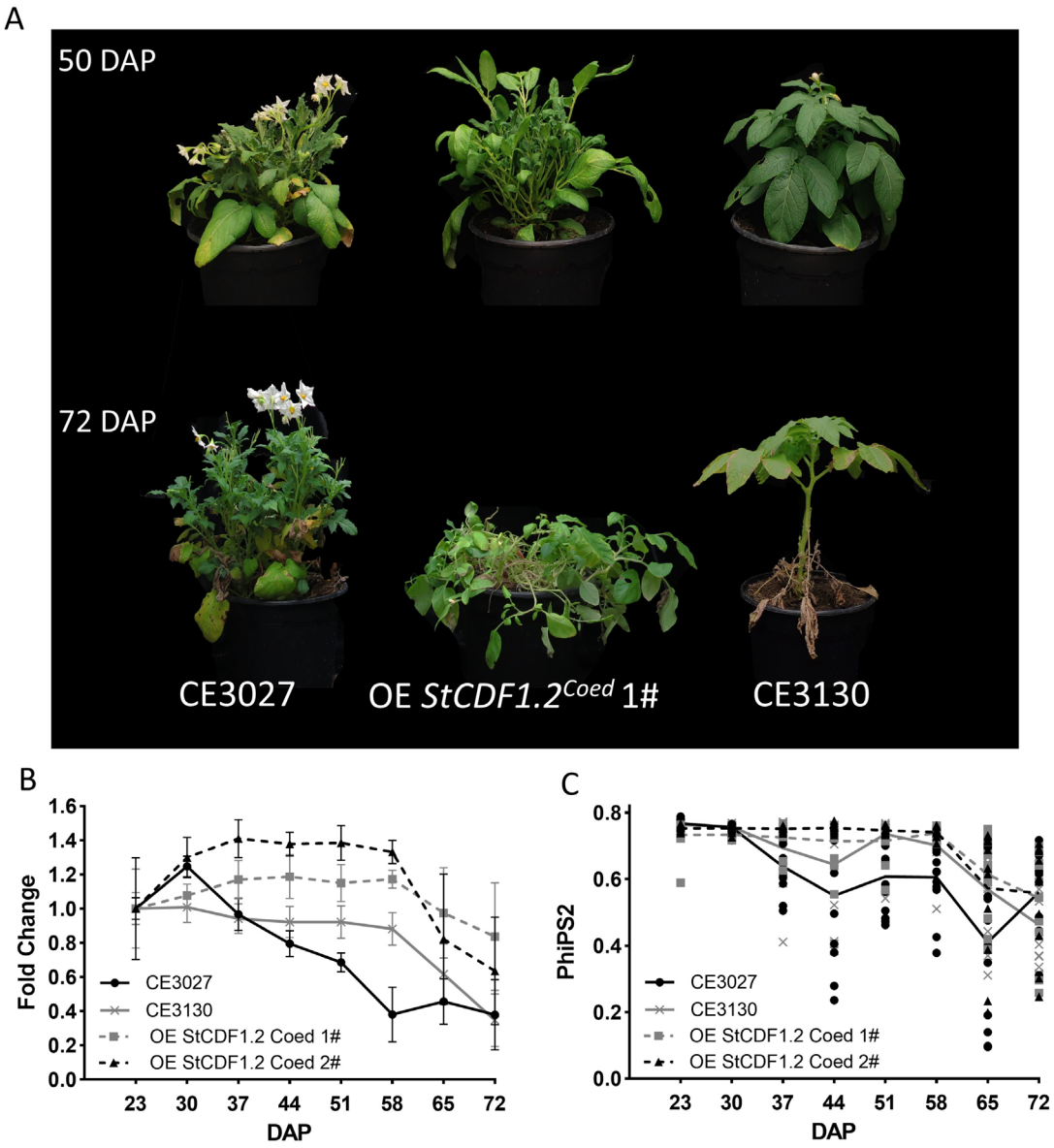

Figure 1. StCDF1 represses senescence onset and shortens growing period.
A. Phenotype of CE3027 (late maturity, homozygous for *StCDF1.1*) , CE3130 (early maturity, containing both the *StCDF1.2* and *StCDF1.3* alleles), OE *StCDF1.2* ^{Coed} 1# at 50 and 79 DAP. **B.** Fold change of chlorophyll content (µmol of chlorophyll per m^2, measured by Apogee MC-100 Chlorophyll Meter) from 23-72 DAP in CE3027, CE3130, OE *StCDF1.2* ^{Coed} 1# and OE *StCDF1.2* ^{Coed} *2#* . The chlorophyll content of each line was standardized to a value of 1 at 23 DAP. Error bars: means ± SE, with n = 12 technical replicates. **C.** Quantum yield of PSII (in light, measured by Licor-600) of the same samples from (**B**). Each measurement was plotted as one data point, n=12 technical replicates. The average of data points from the same time and plant line are connected with a line.

StCDF1 binds to and represses the expression of a positive senescence regulator, *StORE1S02*

To understand how *StCDF1* is involved in the regulation of senescence, this study used the direct target genes of StCDF1. Recently, a DAP-seq of StCDF1 was performed by Gonzales

(2022) and this dataset revealed many novel direct downstream targets of StCDF1. By manually screening for well-known senescence regulators, we found that there are multiple binding sites for StCDF1 on the promoter of *StORE1S02* (*StORESARA1S02*) (Fig. 2A), whose orthologues positively regulate senescence in Arabidopsis and tomato (Lira, B. S. *et al.*, 2017). Based on the DAP-seq results, we hypothesized that *StCDF1* might directly regulate the expression of *StORE1S02*. Therefore, we examined the expression of *StORE1S02* in CE3130 and OE *StCDF1.2* ^{Coed} transgenics and the background of these transgenics (CE3027). The results show that during the morning, transcription levels of *StORE1S02* in CE3130 and OE *StCDF1.2* ^{Coed} transgenics were strongly downregulated compared to in CE3027 (Fig. 2B, Table.S1).

This repression can also be found in the *StORE1S02* expression profile during the development (23-57DAP; Fig. 2C) in CE3130 compared to CE3027. Although the *StORE1S02* transcript level reached its highest point at 37 DAP in both early and late backgrounds, the upregulated period of *StORE1S02* is longer in CE3027 (30 DAP-50 DAP) than in CE3130 (30 DAP-43 DAP). To further confirm that the reduced expression of *StORE1S02* is linked to the repressing function of *StCDF1*, the 35S:*StCDF1.1* construct was co-infiltrated into tobacco leaves with *StORE1S02* promoter constructs driving expression of the firefly luciferase gene (Fig. 2D). The result shows that StCDF1 downregulates the expression of *StORE1S02*. Together, StCDF1 binding to the promoter of *StORE1S02* and the co-expression study confirms that StCDF1 directly negatively regulates the expression of *StORE1S02.*

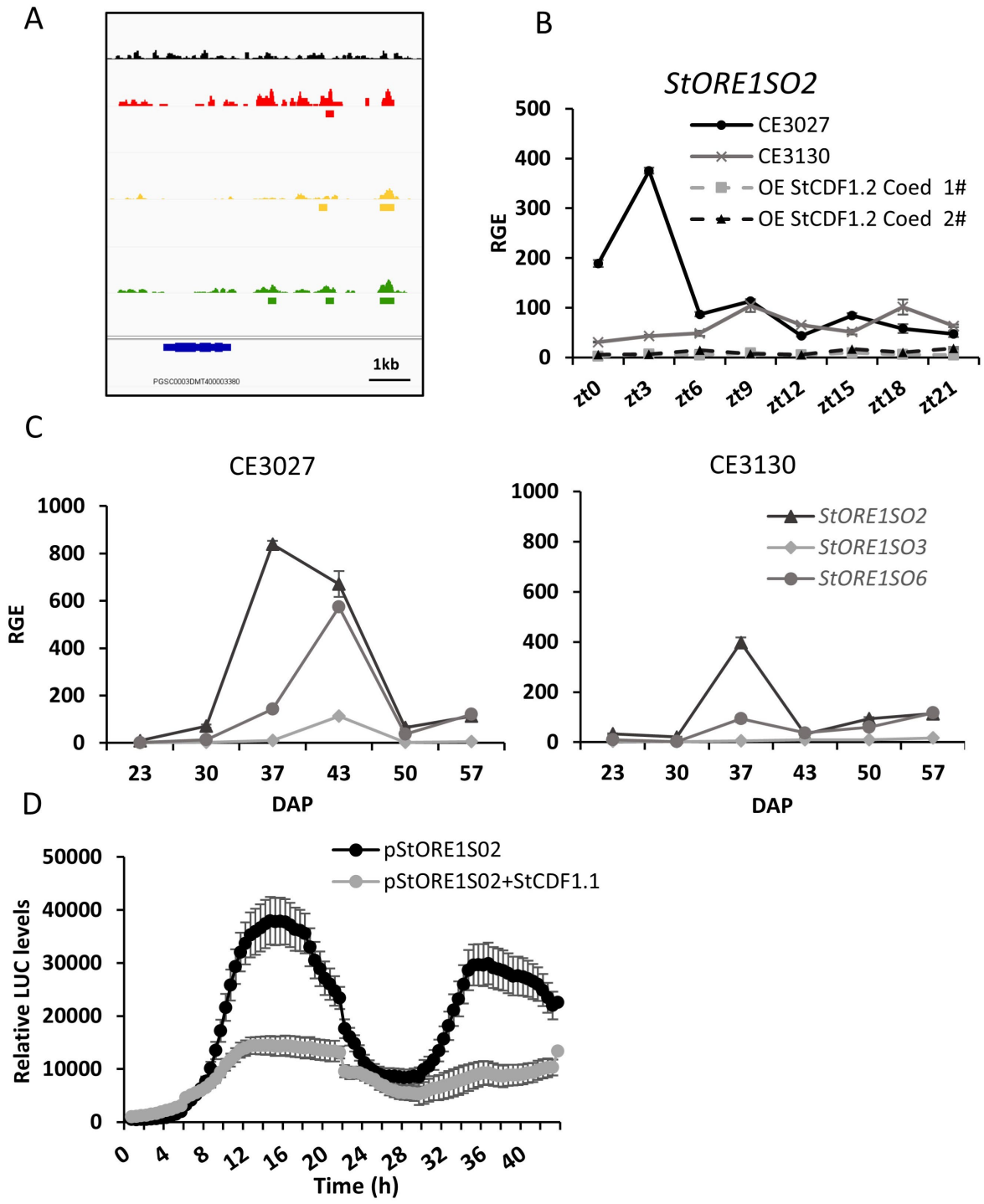

Figure 2.StCDF1 repress expression of *StORE1S02* via directly binding to the promoter of *StORE1S02*. **A**. DAP-Seq binding peaks of StCDF1 in the promoter region of *StORE1S02*. Diagram description from the top: input library as negative control (black bar chart), experiment 1 (red bar chart), experiment 2 (yellow bar chart), experiment 3 (green bar chart). The significant binding sites shows in below bar chart of each experiments. Gene model of *StORE1S02* is represented in blue. In the right bottom corner, the scale represents 1 kb. **B**. Diurnal gene expression analysis of *StORE1S02* in CE3027, CE3130 and OE *StCDF1.2* ^{Coed} 1# and OE *StCDF1.2* ^{Coed} 2# . ZT: Zeitgeber time. Error bars: means ± SE, with n = 3 biological replicates. **C.** Transcript profiles of *StORE1s* throughout development in CE3130 and CE3027 Error bars: means ± SE, with n = 3 biological replicates. **D.** Repression of p*StORE1S02*::*iLUC* luciferase activity by 35S::*StCDF1.1* in *N. benthamiana* leaves. p*StORE1S02* were used as a

negative control. Relative luminescence levels were measured at intervals of 0.5 h for 2 days. Error bars represent the standard error of 4 biological replicates.

ORE1 orthologs in potato

ORESARA1 (ORE1) encodes a NAC transcription factor that positively regulates senescence by promoting nucleic acid degradation and inhibiting chloroplast maintenance (Matallana-Ramirez *et al.*, 2013; Rauf *et al.*, 2013). In this study, we identified 3 ORE1 orthologs in potato by comparing protein sequences from *AtORE1*, *SlORE1S02*, *SlORE1S03*, and *SlORE1S06* against the potato reference genome DM 1-3 516 R44 v6.1. The identified homologues were named *StORE1S02*, *StORE1S03* and *StORE1S06* according to their chromosome localization, as with the tomato *SlORE1* genes. The coding Sequences (CDS) of the genes were aligned and a phylogenetic representation including all *ORE1* sequences from the different crops was created (Fig. 3A). Interestingly, unlike other plant families, all analyzed *Solanaceae* species had 3 copies of *ORE1.*

By retrieving and analyzing the CDS of *ORE1* from ten different crops, we found that all Solanaceae species carry an in-frame insertion of 24 bp in the ORE1S02 homologue (Fig. 3B). This insertion was suggested to disrupt the binding and the cleaving by miR164 (Lira, B. S. *et al.*, 2017). We performed a diurnal gene expression analysis of StORE1 genes in the diploid potato genotype CE3027 and show that *StORE1S02* has a much higher expression than the other two at four different time points (ZT0, ZT3, ZT6 and ZT12; Fig. 3C). The same pattern can also be found over the development period (Fig. 2C). Therefore, the transcript abundance of *StORE1S02* is the highest among all three ORE1 orthologs in potato.

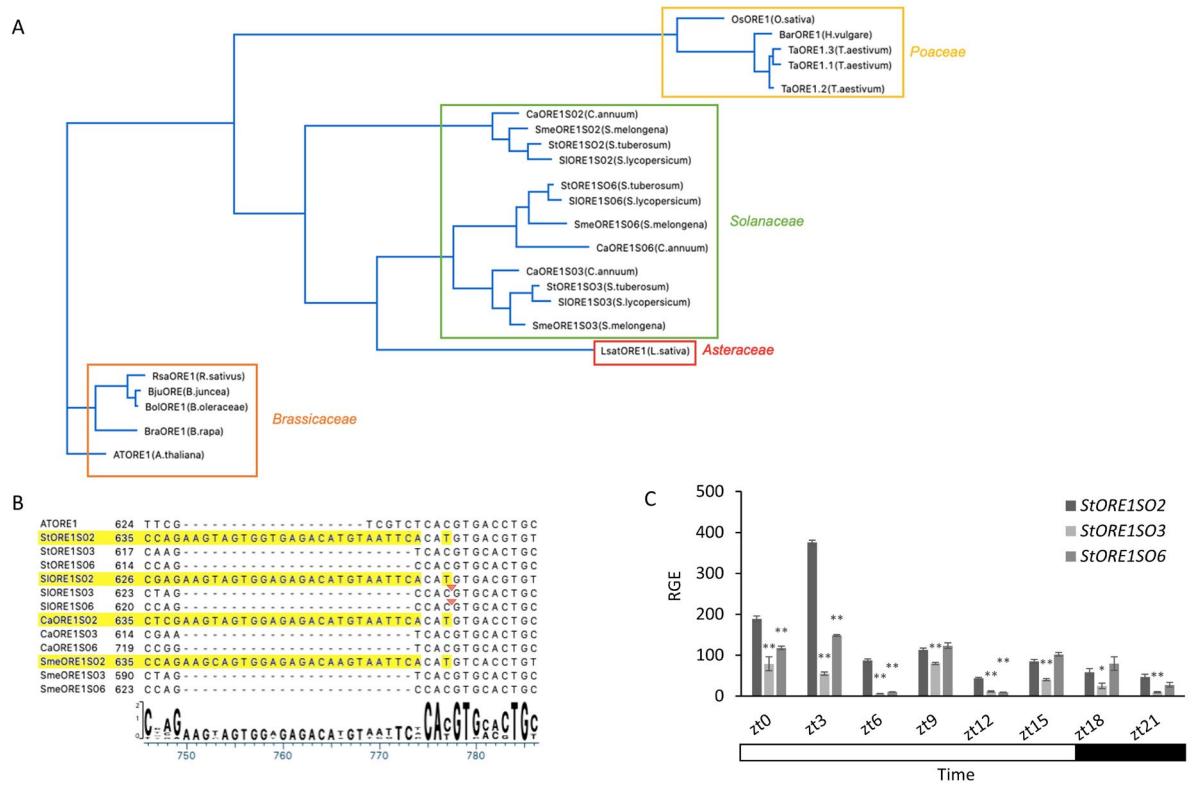

Figure 3. *ORE1* orthologs in potato. **A**. Phylogenetic representation of the *ORE1* genes obtained from the alignment of their protein sequences. The different species are clustered by family. Three *AtORE1* orthologs were found for all *Solanaceae* species. All sequences are detailed in Table S3. In potato, they were named as follows: *StORE1S02*, *StORE1S03*, and *StORE1S06*. **B**. Alignment of *AtORE1* and its orthologs in four *Solanaceae* species. The mir164 binding site in *ORE1S02* genes is highlighted in yellow. The red arrowheads corresponds to the *SlmiR164* cleavage sites detected by Lira et al., 2017, in *StORE1S03* and *StORE1S06*. **C.** Analysis of *StORE1* gene expression in CE3027 across the diel. Error bars: means ±SE, with n = 3 biological replicates. *P < 0.05, **P < 0.01; Compared to *StORE1S02*; t test.

StORE1S02 positively regulates senescence onset

Based on phylogenetic analysis and diurnal gene expression analysis, *StORE1S02* is the closest ortholog to *AtORE1* and has the highest expression among all three *StORE1* genes (Fig. 3A&C). Therefore, for the p35S:*StORE1S02*, 3 transgenic lines were generated in the late senescent diploid potato genotype CE3027. The results show both selected transgenic lines (OE#11, OE #21) displayed higher expression of *StORE1S02* (Fig. S3) and they all showed an early senescence phenotype (Fig. 4A). However, overexpressing *StORE1S02* did not shorten the life cycle compared to the background CE3027 (Fig. 4B).

Interestingly, in both overexpressing *StORE1S02* transgenic lines the expression levels of *StORE1SO3* and *StORE1SO6* were upregulated. This result suggests *StORE1S02* may positively regulate *StORE1SO3* and *StORE1SO6* expression (Fig. 4C).

To further confirm the function of *StORE1s* in potato and avoid possible redundant effects of different homologs, we selected the region which is highly similar among all three *StORE1s* as

RNAi targeting region (Fig. S4). *StORE1s* knockdown plants were generated in CE3130, an early senescent background. Two lines (KD#3 and KD #4) were selected for use in this experiment. A delayed senescence phenotype was found in the *StORE1s* knockdown lines (Fig. 4D). The chlorophyll level also indicates that these transgenic lines contain more chlorophyll a and b compared with the background genotype (Fig. 4E). The life cycle length of KD lines is extended for an extra 3 weeks, but their life cycle still ended earlier than CE3027 and both OE lines (Fig. 4F).

BIFUNCTIONAL NUCLEASE1 (*BFN1)* has been reported to be positively regulated by *ORE1* in *Arabidopsis* (Matallana-Ramirez et al., 2013). In our transgenic lines, we found that *StBFN1* expression was significantly downregulated in KD#3 and KD#4 lines and upregulated in OE#11 and OE#21 lines, compared to their background plants separately (CE3130 and CE3027; Fig. 4G). Thus, we confirmed that this senescence associated gene *StBFN1* is positively regulated by StORE1 transcription factors. By checking the senescence phenotype and senescence related gene expression of both OE and KD lines, we provide strong evidence that StORE1 proteins act as positive regulator for senescence, especially the senescence onset timing, in potato.

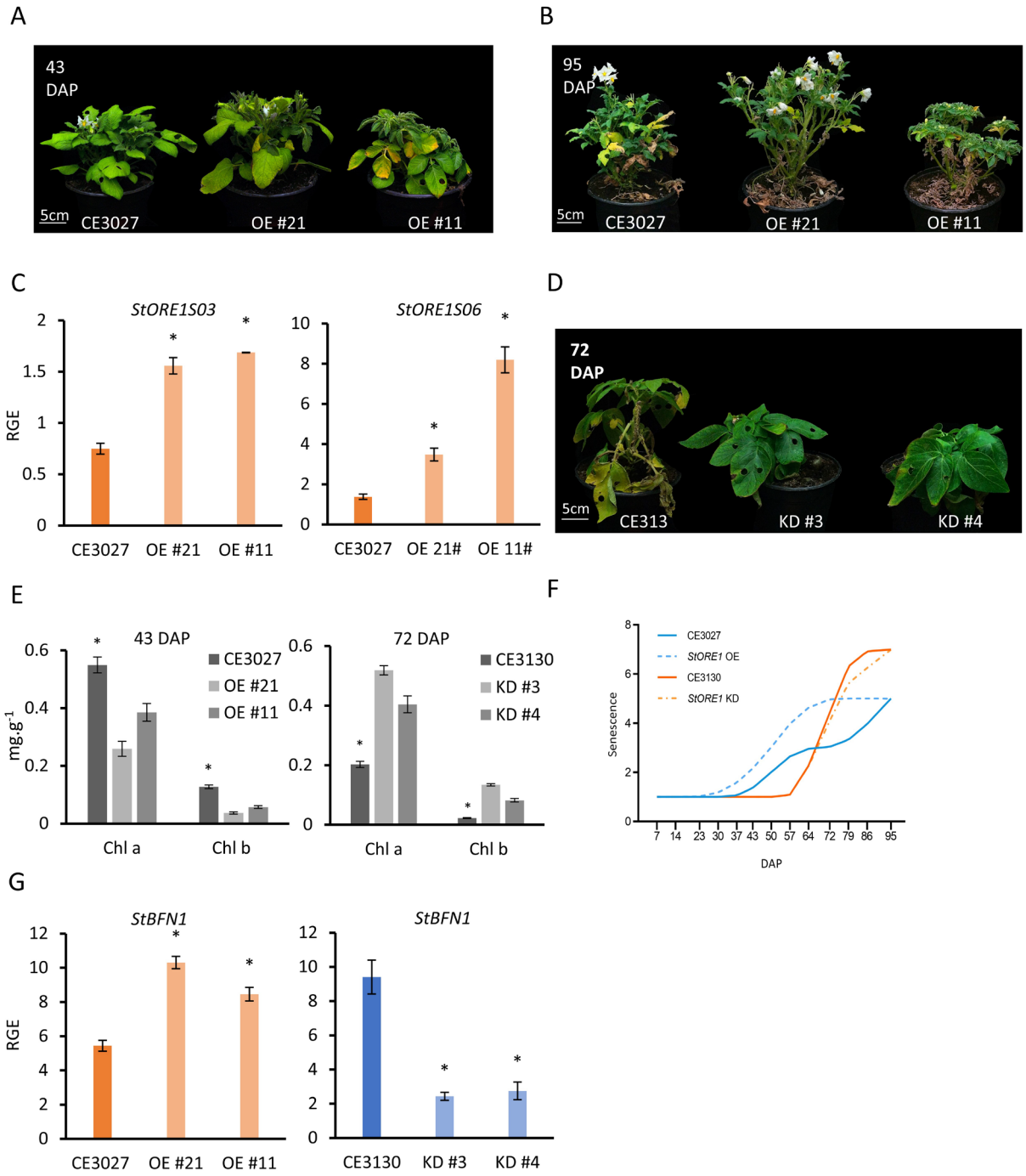

Figure 4. *StORE1S02* positively regulates senescence. **A.** From left to right, CE3027 and CE3027 transformed with 35S::*StORE1S02* lines 21 and 11 (OE #21 and OE #11) at 43 days after planting (DAP). **B.** Same plants in (A), at 95 DAP. **C.** Relative expression of *StORE1SO3* and *StORE1SO6* in CE3027 and CE3027 transformed with 35S::*StORE1S02* lines 21 and 11 (OE #21 and OE #11) at 23 DAP. Data are presented as the mean ± SE biological triplicates. *P < 0.05, **P < 0.01; t test. **D.** From left to right, CE3130 and *StORE1S02* knock-down lines in the CE3130 background (KD #3 and KD #4) at 72 days after planting. **E.** Analysis of chlorophyll content in CE3027, OE #21 and OE #11 at 43 DAP. And chlorophyll content in CE3130, KD #3 and KD #4 at 72 DAP. Data are presented as the mean ± SE biological triplicates. *P < 0.05, **P < 0.01; t test. Samples from each line were pooled (5 individuals) and measured. **F.** Fitted curves showing the senescence development. Senescence scoring according to the instructions from Hurtado, Schnabel et al. 2011, with minor modifications.

Briefly, 1 = green plant; 2 = upper leaves with the first signs of yellowing (light green); 3 = yellow leaves; 4 = 25% of canopy brown; 5 = 50% of canopy brown; 6 = more than 75% canopy brown; 7 = dead plant. **G.** Relative expression of *StBFN1*. The gene expression results of CE3130 and *StORE1S02* knock down lines in CE3130 background (KD #3 and KD #4) at 37 DAP are shown in blue. The gene expression results of CE3027 and CE3027 transformed with 35S::*StORE1S02* lines 21 and 11 (OE #21 and OE #11) at 23 DAP are shown in orange. Data are presented as the mean ± SE biological triplicates. *P < 0.05, **P < 0.01; t test.

StORE1 genes do not affect tuberization initiation but affect sugar transportation

To address whether *StORE1S02* genes have an impact on tuberization, the tuberization phenotype was examined in the *StORE1*-RNAi lines and their background plants (CE3130) at 35 days after planting (DAP). In previous experiments, CE3130 started tuberizing around 30-35 DAP. Both KD lines produced tubers at 35 DAP, as did CE3130 (Fig. 5A). These results demonstrate that StORE1 proteins do not function as a trigger of tuberization.

During the observation period, leaf thickening was found in KD lines (Fig. 5B). We speculated that leaf thickening and cell enlargement could be an indication of increased sugar accumulation. To test our hypothesis, we analyzed the sucrose and glucose content in the leaf at 4 different time points. In the KD lines, the sucrose content increased through time. In contrast, the sucrose content in CE3130 plants remained the same between these 4 time points (Fig. 5C). The glucose content remains relatively stable in all plant lines through these 4 different time points (Fig. S5). We further checked the chlorophyll fluorescence and there was no significant difference between KD plants and their background plants (CE3130) among all the time points (Fig. 5E). Together, we observed that under the same photosynthesis rate, sucrose accumulated in the leaves of *StORE1s* knock down plants throughout development, but not in their background plant (CE3130).

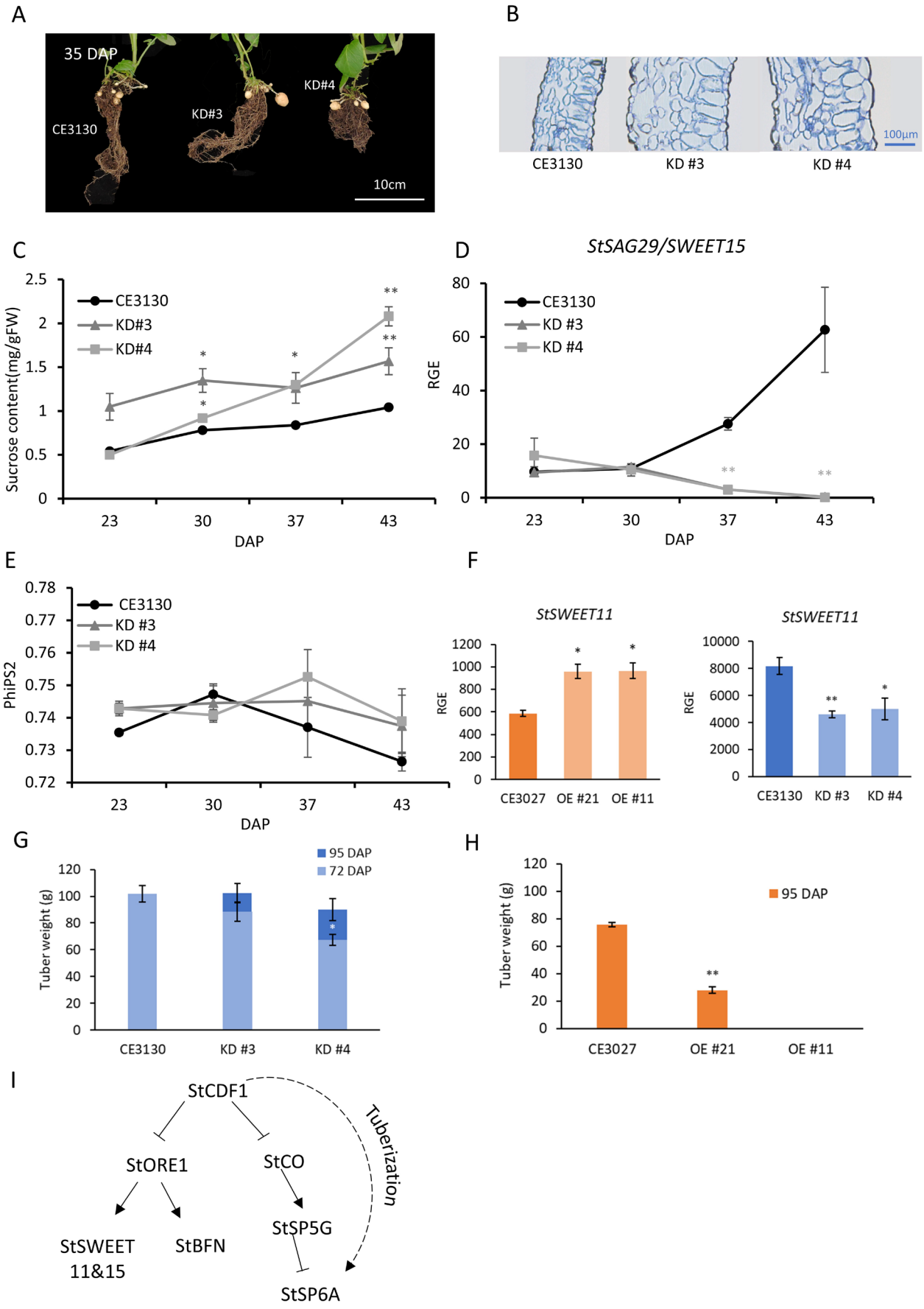
A
35 DAP
CE3130
KD#3
KD#4
10cm
B
CE3130
KD #3
KD #4
100µm
C
Sucrose content(mg/gFW)
CE3130
KD#3
KD#4
DAP
D
StSAG29/SWEET15
RGE
CE3130
KD #3
KD #4
DAP
E
PhiPS2
CE3130
KD #3
KD #4
DAP
F
StSWEET11
RGE
CE3027
OE #21
OE #11
StSWEET11
RGE
CE3130
KD #3
KD #4
G
Tuber weight (g)
95 DAP
72 DAP
CE3130
KD #3
KD #4
H
Tuber weight (g)
95 DAP
CE3027
OE #21
OE #11
I
StCDF1
StORE1
StCO
StSWEET 11&15
StBFN
StSP5G
StSP6A
Tuberization

Figure 5. *StORE1S02* affects sugar transport. **A.** From left to right, underground phenotype of CE3130 and *StORE1S02* knockdown lines in CE3130 background (KD #3 and KD #4) at 35 DAP. **B.** Light microscopy image of a leaf cross section of CE3130 and *StORE1S02* knockdown lines (KD #3 and KD #4). The leaves were harvested at 30 DAP. **C.** Sucrose content in leaves of CE3130 and *StORE1S02* knockdown lines in CE3130 background (KD #3 and KD #4) at different time points (23,30,37 and 43 day after plant, DAP). **D.** Relative expression of *StSAG29/SWEET15* in the same samples as in (C). Data are presented as the mean ± SE biological triplicates. **P < 0.01; t test. **E.** Quantum yield of PSII (in light, measured by Licor-600) of CE3130 and *StORE1* knockdown lines in CE3130 background (KD #3 and KD #4) at different time points (23,30,37 and 43 DAP). **F.** Relative expression of *StSWEET11*. The gene expression results of CE3130 and *StORE1S02* knockdown lines in CE3130 background (KD #3 and KD #4) at 37 DAP are shown in blue. The gene expression results of CE3027 and CE3027 transformed with 35S::*StORE1S02* lines 21 and 11 (OE #21 and OE #11) at 23 DAP are shown in orange. Data are presented as the mean ± SE biological triplicates. *P < 0.05, **P < 0.01; t test. **G.** Average of tuber weight per plant for knocked down plants and their background CE3130. *P < 0.05, **P < 0.01; t test. **H.** Average of tuber weight per plant for overexpressed plants and their background CE3027. *P < 0.05, **P < 0.01; t test. **I.** A hypothetical model for the function of StCDF1 in regulating tuberization and senescence suggesting that StCDF1 represses the expression of *StCO* and *StSP5G*, indirectly promoting *StSP6A* expression to facilitate tuberization. Simultaneously, StCDF1 negatively regulates *StORE1S02* at the transcriptional level. StORE1S02, when activated, promotes leaf senescence by enhancing the expression of genes involved in nucleic acid degradation (*StBFN1*) and sugar transportation processes (*StSWEET11&15*).

Senescence-Associated Genes (SAGs) are a group of genes that have been found to be upregulated during senescence in various species (Lohman *et al.*, 1994; Gepstein *et al.*, 2003). SAGs are therefore used as molecular markers for detecting senescence (Gepstein *et al.*, 2003; Zhang *et al.*, 2021). *SAG29* has been found to be a direct transcriptional target of *ORE1* in Arabidopsis (Matallana-Ramirez *et al.*, 2013) and the induced expression of *SAG29* has been found to be associated with leaf yellowing (Kamranfar *et al.*, 2018). Interestingly, SAG29 is also known as a member of the clade III SWEET proteins (*SWEET15*). We show that the expression of *StSAG29* was strongly repressed throughout different developmental stages (37DAP and 43DAP) in RNAi *StORE1S02* lines compared with CE3130 (Fig. 5D). This is consistent with an increased sucrose content found in the leaves (Fig. 5C). In contrast, *StSAG29* has a higher expression in OE lines than in CE3027 (Fig. S6). Beside *StSAG29/SWEET15*, the expression of *StSWEET11* was also found to be increased in both *StORE1S02* overexpressed lines and decreased in both *StORE1* knockdown lines (Fig. 5F). We also investigated the expression of *StHXK1*, a well-known player in sugar signalling that regulates leaf senescence (Moore *et al.*, 2003). However, no significant difference was found between the KD lines and CE3130 (Fig. S7). These results indicate that *StSWEET11* and *SAG29/SWEET15* expression are associated with senescence and regulated by the StORE1 transcription factors.

Compared to the extended life cycle of KD plants, the CE3130 plants finished their life cycle 3 weeks earlier. We harvested all CE3130 and half of the KD plants and measured total tuber weight at 72 DAP. The other half of the KD plants was harvested at 95 DAP. In the first harvest, the total tuber weight of CE3130 was higher than all KD lines (Fig. 5G). In the second harvest, both KD lines achieved higher yield compared to the first harvest. However, the total yield of

KD lines in the second harvest showed no significant difference to the total yield of CE3130 (Fig. 5G).

We also compared the total yield from *StORE1S02* overexpressing lines with their background CE3027. The yield of both OE #11 and OE #21 plants was significantly reduced compared to the background (CE3027; Fig. 5H). Among these transgenics, the higher expression of *StORE1S02*, the greater the reduction in yield. The OE #11 line, which has the highest expression of *StORE1S02* (Fig. S1), failed to make any tubers. The OE #21 line has a lower expression level of *StORE1S02* compared to line #11 and is able to make tubers but the yield is significantly reduced (Fig. 5H).

These results together indicate that knocking down *StORE1S02* expression may delay the sugar transport from leaf to tuber but has no significant impact on yield in practice. However, overexpressing *StORE1S02* significantly reduced the yield. Thus, *StORE1s* play a key role in sugar transportation and premature senescence caused by overexpressing *StORE1S02* will lead to severe yield loss.

Discussion

Potato above ground maturity is an important trait for potato production, especially regarding the final yield. In many other plants such as wheat, tomato, delayed senescence contributes to longer periods of photosynthesis and can increase final yield (Lira, B. S. *et al.*, 2017; Joshi *et al.*, 2019). However, in potato, previous field studies indicated this link between senescence and final yield is more complicated. A positive correlation between long life cycle and high yield is seen in commercial potato breeding programs (Stöckle *et al.*, 2010; Kleinwechter *et al.*, 2016; Yuan *et al.*, 2016). However, the varieties used in these breeding programs have undergone selection for early tuberization and late senescence in order to achieve high yield and high starch content (Hoopes, G *et al.*, 2022; Clot *et al.*, 2023). Therefore, the genotypes from research populations that have not undergone this selection, could consequently show a different correlation. Because of this, research population materials could provide a better understanding of the correlation between leaf senescence and tuber formation.

Allelic variation of *StCDF1* has been found to influence various developmental traits including tuberization, senescence and yield (Kloosterman, B. *et al.*, 2013). Having a truncated *StCDF1*(*StCDF1.2/1.3*) not only promotes early tuberization and shortens life cycle length but also has major impact on yield (Kloosterman, B. *et al.*, 2013; Manrique-Carpintero *et al.*, 2015; Marand *et al.*, 2019; Hoopes, G *et al.*, 2022; Clot *et al.*, 2023). Thus, it is apparent that StCDF1 plays a complex role in regulating potato plant development.

In this study, we demonstrated that *StCDF1.2* has independent effects on three senescence related traits. Our data indicate that plant senescence is not a single quantitative trait, but a combination of several morphological traits including senescence onset, senescence progression speed and total life cycle length. Constitutive overexpression of *StCDF1* delays senescence onset but promotes more rapid senescence progression and shortened life-cycle

length (Fig. 1A). This result indicates that these senescence related traits are not associated with each other but regulated separately.

We identified a direct downstream target of *StCDF1*, which has been known to act as a positive senescence regulator in other crops, *StORE1S02*. In potato (*Solanum tuberosum*), three *ORESARA1* homologues are present; *StORE1S02*, *StORE1S03*, and *StORE1S06*. Among these three homologues, *StORE1S02* is the closest to *SlORE1S02* and shares the feature of an insertion near the binding sites of the microRNA *miR164* (Lira, B. S. *et al.*, 2017). This is the case also for eggplant (*S. melongena*) and Capsicum (*C. annuum*), which also belong to the *Solanaceae* family of plants.

In this study, we confirmed that *StORE1S02* acts as a positive leaf senescence regulator in potato, as has been seen in other plant species (Rauf *et al.*, 2013; Lira, B. S. *et al.*, 2017), specifically regulating senescence onset. Overexpressing *StORE1S02* in CE3027, which has a late tuberization time and a long life-cycle, induced early yellowing in the lower leaves, but life-cycle length was not affected. In the young/top leaves, overexpressing *StORE1S02* interestingly failed to induce cell death and leaf yellowing. Other than post-transcriptional regulation by miRNA164, a kinase based post-translational mechanism was reported by Durian *et al.* (2020). Their results suggest that ORE1 has to be properly phosphorylated to activate downstream genes to induce senescence. Therefore, we propose that the lack of impact on the top/young leaves when overexpressing StORE1S02 may be attributed to distinct post-translational modifications within various tissues, such as phosphorylation. This result further supports that the onset of plant senescence is regulated separately from life-cycle length of the whole potato plant and more experimentation is required to fully understand the molecular mechanism.

Previous studies in other crops reported that early leaf senescence has a large negative impact on final yield (Xujun *et al.*, 2005; Ma *et al.*, 2018; Yang *et al.*, 2020). In this study, we demonstrate the reduction in final yield, by inducing early senescence in potatoes. In addition, we found that the lower fully expanded leaves play an essential role as source leaves for tuberization and final yield accumulation, while the upper sink leaves do not. This result provides insight into the interesting negative correlation between long life cycle length and low yield in potato genotypes like CE3027. This genotype has a long life-cycle due to apical meristem maintenance keeping young top leaves green. However, the photosynthesis in these top young leaves does not contribute to final yield. Therefore, for late maturing genotypes which already have long growing period, delaying the senescence onset timing or slowing down the senescence progression speed might be the route to improve the final yield.

The increased sucrose content in leaves and reduced expression of *StSWEET11&15*, together with the delayed tuber growth, suggest sugar transport from leaves to tuber was negatively regulated in KD lines. Sugar signalling has a significant impact on leaf senescence (Hoeberichts *et al.*, 2007; van Doorn, 2008; Li, W *et al.*, 2019). However, whether leaf senescence is promoted by sugar accumulation or by sugar deficiency remains unresolved (Pourtau *et al.*, 2006; van Doorn, 2008; Horacio & Martinez-Noel, 2013; Zhaowei *et al.*, 2020; Asim *et al.*, 2022). Here, we found that plants with low *StORE1S02* transcript display enhanced sugar accumulation in leaves and delayed leaf yellowing. This suggests that internal sugar

accumulation is not the decisive factor for promoting early leaf senescence. Furthermore, our work provides a new mechanism for *ORESARA1* in inducing senescence, namely that StORE1s activate the expression of downstream sucrose efflux transporters to promote efficient phloem loading by SUC/SUT transporters. As such, we provide new evidence that leaf senescence contributes to tuber formation through nutrient release and rearrangement. Together, we propose that StORE1 transcription factors induce leaf senescence that contributes to tuber formation, especially as a stimulator for tuber bulking, but not as a tuberization inducer.

In potato, *StCDF1* regulates day length dependent tuberization onset by indirectly inducing the expression of *StSP6A* (Kloosterman, B. *et al.*, 2013). StSP6A interacts with StSWEET11 to block sucrose leakage, promoting symplastic transport of sucrose and tuber formation (Abelenda *et al.*, 2019). The fine balance between *StSP6A* and *StSWEET11* in expression level has a great impact on final yield (Abelenda *et al.*, 2019). In this study, we uncovered that StCDF1 represses senescence onset by directly repressing the expression of *StORE1S02*. StORE1S02, as an activator of *StSWEET* genes, bridges the gap between *StCDF1* and *StSWEETs*. Therefore, in the photoperiod dependent tuberization regulation, StCDF1 promotes tuberization onset by keeping the expression balance of *StSP6A* and *StSWEETs* (Fig. 5I).

This study sheds new light on the mechanisms underlying potato development and yield potential, with important implications for potato breeding, particularly hybrid breeding. Our findings highlight the significant impact of *StCDF1* on regulating potato plant development and reproductive progress. To uncover additional genetic loci that regulate development, StCDF1 allelic variation should be considered in future breeding programs and incorporated into population designs.

Materials and Methods

Plant Materials, Growth Conditions, and Sampling

In this experiment two non-transgenic potato lines were used: CE3130 and CE3027, which were offspring plants from the diploid C x E population (Celis-Gamboa, 2002; Ramírez Gonzales *et al.*, 2021). All plants were propagated in tissue culture by cutting.

The sequences of *StCDF1.2* ^{Coed} was synthesized by Genscript and cloned. Then it was cloned into the pENTR™/D-TOPO vector (Invitrogen™; K240020) and then PK7GW2 by LR reaction (Invitrogen™; 11791020). The destination vector was transformed into the late tuberizing and senescence background potato CE3027 by Agrobacterium-mediated gene transformation (Visser *et al.*, 1989)

To knockdown all *StORE1s*, a 174bp fragment targeted to all three *StORE1* genes was generated by using VIGS tool (https://vigs.solgenomics.net/). The fragment was cloned into pK7GWIWG2(II) to obtain the intron-spliced hairpin RNA(RNAi) construct and introduced into CE3130 (early senescence genotype) plants by Agrobacterium tumefaciens-mediated transformation. The full length *StORE1S02* gene was cloned from CE3027 then insert into the pK7GW2 vector. The plant transformation was done in the same process to CE3027 background.

Tissue culture plants (two week old) were transferred into 19cm diameter pot filled with soil and grown in a controlled-environment chamber at LD condition (16h of light and 8h of dark, 22°C during the daytime and 18°C during the night-time). The plants were regularly watered and received fertilizer as needed. The pots were sorted into lines of 5. At least 10-20cm distance was left in between lines to avoid shading.

Leaf samples for RNA isolation, chlorophyll isolation and sugar analysis were harvested from the mid part of source leaves (fully expanded leaves, normally the 3-4th branch of leaves from the bottom, 1-2 cm up from leaf tip) and then frozen in liquid N_2, powdered, and stored at −80°C.

RNA isolation and quantitative PCR

To quantify expression level of relative genes, RNA was isolated from fully expanded leaves using the MagMAX™ Plant RNA Isolation Kit (A33899) with the KingFisher™ Flex Purification System (5400610). 1µg of total RNA was reverse transcribed in 20 µl mixture with the iScript cDNA Synthesis Kit (Bio-Rad). The cDNA was diluted to a volume of 200 µl with Milli-Q Water. Aliquots (2 µl) were then used as templates for subsequent real-time PCR experiments. *StELF3e* was used as a house keeping control (Kloosterman, B. *et al.*, 2013; Ramírez Gonzales *et al.*, 2021), and primers of relative genes are listed in Supplemental Table S2. The gene expressions were calculated using the delta CT method, normalized against StELF3e expression.

Sugar content analysis

80 mg of leaf power sample was taken to which 500 µl of MilliQ water was added. The samples were then incubated at 80°C for 20 min at 500 rpm. The tubes were centrifuged for 5 min at

10 000 rpm and the supernatant was kept. 500 µl of MiliQ water was again added to the pellet and the steps were repeated 5 more times. To measure the sugar content, the Sucrose Assay Kit (Sigma-Aldrich; SCA20-1KT) was used. The absorbance was measured at 570 nm with TECAN infinite m plex plate reader.

Phylogenetic Analysis

All sequences for phylogenetic analysis were retrieved from Spud DB potato genomic resource (http://spuddb.uga.edu/), The Arabidopsis Information Resource (TAIR, https://www.arabidopsis.org/) and Solanaceae Genomics Network (https://solgenomics.net/)(Table.S3). The CDS were aligned by MUSCLE in the DNASTAR Lasergene software. The phylogenetic tree was made in the software using the default settings.

Chlorophyll extraction and analysis

In figure 3E, the total chlorophyll content was measured following the Lightenthaler (1987) protocol. First, the plant tissue was frozen, grinded, and weighed. Then, it was solubilized in 1 ml of 95% ethanol and heated at 80°C for 20 min. The solution was centrifuged for 5 min at 5000 rpm and the pellet was extracted. This step was repeated two more times with 1 ml ethanol 95 %, and the amount of fresh biomass was calculated. All the supernatants were finally collected to constitute the extract. 200 µl of the extract was diluted in 1800 µl of 95% ethanol and measured at 648.6 and 664.2 nm using a spectrophotometer. Chlorophyll a and b were calculated using the following formulae (Guzzo *et al.*, 2021):

Chlorophyll a = 13.36*(absorbance at 664.2 nm) – 5.19*(absorbance at 648.6 nm) Chlorophyll b = 27.43*(absorbance at 648.6 nm) – 8.12*(absorbance at 664.2 nm).

Chlorophyll measurement by Chlorophyll Meter

The chlorophyll content was measured using the Apogee MC-100 Chlorophyll Meter (https://www.apogeeinstruments.com/chlorophyll-meter-support/), following the manufacturer's guidelines and utilizing the generic settings. The sampling was done with the mid part of source leaves (fully expanded leaves, normally the 3-4th branch of leaves from the bottom, 1-2 cm up from leaf tip).

Chlorophyll fluorescence measurement

The parameters of chlorophyll fluorescence were measured by LI-600 porometer/fluorometer (https://www.licor.com/env/products/LI-600) at ZT3, following the manufacturer's guidelines. The sampling of leaf tissue was performed the same as in the chlorophyll measurement.

Transient dual-luciferase reporter system

The putative promoter regions for *StORE1S02* was amplified from CE3027 using primers designed based on the DM1-3-56-R44 v4.04 genome sequence, as specified in Table S2. The *StORE1S02* promoter region was designed 4 kb upstream the transcription start site which included the sequence bound by StCDF1 obtained from the DAP-Seq analysis (Fig. 1B). The

The PCR amplification products of the promoters was cloned into GATEWAY cloning vector pDONR221 and later inserted into pGWB435-iLUC destination by LR Clonase reaction (Invitrogen).
These reporter constructs were transformed in *Agrobacterium tumefaciens* strain (AGL1) and co-infiltrated into *Nicotiana benthamiana* (rdr6i) leaves with 35S::*StCDF1.1* (full length) constructs. Agrobacterium strains resuspended in MMAi buffer (10 mM MES (pH 5.8), 10 mM MgSO4 and 150 µM acetosyringone). A final concentration of 0.2 OD600 for all constructs was used for infiltration. Two days' post-infiltration leaf discs were incubated in 2MS plant medium supplemented with 0.02 mg/mL D-luciferin (Promega). Luciferase activity was recorded every 30 mins in Centro LB-960 microplate luminometer (Berthold technologies), using Mikrowin 2000 (version 4.29) software.

Acknowledgements

This research is funded by Solynta and Aardevo. L.S. is supported by China Scholarship Council (No. 201807720077). We acknowledge the Wageningen University & Research, Unifarm greenhouse and Klima employees for their help with the maintenance of the plants. We also thank Dirk-Jan Huigen for expert assistance in the glasshouse and growth-room trials.

Author Contributions

LS and CB designed the research. LS and LDB performed a large part of the experiments and analysed data. MAH carried out the Transient assay. LS drafted the manuscript. LS, CB, MDV, SUM and SP revised the manuscript. RGFV helped with overall supervision and critically edited the article. All authors read and approved the final manuscript.

Data Availability

All relevant data are available from the corresponding authors upon request. There are no restrictions on data availability.

Supplementary Material

Figure S1. DNA and protein sequences alignments of *StCDF1.2* and *StCDF1.2* ^{Coed} . The sequences of *StCDF1.2* are retrieved from Solanaceae Genomics Resource (http://spuddb.uga.edu/). The *StCDF1.2* ^{Coed} is synthesised by GenScript (https://www.genscript.com).The multiple-alignment was done using Multiple sequence alignment by Florence Corpet (http://multalin.toulouse.inra.fr/multalin/).

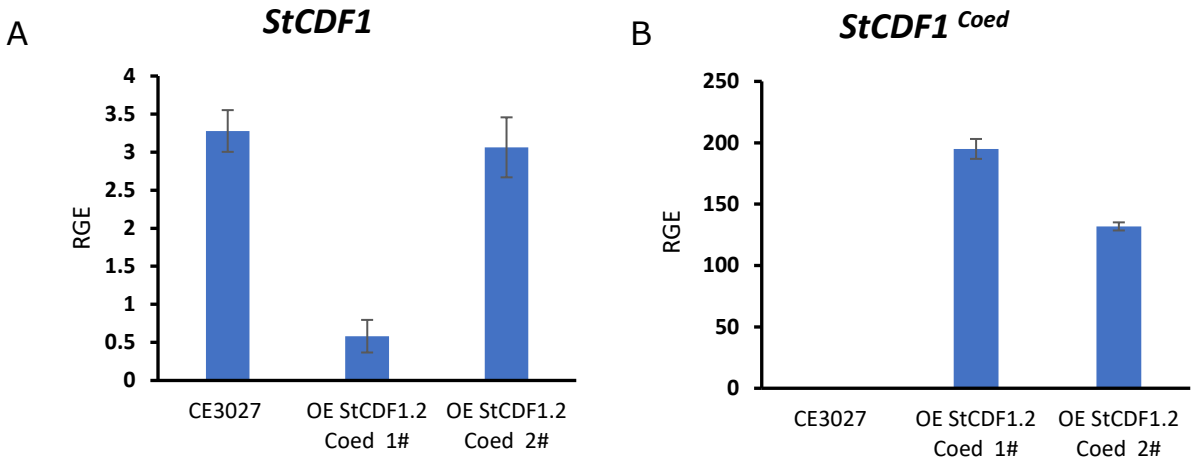

Figure S2. Characterization of transgenic potato plants overexpressing *StCDF1.2 Coed*. A&B. The relative expression of *StCDF1* and *StCDF1.2Coed* in in four-week-old long day (LD) grown CE3027, OE *StCDF1.2 Coed* 1# and OE *StCDF1.2 Coed* 2# at ZT 9. Error bars: means ± SE, with n = 3 biological replicates.

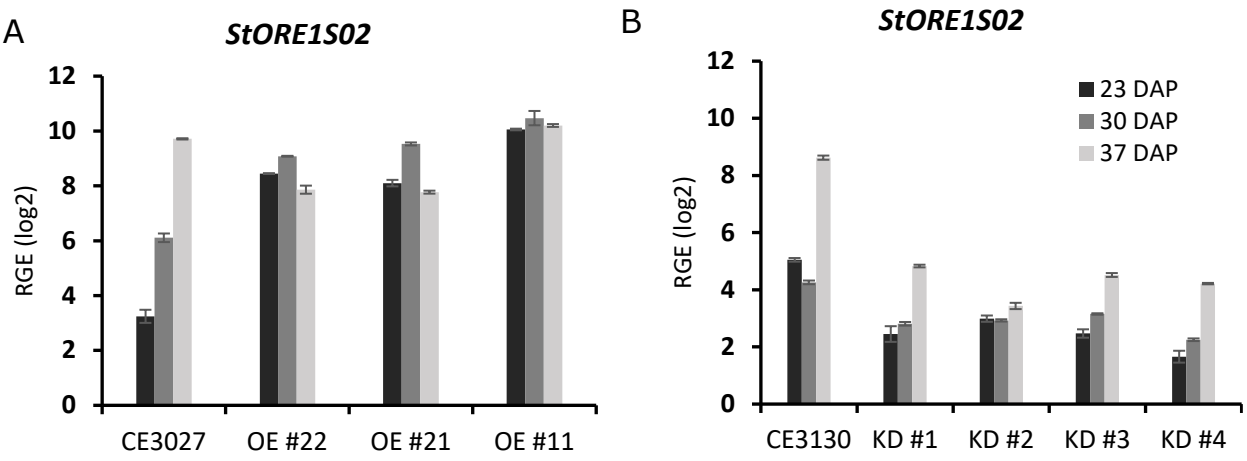

Figure S3. Log scale of the relative expression of *StORE1S02* for the first three weeks of sample harvesting. A, Expression levels of *StORE1S02* for CE3027 and OE lines. The values gradually increase with time for CE3027 plants, in all OE lines the values stay consistently high. **B**, The graph represents the values for CE3130 and all the *StORE1s* knocked down lines. Expression levels of *StORE1S02* generally increase with time for all the lines and stay significantly lower for KD lines compared to their background, CE3130.

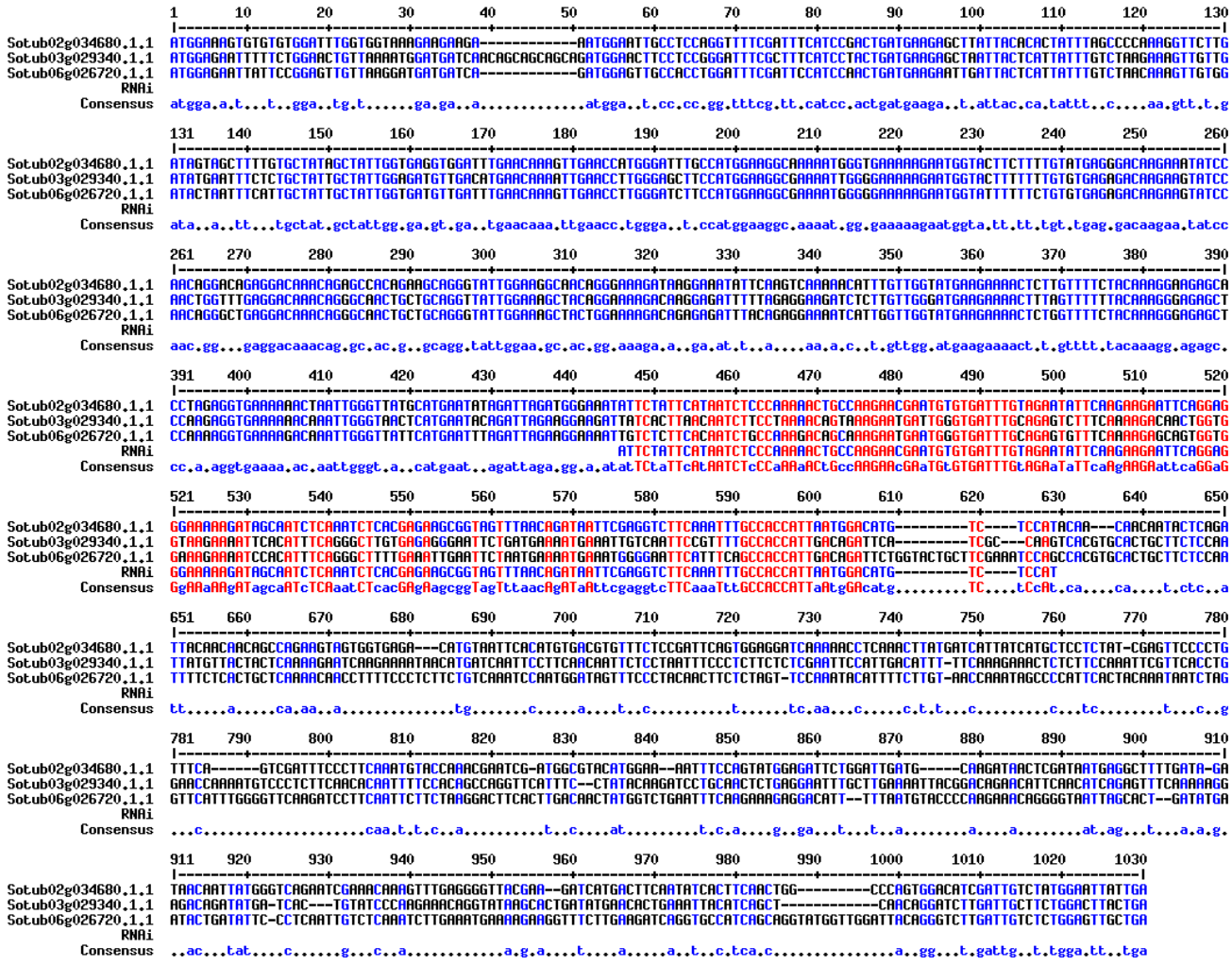

Figure S4. Alignments of *StORE1* genes and the RNAi targeting region.
The sequences of *StORE1* are retrieved from Solanaceae Genomics Resource (http://spuddb.uga.edu/). The multiple-alignment was done using Multiple sequence alignment by Florence Corpet (http://multalin.toulouse.inra.fr/multalin/). The RNAi targeting region was designed by using SGN VIGS Tool (https://vigs.solgenomics.net/).

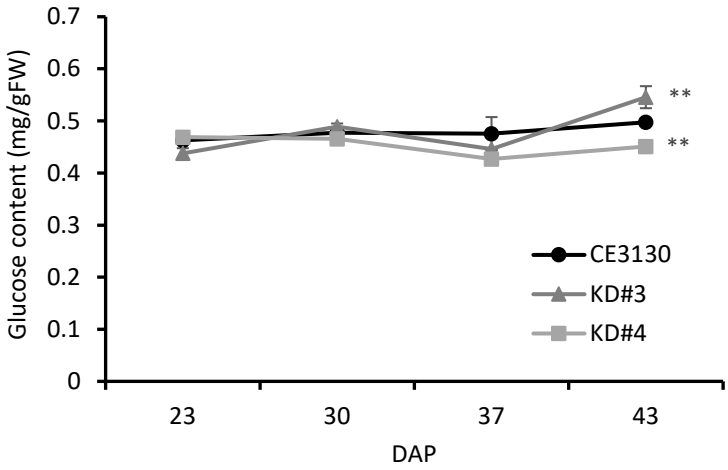

Figure S5. Glucose content in leaves of CE3130 and StORE1S02 knockdown lines in CE3130 background (KD #3 and KD #4). The same samples used in Figure 4C were used in this experiment. 4 different time points (23,30,37 and 43 day after plant, DAP) are included.

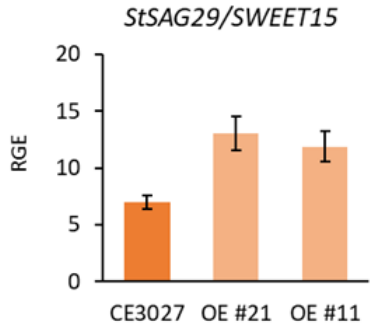

Figure S6. Relative expression of the *StSAG29/SWEET15* in the same samples as in (Fig 2D).

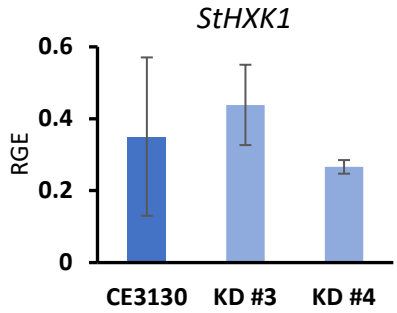

Figure S7. Relative expression of the *StHXK1* in the same samples as in CE3130 and *StORE1S02* knockdown lines in CE3130 background (KD #3 and KD #4) at 37 DAP

Table S1. Statistical analysis for Fig1 E.

Sig	CE3027 vs OE StCDF1.2 Coed 1#	CE0327 vs OE StCDF1.2 Coed 2#	CE0327 vs CE3130
zt0	**	**	**
zt3	**	**	**
zt6	**	**	**
zt9	**	**	
zt12	**	**	**
zt15	**	**	**
zt18	**	**	
zt21	**	*	

Table S2. Specific primer pairs for qRT-PCR reaction.

Name	primer sequence	Discrption	Gene ID
qStORE1SO6 F	ATGTACCCCAAGAAACAGGGG	qpcr	Soltu.DM.06G025800.1
qStORE1SO6 R	ACCATACCTGCTGATGGCAC		
qStORE1SO3 F	ACCTGGAACCAAAATGTCCCT	qpcr	Soltu.DM.03G029980.1
qStORE1SO3 R	GCAATCAAGATCCTGTTGAGCTG		
qStORE1SO2 F	CGAATCGATGGCGTACATGG	qpcr	Soltu.DM.02G031550.1
qStORE1SO2 R	TGGGCCAGTTGAAGTGATATTGA		
qStELF-F	GGAGCACAGGAGAAGATGAGGAG	qpcr	Soltu.DM.10G027530.1
qStELF-R	CGTTGGTGAATGCGGCAGTAGG		
qStBFN1 F	CATGGAGCAAAGAGGGGCAT	qpcr	Soltu.DM.02G018270.1
qStBFN1 R	CACACACAGAGGGCCGATAA		
qStSAG29 F	TAGCTCCAGTGCCAGCATTC	qpcr	Soltu.DM.05G012430.1
qStSAG29 R	AAACACCCACTGCTACGGTT		
qStSWEET11 F	GTGATGCATGTGCATGTTTG	qpcr	Soltu.DM.03G019570.1□
qStSWEET11 R	CAACGGCCAATCTCCTCTAA		
qStCDF1.2^{Coed} F	GAGGCTGCTCATGGTAT	qpcr	
qStCDF1.2^{Coed} R	AGCTGGCATCCTTCTTTCAGA		
qStCDF1 F	CGAAGAATGCCTGCAATCGG	qpcr	Soltu.DM.05G005140
qStCDF1 R	CCAGTACGGTGTTGCTGGAT		
qStHXK1 F	TGCTGCTGTAGTATGTGGGG	qpcr	Soltu.DM.12G025470
qStHXK1 R	GGATTCGCCTCTGTGGACTG		
StORE1SO2 RNAi F	CACCATTCATAATCTCCCAAAAACTGCCA	Cloning	Soltu.DM.02G031550.1
StORE1SO2 RNAi R	ATGGAGACATGTCCATTAATGGTGG	Cloning	
StORE1SO2 35s F	CACCATGGAAAGTGTGTGTGGATTTGG	Cloning	Soltu.DM.02G031550.1
StORE1SO2 35s R	TCAATAATTCCATAGACAATCGATGTCC	Cloning	
StORE1SO2 prR	ggggaccactttgtacaagaaagctgggtgCTGTGGCTCTGTTTG	Cloning	
StORE1SO2 prF	ggggacaagtttgtacaaaaaagcaggctggGAAAGGCACCAATA	Cloning	
StCDF1.2Coed F	CACCATGAGTGAAGTGAGAGAT	Cloning	
StCDF1.2^{Coed} R	TCACTCCTGATACCTTGTCACCA		

Table S3. ORE1 homologues in 13 plant species.

Species name	Gene name	Gene ID	Source of the gene ID
Arabidopsis thaliana	AtORE1	AT5G39610.1	https://www.arabidopsis.org/
Solanum tuberosum	StORE1S02	Soltu.DM.02G031550.1	http://spuddb.uga.edu/index.shtml https://solgenomics.net/tools/blast
	StORE1S03	Soltu.DM.03G029980.1	
	StORE1S06	Soltu.DM.06G025800.1	
Solanum lycopersicum	SlORE1S02	Solyc02g088180.2	https://solgenomics.net/tools/blast
	SlORE1S03	Solyc03g115850.2	
	SlORE1S06	Solyc06g069710.2	
Capsicum annuum	CaORE1S02	CA02g28070	https://solgenomics.net/tools/blast
	CaORE1S03	CA12g13470	
	CaORE1S06	CA06g18770	
Solanum melongena	SmeORE1S02	Sme2.5_00161.1_g00008.1	https://solgenomics.net/tools/blast
	SmeORE1S03	Sme2.5_00136.1_g00021.1	
	SmeORE1S06	Sme2.5_00298.1_g00016.1	
Lactuca sativa	LsatORE1	Lsat_1_v5_gn_4_109600.1	https://lgr.genomecenter.ucdavis.edu/
Oryza sativa	OsORE1	LOC_Os04g38720.1	http://rice.uga.edu/
Hordeum vulgare	BarORE1	BART1_0-u12809.010	https://ics.hutton.ac.uk/barleyrtd/index.html
Triticum aestivum	TaORE1.1	TaORE1.1 MN747242.1	https://academic.oup.com/plphys/article/180/3/1740/6117747#supplementay-data
	TaORE1.2	TaORE1.1 CM022216.1	
	TaORE1.3	TaORE1.3 CM022214.1	
Brassica oleraceae	BolORE1	BolC04g044910.2J	http://brassicadb.cn/
Brassica rapa	BraORE1	BraA07g020590.3.5C	http://brassicadb.cn/
Brassica juncea	BjuORE1	BjuVA04G12730	http://brassicadb.cn/
Raphanus sativus	RsaORE1	Rsa10035257	http://brassicadb.cn/

Chapter 3

Hot Potatoes and Cool Genes: Uncovering the Mechanisms of StCDF1 in Heat Tolerance and ABA Production

Li Shi[1,2], Wendi Zhao[1], Maroof Ahmed Shaikh[3], Wouter Kohlen[4], Michiel E. de Vries[5], Sybille Ursula Mittmann[6], Salome Prat[3], Richard G.F. Visser[1] and Christian W.B. Bachem[1]

[1]Plant Breeding, Wageningen University & Research, 6708PB, Wageningen, The Netherlands.
[2]Gradute School Experimental Plant Sciences, Wageningen University & Research, 6708PB, Wageningen, The Netherlands
[3]Center for Research in Agriculture Genomics (CRAG), Barcelona, 08193, Spain.
[4] Horticulture and Product Physiology Group, Wageningen University and Research, P.O. Box 16 6700AA, Wageningen, the Netherlands.
[5] Solynta, Dreijenlaan 2, 6703 HA, Wageningen. The Netherlands.
[6] Aardevo B.V. Johannes Postweg 8, 8308 PB, Nagele, The Netherlands.

Abstract

Potato tuberization, a crucial developmental process, is greatly influenced by various environmental factors. The growth of potato tubers is significantly impacted by temperature, and tuberization can be suppressed by high temperatures, making it a major environmental factor to consider. In this study, two individuals of a potato population with different StCDF1 allele combinations, as well as two transgenic lines overexpressing *StCDF1* were grown under normal and high temperature conditions. Results showed that *StCDF1* promotes heat tolerance and promotes tuberization under different temperatures. Specifically, plants overexpressing *StCDF1* or expressing a truncated *StCDF1* allele showed less premature leaf senescence and gained 16-47% yield increase by exposing to higher temperatures. Moreover, high transpiration associated with low endogenous levels of ABA was found in *StCDF1* overexpressing transgenic plants and plants carrying a truncated allele under both conditions. This study provides insight into the mechanisms of potato heat tolerance and suggests a potential target for improving potato yield under adverse temperature conditions.

Introduction

Potato is one of the most important non grain food crops in the word (FAO, 2019). The origin of the potato lies in the Andes of South America, which has a relatively cool climate and thus characterizes the potato crop as a relatively cool climate crop (Spooner *et al.*, 2005; Lehretz *et al.*, 2019). The susceptibility of potato to elevated temperatures has been reported in several studies (Ewing, 1981; Hijmans, 2003; Struik, 2007; Park *et al.*, 2022). High temperature, typically above 25°C, stimulates shoot growth, while negatively affects many aspects of potato plant physiology, including carbon synthesis and tuberization signalling. Eventually these negative impacts lead to yield losses (Ewing, 1981; Timlin *et al.*, 2006; Struik, 2007; Dahal *et al.*, 2019). Due to a rise in temperature in most potato growing regions due to climate change, yield losses due to heat stress will become more prominent.

Recently, an interesting study of 50 potato varieties tested under heat revealed that early maturing cultivars are usually less affected by heat than late cultivars (Zhang, G *et al.*, 2020). Moreover, several previous studies in different years and regions demonstrated the same correlation (Marinus & Bodlaender, 1975; Khedher & Ewing, 1985; Levy, 1986). In potato breeding programs, maturity has long been recognized as an important genetically controlled trait. Phenotyping maturity provides an estimation for proper harvest time and impact on yield (Wallace *et al.*, 1993; Prat, 2006). Previous studies have found a major locus for foliage maturity on chromosome 5, by using quantitative trait locus mapping (Visker *et al.*, 2003; Kloosterman, B. *et al.*, 2013; Li, J *et al.*, 2019). Later, this locus was identified as *CYCLING DOF FACTOR1* (*StCDF1*), which has a decisive influence on foliage maturity and daylength dependent tuberization (Kloosterman, B. *et al.*, 2013). Allelic variation at the 3′ end of the *StCDF1* gene can result in truncated allelic variants (*StCDF1.2* and *StCDF1.3*). The protein produced by the wild type *StCDF1* (*StCDF1.1*) is destabilized by binding to StGIGANTEA (StGI) and FLAVIN-BINDING KELCH REPEAT F-BOX PROTEIN 1 (StFKF1) in the afternoon under long-day conditions (Kloosterman, B. *et al.*, 2013; Hoopes, GM *et al.*, 2022). However, StCDF1.2 and StCDF1.3 protein levels remain constant throughout the day as they are unaffected by this post-translational degradation (Kloosterman, B. *et al.*, 2013). Under long day conditions, the plants that carry the *StCDF1* mutant alleles (*StCDF1.2* or *StCDF1.3*) display an early maturing and early tuberizing phenotype (Kloosterman, B. *et al.*, 2013). Recently we showed that *StCDF1* has a long non-coding counterpart, called *StFLORE* thought to act as a natural antisense transcript (Ramírez Gonzales *et al.* (2021). Both transcripts function in regulating drought stress responses by affecting stomatal density, size and diurnal movement (Ramírez Gonzales *et al.*, 2021). Although the *StCDF1* locus has been implicated in controlling maturity and regulating responses to drought, its involvement in other abiotic stresses such as heat stress remains to be determined.

StCDF1 plays an important role in regulating photoperiod-dependent tuberization by indirectly promoting expression of a homolog of *FLOWERING LOCUS T* (*FT*) in potato, namely *SELF-PRUNING 6A* (*StSP6A*) (Navarro *et al.*, 2011; Abelenda *et al.*, 2014). StSP6A, as a mobile signal, is produced in the leaves and then transported to the stolons to initiate tuber formation (Navarro *et al.*, 2011), while at the same time repressing flower development (Plantenga *et al.*, 2019a). The photoperiod-dependent expression of *StSP6A* is controlled by another *FT*

homolog, called *SELF-PRUNING 5G* (*StSP5G*). *StSP5G* negatively regulates the expression of *StSP6A* after activation by CONSTANS-LIKE 1 (StCOL1) (Abelenda *et al.*, 2016), whose expression is determined by the length of the dark period (Plantenga *et al.*, 2019b). Previous studies show that StCDF1 directly binds to the promotor of *StCOLs* and represses the expression of all *StCOLs* (Kloosterman, B. *et al.*, 2013; Ramírez Gonzales *et al.*, 2021). Therefore, StCDF1 indirectly activates the expression of *StSP6A* to promote tuberization by repressing expression of *StCOLs* and *StSP5G*.

The expression of *StSP6A* is not only under the regulation of photoperiod, but also of environmental temperature (Hancock *et al.*, 2014; Hannapel *et al.*, 2017; Lehretz *et al.*, 2021). Many studies have reported that high temperature negatively affects the expression of *StSP6A*. Moreover, this reduction correlates with delayed tuberization and yield loss (Lehretz *et al.*, 2019; Park *et al.*, 2022). Recently, Lehretz *et al.* (2019) uncovered a novel negative post-transcriptional regulator of *StSP6A*, a microRNA (miRNA) named *SUPPRESSING EXPRESSION OF SP6A* (*StSES*) (Lehretz *et al.*, 2019; Park *et al.*, 2022). Interestingly, the expression of *StSES* is stimulated by elevated temperatures (Lehretz *et al.*, 2019; Park *et al.*, 2022). Tuberization can be achieved by overexpressing a special variant of *StSP6A*, which is codon edited to prevent post-transcriptional regulation, whereas this cannot be achieved by simply overexpressing the unmodified StSP6A gene (Lehretz *et al.*, 2019; Park *et al.*, 2022). These studies uncovered a post-transcriptional regulation of StSP6A at elevated temperature. However, how elevated temperature influences the photoperiod regulation of *StSP6A* remains unclear.

Abscisic acid (ABA) is a crucial phytohormone that regulates plant development and response to abiotic stress factors such as drought and heat (Suzuki *et al.*, 2016). ABA-deficient mutant *Arabidopsis* plants have reduced heat tolerance, and this phenotype can be rescued by exogenous addition of ABA (Larkindale & Knight, 2002). However, a study in rice suggests applying exogenous ABA on different rice genotypes leads to an opposite response to heat stress (Li *et al.*, 2020). These studies show that both ABA biosynthetic and signaling pathways are involved in heat stress response. A member of the CDF family in *Arabidopsis*, namely CDF4, controls the expression of ABA biosynthesis genes *NCED2* and *NCED3* (9-cis-epoxycarotenoid dioxygenase 2, 3), leading to increased production of ABA (Xu *et al.*, 2020). Recently, Gonzales (2022) reported that *StNCED3*, which encodes a key enzyme in the final step of ABA biosynthesis, is one of the direct downstream targets of StCDF1. This result indicates that StCDF1 may play a role in regulating abiotic stress response by influencing ABA biosynthesis.

In plants, the *CDF* family of proteins plays a role in various developmental processes, including flowering time regulation, light response, secondary metabolism, response to nitrate and root growth (Kloosterman, B. *et al.*, 2013; Corrales *et al.*, 2017; Goralogia, G. S. *et al.*, 2017). In this study, we show that *StCDF1* regulates plant response to high temperature. Our analysis revealed that *StCDF1* is a positive regulator for both plant maturity and heat tolerance. Constitutive overexpression of *StCDF1.2* in a heat-sensitive, late-maturing genotype, rescues its heat-sensitive phenotype and improved its yield after heat treatment. Moreover, we show that *StCDF1* negatively affects ABA biosynthesis by repressing the expression of several key

enzymes, such as *β-carotene hydroxylase* (*StBCH*), *9-cis-epoxycarotenoid dioxygenase 3* (*StNCED3*) and *9-cis-epoxycarotenoid dioxygenase 4* (*StNCED4*). This study sheds new light on the role of *StCDF1* in regulating abiotic stress by impacting endogenous ABA levels.

Results

StCDF1 promotes a heat tolerant phenotype

To study the effect of *StCDF1* regulation under moderate heat and the effects on downstream genes, we used an early diploid genotype (CE3130; *StCDF1.2/1.3*, Supplemental Table S1) and a contrasting late diploid genotype (CE3027; *StCDF1.1/1.1*, Supplemental Table S1). To eliminate post-transcriptional regulation on StCDF1 by ubiquitination or cis-NAT regulation by *StFLORE* (Ramírez Gonzales *et al.*, 2021), we over expressed a synthetic codon edited *StCDF1.2* variant that we called *StCDF1.2* ^{Coed} using the 35S CaMV promoter in the CE3027 background. In this study, two transgenic lines (OE *StCDF1.2* ^{Coed} 1#& 2#) resulting from two independent transgenic events of the same construct were sampled and tested separately, the data were considered as a single set for statistical analysis. All the plants were propagated by tissue culture, 2-week old tissue culture plantlets were transferred to soil in pots. In the first four weeks, all plants were grown under control conditions (22 °C light, 18°C dark) under long days (LD; 16h light:8h dark). From 35 days after planting (DAP), half of the plants were exposed to heat (Heat; 30 °C light: 28°C dark) with LD light conditions for 14 days. Then, plants were moved back to control conditions for 5 more weeks until most of the plants had completed their life cycle (Fig. 1A). In this experiment, Zeitgeber Time (ZT) is used to indicate the light period. ZT is a timekeeping system that is based on the timing of environmental cues, such as the light-dark cycle. ZT0 represents the time when the light period begins, and each subsequent hour is represented by the next sequential number (e.g., ZT1 represents one hour after the start of the light period).

Interestingly, the CE3027 plants lost most of their lower source leaves during the heat treatment (Fig.1B). Overexpressing *StCDF1.2* ^{Coed} in CE3027 or carrying a truncated *StCDF1* allele (*StCDF1.2/1.3*) like CE3130 prevented premature leaf senescence caused by exposure to heat. In addition, the early maturing genotypes (OE *StCDF1.2* ^{Coed} transgenic lines and CE3130) showed repressed development phenotypes due to heat exposure, such as suppressed elongation of stems and decreased canopy size (Fig. 1B). However, these phenotypes were not found in the late maturing genotype (CE3027).

During the heat treatment, the total conductance to water vapor (gtw) (Buckley *et al.*, 1999) and Photosystem II efficiency (PhiPS2) were measured at 3 hours after light start (ZT3; Zeitgeber Time 3) in 3 days and 8 days after exposure to heat. Both CE3027 and CE3130 exhibited increased total conductance under heat treatment in both measurements (Fig.1C & D). However, the heat treatment had no significant impact on the gtw of OE *StCDF1.2* ^{Coed}.. Interestingly, under control conditions, the gtw of OE *StCDF1.2* ^{Coed} and CE3130 were significantly higher than that of CE3027 in both measurements (Fig.1C & D). The PhiPS2 were not altered by high temperature treatment in all lines (Fig.1E & F).

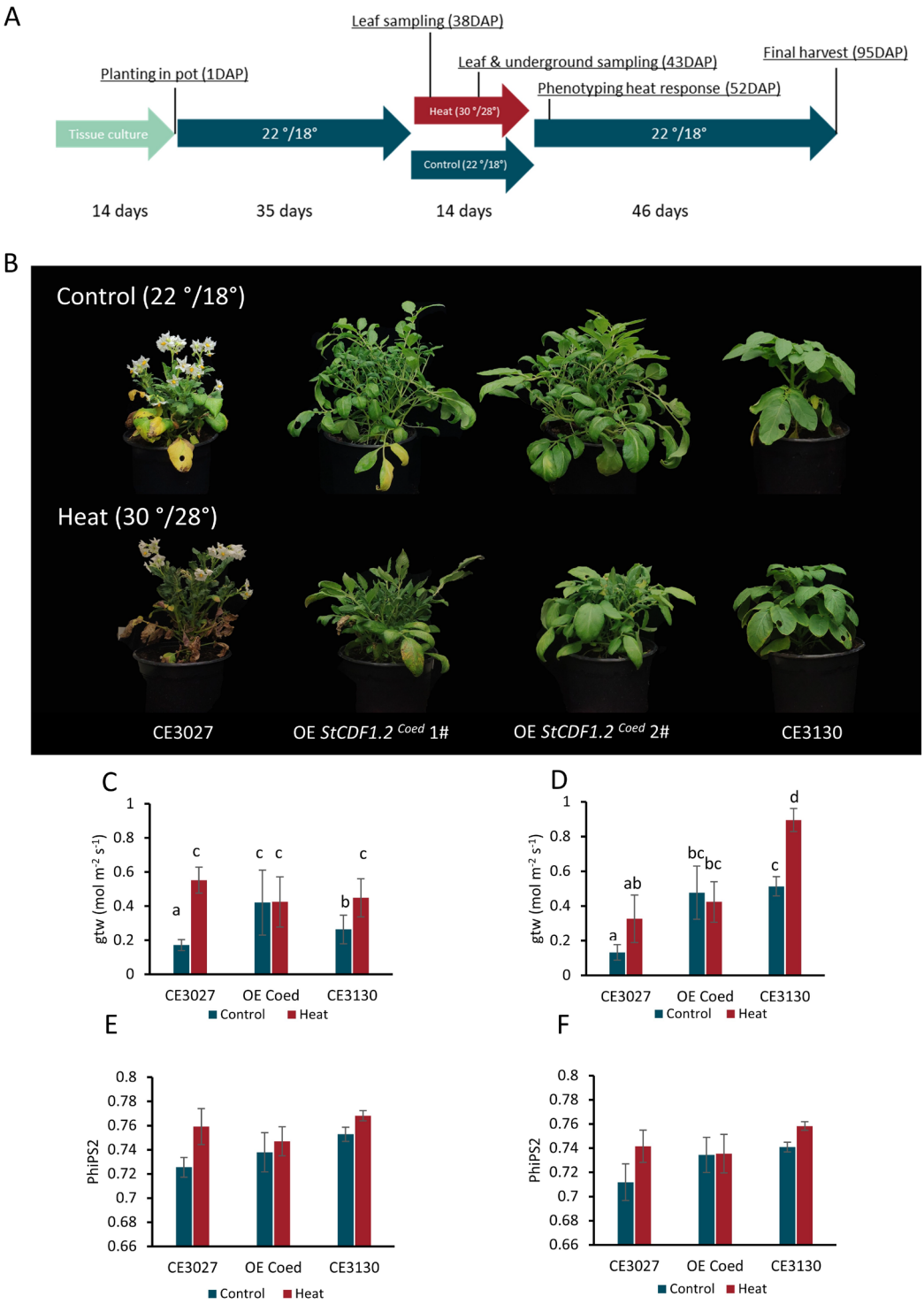

Figure 1. StCDF1 promotes heat tolerant phenotype.
A. Potato plantlets were prepared as follows: 2-week-old tissue culture plantlets were transferred to soil in pots. In the first 35 days after planting (DAP), all plants were grown under control conditions (Control; 22 °C light: 18°C dark) with long days (LD; 16h light:8h dark). From 35 DAP, half of the plants were exposed to heat (Heat; 30 °C light: 28°C dark) with LD light condition for 14 days. Two independent transgenic lines were sampled separately, with the data combined into one for statistical analysis. **B.** Phenotype of CE3027 (late maturing, homozygous for *StCDF1.1*) OE *StCDF1.2* ^{Coed} 1# & 2#, and CE3130 (early maturing, containing both the *StCDF1.2* and *StCDF1.3* allele), at 52 DAP (3 days after the end of heat treatment). **C&D.** Measurement of transpiration using total conductance (gtw). Plants were grown at

different temperatures for 3 (C) and 8 days (D). Error bars: means ± SD, with n = 9 replicates. Letters indicate groups that are statistically significantly different from each other (t-test, *p < 0.05). **E&F.** Measurement of photosynthetic performance using Photosystem II efficiency (PhiPS2). Same sampling as in **C&D**.

StCDF1 regulates tuberization at different temperatures

Previous studies suggested that *StCDF1* positively regulates *StSP6A* expression to induce tuberization (Kloosterman, B. *et al.*, 2013). However, high temperature has a negative impact on the expression of *StSP6A* (Lehretz *et al.*, 2019; Park *et al.*, 2022). To study the function of *StCDF1* in regulating tuberization under high temperature, we tested the expression of key tuberization regulators in CE3130 and OE *StCDF1.2* ^{Coed} transgenic lines and the background of these transgenic lines (CE3027) under different temperatures.

Without heat treatment, we found that CE3130 and OE *StCDF1.2* ^{Coed} transgenic lines displayed reduced expression of *StSP5G* and increased expression of *StSP6A* compared to CE3027 (Fig. 2A & B). These results are consistent with our previous findings (Kloosterman, B. *et al.*, 2013). Under heat treatment, *StSP6A* expression was significantly downregulated in CE3130 and OE *StCDF1.2* ^{Coed} transgenic lines, but vice versa in CE3027 (Fig.2A). Notably, the reduction of *StSP6A* expression in CE3130 and OE *StCDF1.2* ^{Coed} transgenic lines didn't bring the *StSP6A* expression down to the same level of expression as that observed in CE3027. In fact, the early maturing lines (CE3130 and OE *StCDF1.2* ^{Coed} transgenic lines) still had an over 100 fold higher expression of *StSP6A* compared to the late maturing CE3027 under heat treatment.

In addition, we analyzed the expression of *StSP5G* in our plants at different temperatures as it is known as one of the key negative regulators of *StSP6A* (Navarro *et al.*, 2011; Abelenda *et al.*, 2014). The expression of *StSP5G* in CE3130 and OE *StCDF1.2* ^{Coed} transgenic lines was significantly increased by heat treatment, whereas this was not the case in CE3027 (Fig. 2B). Together, we found that heat treatment increased expression of *StSP5G* while decreasing expression of *StSP6A* in early maturing plants.

While *StCDF1* is a well-known regulator for *StSP5G* and *StSP6A* expression, very little is known about the way that *StCDF1* expression is affected by high temperature. To study this, we examined the expression of *StCDF1* and its long non-coding counterpart *StFLORE* under different temperatures. Considering the fact that *StCDF1* is mainly expressed when the light starts (ZT0), we chose ZT0, ZT3 and ZT6 to harvest samples and examine gene expression. Without the heat treatment, the highest expression *of StCDF1* was found in OE *StCDF1.2* ^{Coed} transgenic lines, which confirmed the genotypes were overexpressing *StCDF1.2*, followed by CE3130 and CE3027 (Fig. 2C). A significant decrease in expression of *StCDF1* was found at ZT0 in all lines under heat treatment. Interestingly, heat induced expression of *StFLORE* was observed in all lines at ZT0 (Fig. 2D), and this induction was most pronounced from ZT0 to ZT3 (Supplemental Fig. S1). These results suggest that high temperature has an impact on the expression of genes which are involved in regulating photoperiod-dependent tuberization.

To gain knowledge on how *StCDF1* influences tuberization at different temperatures, two harvests were performed at 43DAP and 95DAP (Fig. 1A). The results indicate that exposing plants to high temperature had no effect on tuber number (Fig. 2E & F), except for a significant difference in CE3130 at 8 days post-heat (Fig. 2E), but this difference was no longer significant after 6 weeks under control conditions (Fig. 2F). A slight decrease in final yield under heat was observed in CE3027 (Fig. 2F). Interestingly, both OE *StCDF1.2*^{Coed} transgenic plants and CE3130 plants exposed to heat showed significantly higher yield by 16-47% compared to the control plants (Fig. 2F). Consistent with the above ground heat tolerance phenotype, tuberization in OE *StCDF1.2*^{Coed} transgenic plants and CE3130 was not negatively affected by exposure to heat.

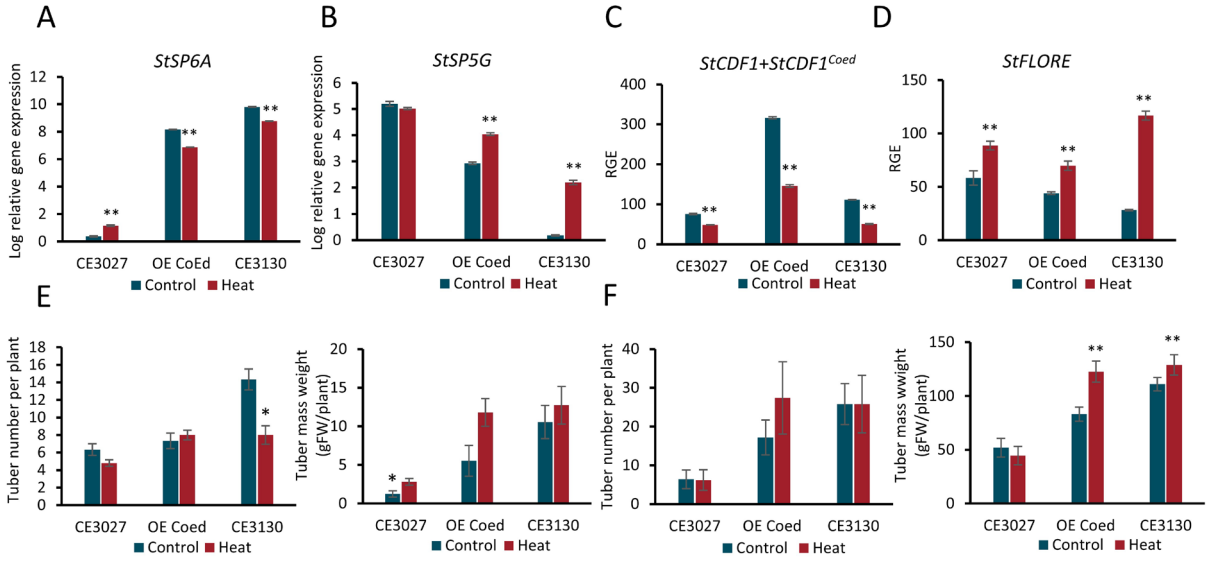

Figure 2. StCDF1 regulates tuberization at different temperatures.
A. Expression of *StSP6A* at different temperatures. Leaf samples were harvested at ZT3, 3 days after heat treatment started (38DAP). Data are presented as the mean ± SE with n = 3 replicates (t test, *P < 0.05, **P < 0.01, compared to control). **B.** Relative expression of *StSP5G* in the same samples as in (**A**). **C.** Relative expression of *StCDF1* (unmodified) and *Codon edited StCDF*1 at different temperatures. Leaf samples were harvested at ZT0, 3 days after heat treatment started. Data are presented as the mean± SE with n = 3 replicates (t test, *P < 0.05, **P < 0.01, compared to control). **D.** Relative expression of *StFLORE* in the same samples as in (**C**). **E.** Measurement of tuber of tuber number and of tuber mass weight at 43DAP. The number of tubers (including very small tubers and or swelling stolons) and tuber mass weight were recorded at 8 days (**F**) after heat treatment started (43DAP). .Error bars: means ± SD, with n = 3 replicates. (t test, *p < 0.05 compared to control). **F.** Measurement of tuber number and of tuber mass weight at final harvest. The final harvest was conducted at 95DAP when almost all of the plants had finished their lifecycle. Error bars: means ± SE, with n = 5 replicates. (t test, *p < 0.05,**p < 0.01 compared with Control).

StCDF1 is involved in regulating ABA biosynthesis by directly repressing the transcription of ABA synthesis related genes

Our data shows that, overexpressing *StCDF1.2* ^{Coed} in a late maturing background (CE3027) or carrying a truncated *StCDF1* allele (CE3130) significantly promoted gtw (Fig.1B & C). The gtw can be divided into stomatal conductance (gsw) and boundary layer conductance (gbw).

By analyzing in more detail, we found the change caused by *StCDF1* mainly happened in stomatal conductance (gsw) (Fig. 3A & B), rather than boundary layer conductance (gbw) (Fig. 3C & D). Stomatal conductance can be affected by diverse causes and ABA has been known as one of the most important regulators for stomatal opening and closure (Yari Kamrani *et al.*, 2022). Moreover, StCDF1 has been reported to directly repress the expression of *StNCED3*, which is a key enzyme in the biosynthesis of ABA (Gonzales, 2022). These results led us to hypothesize that *StCDF1* promotes stomatal opening by repressing ABA biosynthesis.

To understand how *StCDF1* regulates ABA biosynthesis, this study used the direct target genes of *StCDF1*, identified by DAP-seq and RNA-seq (Gonzales, 2022) (Fig. 3E & F). Notably, several ABA biosynthesis related genes are significantly down regulated by overexpressing *StCDF1.2* (Fig. 3E). Moreover, we found *StCDF1* has predicted binding sites on the promoters of 3 specific ABA biosynthesis related genes encoding *β-carotene hydroxylase* (*StBCH-2: PGSC0003DMG400028897*), *9-cis-epoxycarotenoid dioxygenase 3* (*StNCED3-2: PGSC0003DMG400027633*) and 9-*cis-epoxycarotenoid dioxygenase 4* (*StNCED4: PGSC0003DMG400001969*) (Fig. 3F).

To verify the direct regulation between StCDF1 and these ABA biosynthesis related genes, we selected the following ABA biosynthesis related genes based on expression level for analyzing expression: *StBCH-2*, *StZEP*, *StNCED3-2, StNCED4, StABA2-2* and *StABA3*. The diurnal gene expression of these selected genes in OE *StCDF1.2* ^{Coed} transgenic plants and the untransformed control plants (CE3027) was analyzed. The results show that the expression of all these six genes in CE3027 reached the highest level within 6 hours (ZT0-6) after the lights were turned on. Moreover, the level of transcription of these genes is differentially reduced in OE *StCDF1.2* ^{Coed} transgenic plants compared to CE3027, especially in the early daytime (ZT0-6) (Fig. 3G). To further test the transcriptional regulatory link between *StCDF1* and these ABA biosynthesis related genes, a transient assay was performed by co-infiltrating the *35S::StCDF1* construct and *StNCED3* and *StNCED4* promotor constructs driving expression of the firefly luciferase gene into tobacco leaves. The results indicated that StCDF1 directly suppresses the expression of both *StNCED3* and *StNCED4* (Fig. 3H).

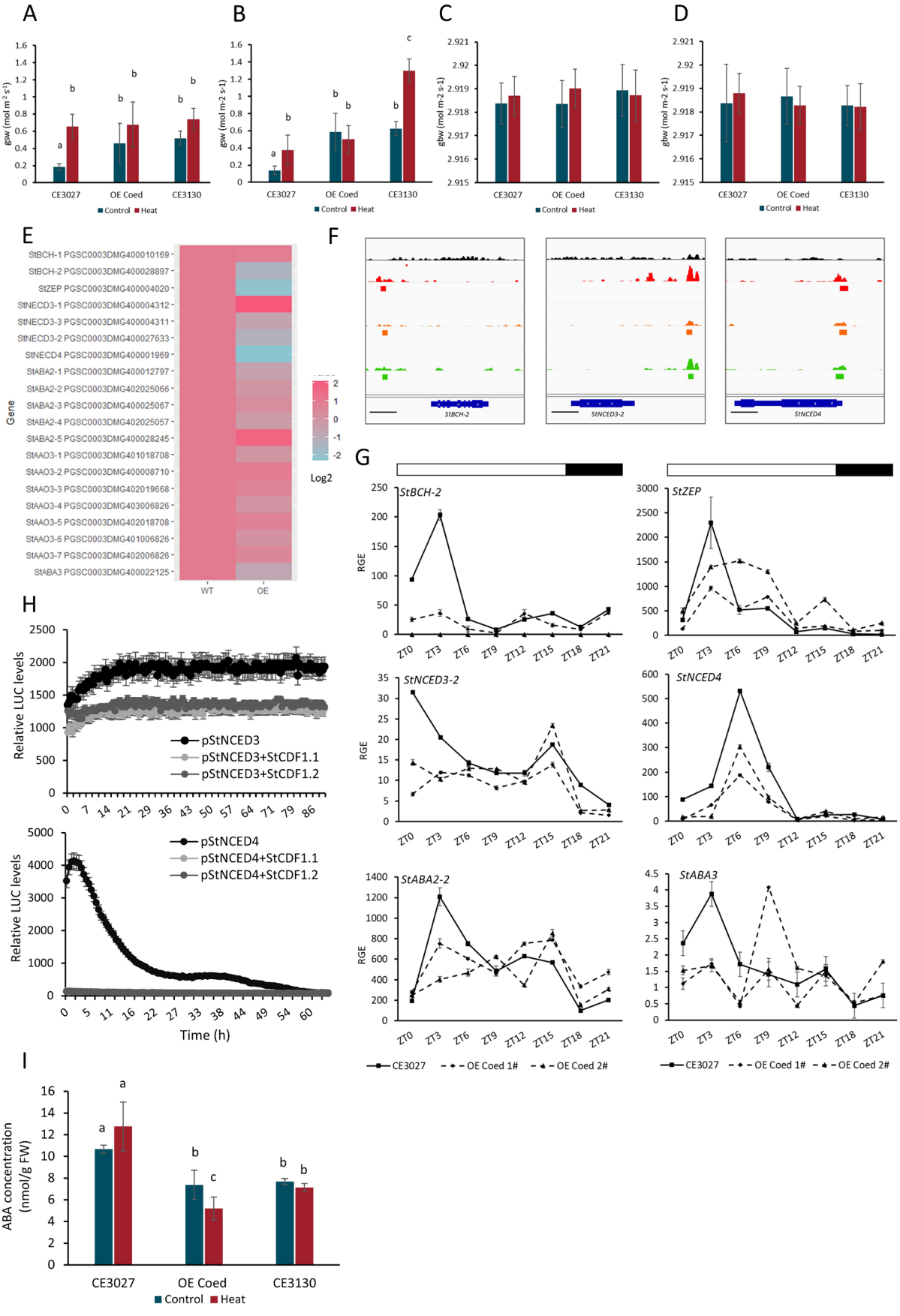
A
B
C
D
gsw (mol m-2 s-1)
gbw (mol m-2 s-1)
CE3027
OE Coed
CE3130
Control
Heat
E
Gene
StBCH-1 PGSC0003DMG400010169
StBCH-2 PGSC0003DMG400028897
StZEP PGSC0003DMG400004020
StNECD3-1 PGSC0003DMG400004312
StNECD3-3 PGSC0003DMG400004311
StNECD3-2 PGSC0003DMG400027633
StNECD4 PGSC0003DMG400001969
StABA2-1 PGSC0003DMG400012797
StABA2-2 PGSC0003DMG402025066
StABA2-3 PGSC0003DMG400025067
StABA2-4 PGSC0003DMG402025057
StABA2-5 PGSC0003DMG400028245
StAAO3-1 PGSC0003DMG401018708
StAAO3-2 PGSC0003DMG400008710
StAAO3-3 PGSC0003DMG402019668
StAAO3-4 PGSC0003DMG403006826
StAAO3-5 PGSC0003DMG402018708
StAAO3-6 PGSC0003DMG401006826
StAAO3-7 PGSC0003DMG402006826
StABA3 PGSC0003DMG400022125
WT
OE
Log2
F
StBCH-2
StNCED3-2
StNCED4
G
StBCH-2
StZEP
StNCED3-2
StNCED4
StABA2-2
StABA3
RGE
ZT0
ZT3
ZT6
ZT9
ZT12
ZT15
ZT18
ZT21
CE3027
OE Coed 1#
OE Coed 2#
H
Relative LUC levels
pStNCED3
pStNCED3+StCDF1.1
pStNCED3+StCDF1.2
pStNCED4
pStNCED4+StCDF1.1
pStNCED4+StCDF1.2
Time (h)
I
ABA concentration (nmol/g FW)
CE3027
OE Coed
CE3130
Control
Heat

Figure 3. StCDF1 is involved in ABA biosynthesis by directly repressing the transcription of ABA synthesis related genes. A&B. Measurement of stomatal conductance (gsw). Plants were grown at different temperatures for 3 (A) and 8 days (B). Error bars: means ± SD, with n = 9 replicates. Letters indicate groups that are statistically significantly different from each other (t-test, $p < 0.05$). **C&D.** Measurement of boundary layer conductance (gbw). Same sampling as in A&B. **E.** Expression of the candidate genes for the ABA biosynthesis related genes (Gonzales, 2022). Genes were selected based on annotation. Fold changes in gene expression were visualized using a heatmap. The color scale represents $\log_2$ fold changes. WT: CE3027, OE: overexpressing *StCDF1.2* in CE3027. **F.** DAP-Seq binding peaks of StCDF1 in the promoter region of *StBCH-2*, *StNCED3-2*, *StNCED4*. Diagram description from the top: input library as negative control (black bar chart), experiment 1 (red bar chart), experiment 2 (orange bar chart), experiment 3 (green bar chart). The significant binding sites are shown below the bar chart of each experiment. Gene models are represented in blue. In the right bottom corner, the scale represents 1 kb. **G.** Gene expression analysis of CE3027 wild type and transgenic plants carrying the *StCDF1.2* overexpression construct (*35S*::*StCDF1.2 Coed*). Expression of selected ABA biosynthesis related genes, mRNA levels were measured in long-day control conditions. Leaf samples were harvest at 32 DAP. ZT: Zeitgeber time. Error bars: mean ± SE with n = 3 replicates. **H.** Repression of p*StNCED3*::*iLUC* and p*StNCED4*::*iLUC* luciferase activity by 35S::*StCDF1.1 and* 35S::*StCDF1.2* in *N. benthamiana* leaves. Relative luminescence levels were measured at intervals of 0.5 h for 2-3 days. Error bars represent the standard error of 24 biological replicates. **I.** Measurement of free ABA levels. Error bars: means ± SE, with n = 3 replicates. Letters indicate groups that are statistically significantly different from each other (t-test, *$p < 0.05$).

Furthermore, we isolated and measured the ABA concentration within the same leaf samples we used for RNA isolation, which were harvested at ZT3 (38DAP). Exposure to heat resulted in a slight but non-significant increase in the endogenous levels of ABA in CE3027 plants. Moreover, it was observed that the ABA concentration in CE3130 and OE *StCDF1.2* ^{Coed} transgenic plants experienced significant decreases ranging from 10% to 41% compared to CE3027, under both conditions (Fig. 3I). The expression of ABA biosynthesis related genes was also altered by exposure to heat (Supplemental Fig. S2). Of the selected genes related to ABA biosynthesis, only *StNCED3* expression showed continuous repression under heat conditions in CE3130 and OE *StCDF1.2* ^{Coed} transgenic plants, compared to CE3027 (Supplemental Fig. S2B). Together, we conclude that *StCDF1* plays a critical role in regulating endogenous levels of ABA under different temperature conditions and its repression of *StNCED3* is the most constant repression across different temperatures. This regulation may ultimately lead to improved plant performance under heat stress and increased yield.

Discussion

In this study, we investigated the effect of *StCDF1*, a central regulator of daylength-dependent potato tuberization, on heat stress response. Our results uncovered a novel connection between two pathways: photoperiod-dependent tuberization and heat stress response.

CDF family members have been known to be involved in regulating different aspects of plant growth and development like photoperiodic flowering/tuberizing-time control or root and shoot growth in different plant species. In the last decade, several studies have suggested the genes

of this family are also involved in regulating abiotic stress (Renau-Morata *et al.*, 2020). In *Arabidopsis*, the expression of all 5 *CDF* members can be altered by different abiotic stresses (Renau-Morata *et al.*, 2020). Moreover, both *AtCDF3* and *SlCDF3* have been reported to play a positive role in response to different abiotic stresses, such as drought, low temperature, osmotic stress and salt tolerance (Corrales *et al.*, 2017; Renau-Morata *et al.*, 2017).

In *Arabidopsis*, only the quadruple mutant (*cdf1*, *cdf2*, *cdf3*, and *cdf5*) shows a substantial change in flowering timing (Fornara *et al.*, 2009). In potatoes however, the suppression of *StCDF1* alone leads to a significant delay in the onset of tuberization (Ramírez Gonzales *et al.*, 2021), suggesting *StCDF1* is the major regulator of tuberization regulation among all *StCDF* members. Our previous work has shown that *StCDF1* has a negative effect on potato drought tolerance, resulting in increased water loss during stress conditions (Ramírez Gonzales *et al.*, 2021). We found here that *StCDF1* has the opposite role in regulating heat stress response compared to drought stress response. Our data revealed that overexpressing *StCDF1* in the heat stress sensitive background (CE3027) restored the phenotype to heat tolerant and produced more yield than the heat-sensitive background under both heat and control conditions. Therefore, our study provides definitive evidence to demonstrate that *StCDF1* positively influences potato heat tolerance.

In this study, we tested the expression of genes which are involved in photoperiod-dependent tuberization regulation under different temperatures. Our results agree with previous studies that *StSP6A* expression is decreased under high temperatures (Fig. 2A). However, this reduction was only found in the early maturing genotypes (OE *StCDF1.2* ^{Coed} transgenic plants and CE3130). In a previous study, it was observed that high temperature did not alter the expression of *StSP5G*, the repressor of *StSP6A*, leading to the conclusion that the temperature-dependent regulatory mechanisms of tuberization are distinct from those related to photoperiod (Park *et al.*, 2022). However, we found here an increase in *StSP5G* expression in early maturing genotypes under heat treatment, which was associated with a decrease in *StSP6A* expression (Fig. 2A & B). These different observations may result from the different leaf sample harvesting time. Based on previous data, Zeitgeber Time 3 (ZT3) was selected for sampling in this experiment, as it is the time that *StSP5G* reaches the highest expression under long day conditions (Fig. S3). Any changes caused by external factors, like high temperature, were expected to be most visible at this time point, making it an ideal choice for analysis. On the other hand, the different high temperature treatments could also contribute to this difference in expression pattern of *StSP5G*. For instance, in this study, *StSP5G* expression was analyzed after subjecting the plants to a high temperature treatment of 30/28°C. In another experiment where no change in *StSP5G* expression was observed, the plants were exposed to an even higher temperature treatment of 35/29°C (Park *et al.*, 2022). Furthermore, the expression of further upstream regulators of *StSP6A* in the photoperiod pathway, like *StCDF1* and *StFLORE*, are also influenced by exposure to high temperature. Altogether, our data suggests that high temperature influences the expression of several genes in the photoperiod-dependent tuberization pathway.

In many potato farming regions, drought and heat waves often coincide and both stresses can significantly impact the final yield. Interestingly, we found that *StCDF1* plays a different role in

response to these two stresses. *StCDF1* was found to have a negative impact on drought tolerance by affecting stomatal density, size and diurnal opening, leading to increased water loss (Ramírez Gonzales *et al.*, 2021). In this study, we provide supporting evidence that overexpressing *StCDF1* leads to increased transpiration under control conditions (Fig. 1C & D). Notably, transpiration in plants provides the necessary components for photosynthesis, such as carbon dioxide and water, by regulating transpiration pull (von Caemmerer & Baker, 2007). It is reasonable to postulate that high transpiration promoted by *StCDF1* may contribute to promoting carbon fixation and eventually leads to promoting better yield under non-stress conditions.

A previous study suggests that *StCDF1* promotes early tuberization under long day condition through indirectly promoting the expression of the tuberigen, *StSP6A* (Kloosterman, B. *et al.*, 2013). Moreover, *StCDF1* was found to regulate the expression balance between *StSP6A* and *StSWEETs*, which is important for nutrient release and rearrangement at the tuber formation stage **(chapter 2)**. Here we find that *StCDF1* also promotes transpiration, which likely contributes to improving photosynthesis and carbohydrate synthesis. Together, these findings suggest that *StCDF1* plays a critical role in inducing early tuberization by coordinating several critical steps.

In response to high temperatures, plants often exhibit increased transpiration. We found here that all genotypes showed increased transpiration when exposed to high temperature, except the OE *StCDF1.2* ^{Coed} transgenic plants (Fig. 1C & D). This increase in transpiration is considered a cooling strategy for leaves, and previous research has shown that enhancing leaf cooling through increased transpiration can improve heat tolerance in several crops (Zandalinas *et al.*, 2016; Deva *et al.*, 2020; Rajametov *et al.*, 2021). Under heat conditions, the transpiration of CE3027 increased to the same level as in the OE *StCDF1.2* ^{Coed} transgenic plants. However, CE3027 still lost most of its lower source leaves during the heat treatment and can be regarded as heat susceptible (Fig. 1B). It is likely that *StCDF1* affects heat tolerance through pathways other than just transpiration. Campbell *et al.* (2023) recently identified a candidate gene, *HEAT SHOCK COGNATE 70* (*StHsc70*), which regulates potato heat tolerance by protecting PSII against photooxidative damage induced by environmental stress. To investigate whether StCDF1 also regulates heat tolerance by modulating *StHsc70* expression, we examined the expression of *StHsc70* in transgenic and wild-type plants under both heat and control conditions (Fig. S4). Our results indicate that StCDF1 is unlikely to be involved in the same pathway as StHsc70 in regulating heat tolerance. However, combining both heat tolerance alleles of *StCDF1* and *StHsc70* may further improve potato's heat tolerance.

Plant transpiration is largely regulated by the opening and closing of stomata. *StCDF1* has been speculated to regulate stomatal movement (Ramírez Gonzales *et al.*, 2021), but the exact mechanism remains unknown. In this study, we discovered that *StCDF1* represses the biosynthesis of abscisic acid (ABA), which is a key phytohormone for regulating the opening and closing of stomata. This reduced endogenous ABA level correlates with the high transpiration in OE *StCDF1.2* ^{Coed} transgenic plants and CE3130. StCDF1 has been known to be one of the most important circadian regulators (Kloosterman, B. *et al.*, 2013). Our findings

suggest that *StCDF1* may play an important role in regulating circadian control of ABA biosynthesis and stomatal movement, especially in the morning time (ZT0-ZT6).

ABA has always been considered one of the most important plant hormones for abiotic stress responses. However, whether ABA promotes or represses heat tolerance is not clear. Current research suggests that the effect of ABA on regulating heat stress response varies among different plant species and even among different genotypes within a single species (Zandalinas *et al.*, 2016; Li *et al.*, 2020; Li, Ning *et al.*, 2021; Zhu *et al.*, 2022). In this study, we found that the reduced endogenous ABA level is associated with enhanced heat tolerance in early maturing genotypes, like OE *StCDF1.2* ^{Coed} transgenic plants and CE3130. Further research is necessary to fully understand the link between ABA and heat tolerance.

Interestingly, *AtCDF4* has been shown to promote ABA biosynthesis by activating the expression of the same key ABA biosynthesis genes that are repressed by *StCDF1*, including *NCED3* (Xu *et al.*, 2020). The activation function was found to be independent from the dof DNA binding domain (Xu *et al.*, 2020). Recently, Gonzales (2022) reported that *StCDF1* could also function as an activator. However, our 24h time course results only show the repressing effect of *StCDF1* on genes involved in regulating ABA biosynthesis. To understand the intriguing difference between *StCDF1* and *AtCDF4* in function, more research is required in the future.

Previous studies have established StCDF1 as a regulator of several processes, including maturity, yield, drought stress response, and biotic resistance. This study has expanded on this understanding by highlighting StCDF1's role in regulating heat tolerance and ABA biosynthesis, demonstrating its capacity to serve as a central hub that coordinates various pathways. Consequently, investigating this locus can significantly enhance our comprehension of how plants balance different pathways. In breeding programs, markers used to distinguish between early and late alleles of StCDF1 could also be employed to predict heat tolerance. Additionally, because of the distinct mechanism of StCDF1 in regulating heat response, it could be combined with other known loci to further improve heat tolerance, particularly in hybrid breeding programs.

Materials and Methods

Plant materials, growth conditions, sampling and phenotyping

For this experiment, we used two non-transgenic potato plants, CE3130 and CE3027, which are progeny of the diploid C x E population (Celis-Gamboa, 2002; Ramírez Gonzales *et al.*, 2021)**.** The Condon edited *StCDF1.2* was synthesized by Genscript and cloned into into the pENTR™/D-TOPO vector (Invitrogen™; K240020) and then PK7GW2 by LR reaction (Invitrogen™; 11791020). Then, performed Agrobacterium-mediated gene transformation to introduce the destination vector into the late-tuberizing and senescence background potato, CE3027. Two transgenic lines (OE *StCDF1.2* ^{Coed} 1#& 2#) from independent transformation even were used in this study.

The plants were propagated in tissue culture with Murashige and Skoog medium 20 (MS20) by cutting (Murashige & Skoog, 1962). Two weeks after subculture, *in vitro* plantlets were

transferred to 19 cm pots containing compost and grown in a climate chamber, under control conditions of 16 h light (22 °C) and 8 h dark (18 °C)(LD, long day condition). After growing for 4 weeks, half of the plants were transferred to the second climate chamber, which provided a different temperature treatment, 30° C/28 °C LD and were watered daily. The heat treatment was continued for 14 days. Then, all plants were grown under control conditions for another 6 weeks (95DAP) until most of the plants had finished their life cycle (Fig. 1A).

On the third day of heat treatment, source leaves were harvested for RNA isolation and ABA content analysis. The leaf samples were quickly frozen in liquid nitrogen, ground into powder, and stored at -80°C for preservation. Eight days into the heat treatment, three plants from each genotype were harvested to observe the underground developmental phenotype. At 3 and 8 days after heat treatment started, the parameters of leaf photosynthesis were measured by LI-600 porometer/ fluorometer (https://www.licor.com/env/products/LI-600) at ZT3. The final harvest was done at 95DAP, the tuber number and weight were recorded (Fig. 1A).

RNA isolation and quantitative PCR

The RNA was isolated using MagMAX™ Plant RNA Isolation Kit (A33899) with the KingFisher™ Flex Purification System (5400610). The cDNA synthesis was done as described previously (Ramírez Gonzales *et al.*, 2021). *StELF3e* was used as a house keeping control, and primers for qPCR are listed in Supplemental Table 2.

Determination of endogenous ABA concentration

Leaf samples were collected at 3 days after heat treatment started (43DAP) and immediately frozen in liquid nitrogen. Frozen leaves were ground, and ABA was extracted as described previously (Gühl *et al.*, 2021; Larsen *et al.*, 2023). Briefly, the samples were weighed at 20 ± 2 mg in 2mL Eppendorf tube. After adding 1 mL of methanol and briefly vortexing, the samples were incubated at 4°C overnight with gentle shaking. The following day, the samples were centrifuged for 10 minutes at 13000 rpm, and the supernatant was transferred to a 4.5mL brown glass vial. All supernatant-containing vials were placed in a speed vacuum system (SPD121P, ThermoSavant, Hastings, UK) for 1 hour to evaporate. 1mL of formic acid (40mL 98% FA + 960ML pure H2O) was added to the pellets and briefly vortexed. Next, an Oasis MCX 1CC extraction cartridge was placed on a solid phase extraction manifold pre-washed with 1mL of absolute methanol. Each sample was then pipetted into the cartridge and run through, followed by a wash with 1mL of formic acid. The collection tube was placed underneath the cartridge, and the sample was eluted with 1mL methanol. Quantification of ABA levels was performed using Thermo Scientific GC-MS systems with 3 replicates (each 20 ± 2 mg of frozen tissue) as described elsewhere (López-Ráez *et al.*, 2010; Gühl *et al.*, 2021).

Chlorophyll fluorescence and respiration measurement

The parameters of chlorophyll fluorescence and transpiration were measured by LI-600 porometer/fluorometer (https://www.licor.com/env/products/LI-600) at ZT3, following the manufacturer's guidelines. The sampling of leaf tissue was performed the on the source leaves.

Transient dual-luciferase reporter system

The putative promoter regions of *StNCED3-2* and *StNCED4* were amplified from CE3027 by using primers using primers designed based on the DM1-3-56-R44 v4.04 genome sequence, as specified in Table S2. The regions 4 kb and 2 kb upstream of the transcription start sites of *StNCED3-2* and *StNCED4* respectively were cloned out, which included the putative binding sites of StCDF1, as obtained from the DAP-Seq analysis (Fig. 3F). The cloning processes, Agrobacterium infiltration and luciferase activity screening followed the same steps as described in **Chapter 2**.

Acknowledgements

This research is supported by Solynta and Aardevo. L.S. is supported by China Scholarship Council (No. 201807720077). We acknowledge the Wageningen University & Research, Unifarm greenhouse and Klima employees for their help with the maintenance of the plants.

Author Contributions

LS and CB designed the research. LS and WZ performed a large part of the experiments and analysed data. MAH carried out the Transient assay. WK provided the equipment and protocol for hormone isolation and analysis. LS drafted the manuscript. LS, CB, MDV, SUM and SP revised the manuscript. RGFV helped with overall supervision and critically edited the article. All authors read and approved the final manuscript.

Data Availability

All relevant data are available from the corresponding authors upon request. There are no restrictions on data availability

Supplementary Material

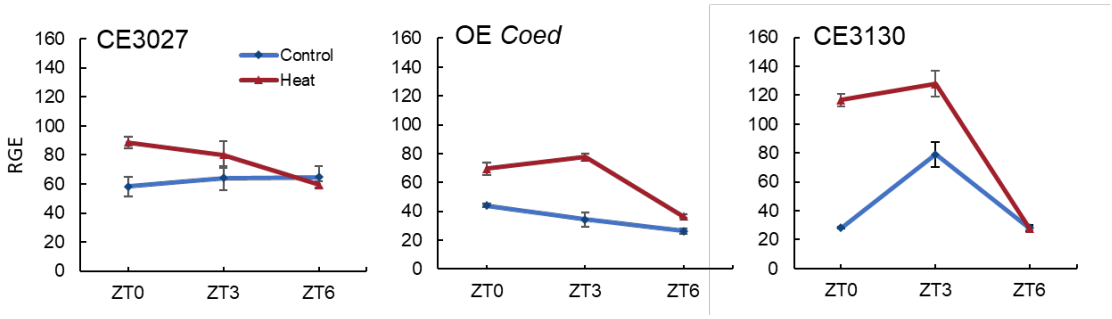

Figure S1. Expression of *StFLORE* under control and heat conditions.
Plants were grown as described in Figure 1. ZT0,ZT3 and ZT6 were selected for harvesting leaves. Error bars: means ± SE, with n = 3 biological replicates.

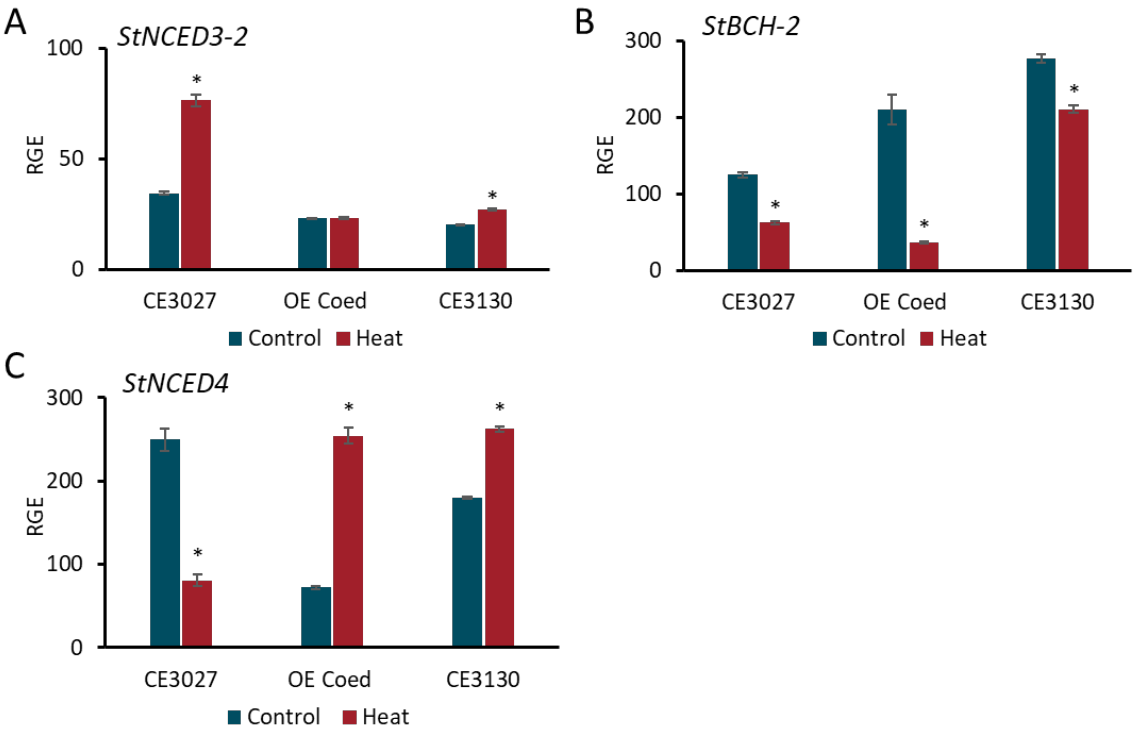

Figure S2. Expression of ABA biosynthesis related genes under control and heat conditions. A-C. Same sampling as in **Figure2 A-D**. Error bars: means ± SE, with n = 3 biological replicates.

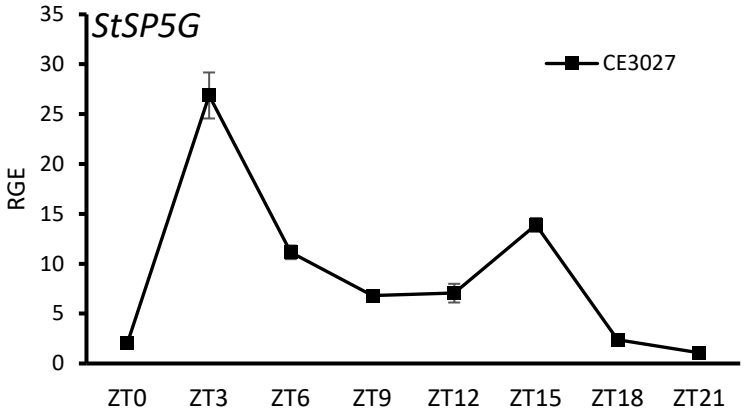

Figure S3. Time course expression of the *StSP5G* under LD condition.
Same sampling as in Figure 3G. Error bars: means ± SE, with n = 3 biological replicates.

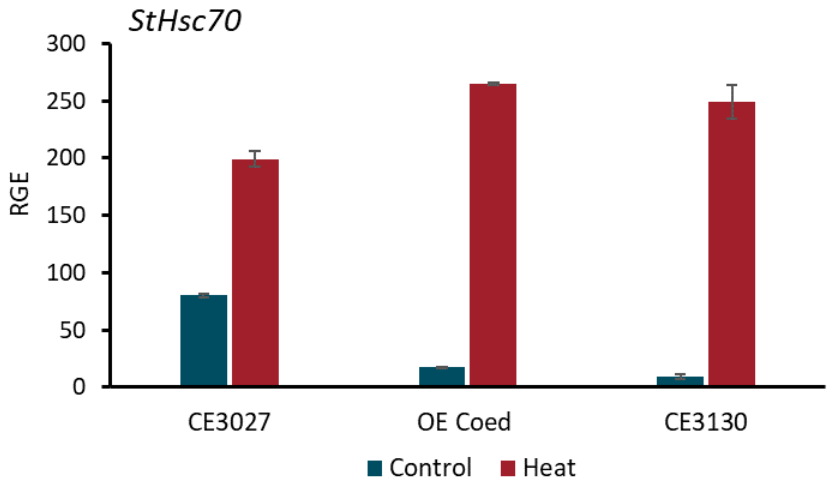

Figure S4. Expression of StHsc70 under control and heat conditions. Same sampling as in Figure2 A-D. Error bars: means ± SE, with n = 3 biological replicates.

Table S1. Plants used in the experiment with description.

Line	GMO	StCDF1 alleles (background)	Ploidy	Tuberization
CE3027	No	1.1/1.1	Diploid	Late tuberization
CE3130	No	1.2/1.3	Diploid	Early tuberization
OE *StCDF1.2* ^{Coed} 1#	Yes	1.1/1.1	Diploid	Early tuberization
OE *StCDF1.2* ^{Coed} 2#	yes	1.1/1.1	Diploid	Early tuberization

Table S2. Specific primer pairs in this experiment.

Primer name	Sequence (5'--->3')	Gene identifier
StELF_F	GGAGCACAGGAGAAGATGAGGAG	Sotub10g021590.1.1
StELF_R	CGTTGGTGAATGCGGCAGTAGG	
StBCH-2_F	GCACGAGTCACACCACAAAC	Soltu.DM.06G013450.1
StBCH-2_R	CAGGTCCAACCGGGAATCTC	
StNECD3-2_F	TGAATGTGATGAAGGACTAAAAGCG	Soltu.DM.07G022620.1
StNECD3-2_R	GCCATGGTTCAGCAATAGCC	
StNECD4_F	ACTTTTCGCCCTCGGTGAAT	Soltu.DM.08G020370.1
StNECD4_R	AAGCCTCGTTAGTTTCGGGG	
StHSc70_F	GGAACACCACGATTCCGACT	Soltu.DM.04G007430.1
StHSc70_R	CTGGAGGAATGCCAGTGAGT	
StFLORE_F	TGCAGACTCGTCGATTGAAC	
StFLORE_R	GAGTGCCTTTTCCTCACTCG	
StCDF1_F	CGAAGAATGCCTGCAATCGG	Soltu.DM.05G005140.1
StCDF1_R	CCAGTACGGTGTTGCTGGAT	
StSP5G_F	GGTGTGTAGACTTTGGTGTGGTTT	Soltu.DM.05G024030.1
StSP5G_R	GGCCTCAAGGCACATCCAT	
StSP6A_F	GACGATCTTCGCAACTTTTACA	Soltu.DM.05G026370.1
StSP6A_R	CCTCAAGTTAGGGTCGCTTG	
qStZEP F	ACATGGCACCTGGGTTACAG	Soltu.DM.02G028820.1
qStZEP R	TGCTCAATGTCTGATGTTTGC	
qStABA2-2 F	GGAGAGAGCATTGTACGCTGT	Soltu.DM.04G027720.1
qStABA2-2 R	AACACGCGCTCTCTTCATCA	
qStABA3 F	GCAGAAACAGTTGCGTAGATGG	Soltu.DM.07G028460.2
qStABA3 R	GGGGCTTTCTGATTCACCCA	
qStCDF1.2Coed F	GAGGCTGCTGCTCATGGTAT	
qStCDF1.2Coed R	AGCTGGCATCCTTCTTTCAGA	
pNCED4 F	ggggacaagtttgtacaaaaaagcaggctggATTGTTTTCTTATACTTTACGCCATC	
pNCED4 R	ggggaccactttgtacaagaaagctgggtgATAGGTTTTCTTGAGGGTATTGGTTC	
pNCED3 F	ggggacaagtttgtacaaaaaagcaggctggTGGTAGTGCAAATTTTATGTTATGTC	
pNCED3 R	ggggaccactttgtacaagaaagctgggtgTTTGTAGCATGTGAAGTAGTAGTGGC	

Chapter 4

Transient TurboID-Based Proximity Labelling for identification of Protein-Protein Interaction Networks in *Solanum tuberosum*

Li Shi[1,2,#], Tatiana Marti Ferrando[1,2,#], Sergio Landeo Villanueva[2,3], Matthieu Joosten[3], Vivianne Vleeshouwers [1,#,*], and Christian W.B. Bachem [1,#,*]

[1]Plant Breeding, Wageningen University & Research, 6708PB, Wageningen, The Netherlands.
[2]Gradute School Experimental Plant Sciences, Wageningen University & Research, 6708PB, Wageningen, The Netherlands.
[3]Laboratory of Phytopathology, Wageningen University & Research, 6708PB, Wageningen, The Netherlands.
[#]Equal-contribution
*Correspondence: vivianne.vleeshouwers@wur.nl & christian.bachem@wur.nl

Summary

Protein-protein interactions (PPIs) in crop plants remain largely unexplored. Here, we provide a protocol for identifying PPIs in potato (*Solanum tuberosum*) using TurboID-mediated Proximity Labelling (PL). We evaluated the use of the nucleus-located transcription factor CYCLING DOF FACTOR1 (StCDF1) of potato, and the plasma membrane-localized receptor-like kinase SOBIR1 (NbSOBIR1) of *Nicotiana benthamiana* fused to TurboID. The constructs were transiently expressed as baits in potato leaves to identify PPIs. We describe the plant material that was used, agroinfiltration, biotin treatment, protein isolation, free biotin removal, and enrichment of biotinylated proteins. This study provides a protocol for applying PL in potato for the analysis of protein complexes involved in plant development and disease resistance.

Graphical abstract

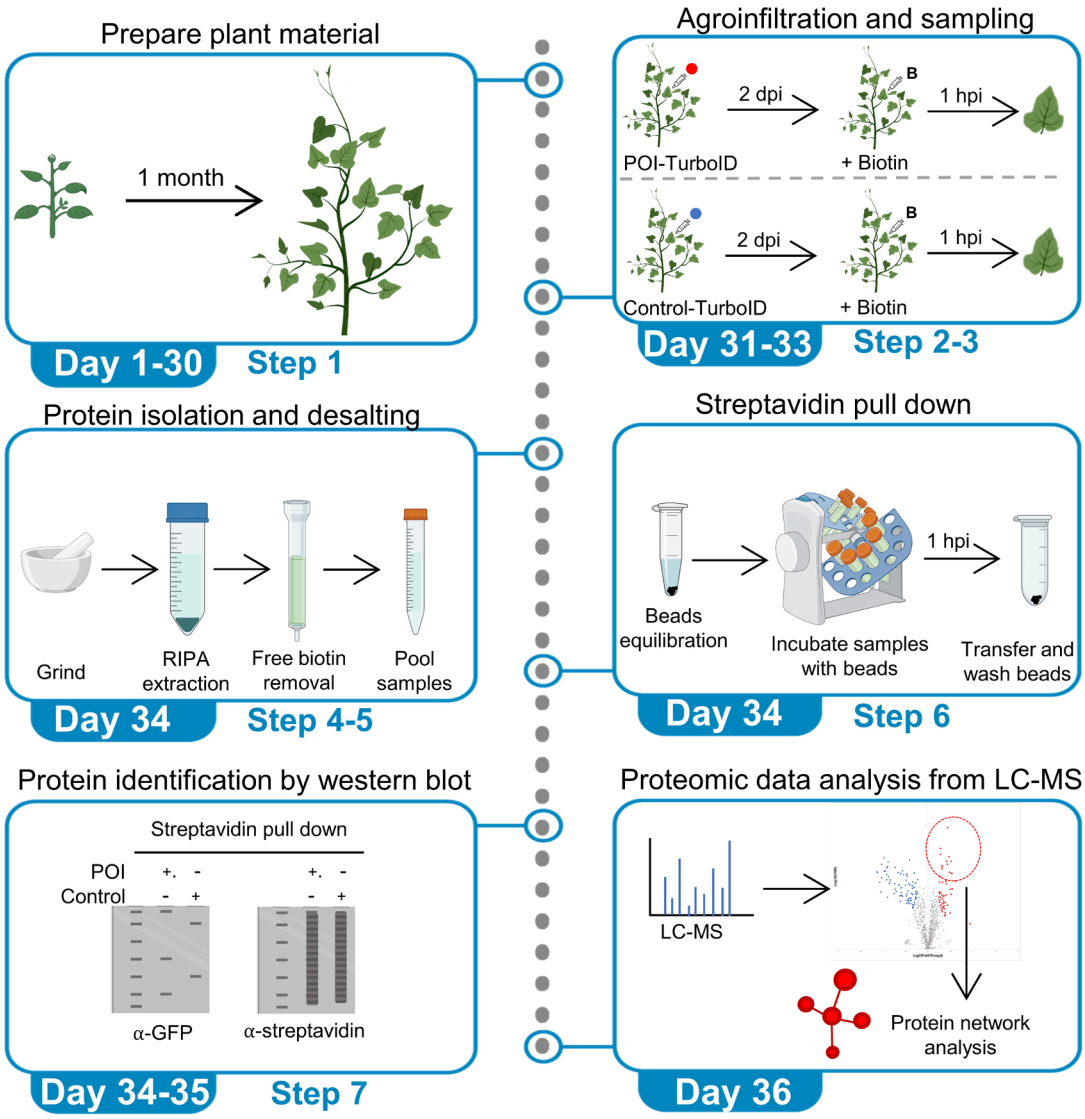

Before you begin

Experimental design considerations

Selection of genotypes*:* This protocol describes the procedure for transient TurboID-based proximity labelling of the transcription factor StCDF1 in CE3027 and the receptor-like kinase NbSOBIR1 in MCD-321. CE3027 is an offspring plant of the diploid C x E population and it was selected to study the role of StCDF1 in tuberization in previous research (Kloosterman, B. *et al.*, 2013; Ramirez Gonzales *et al.*, 2021). MCD-321 is an offspring plant of a cross between the wild potato plants *Solanum microdontum* subsp*. microdontum* and an F1 clone from a *S. microdontum* subsp*. gigantophyllum* x *S. verrucosum* cross (Lin *et al.*, 2022)*. S. microdontum* is a source of resistance against the oomycete pathogen *Phytophthora infestans (van den Berg & Spooner, 1992; Domazakis et al., 2018; Meade et al., 2020). SOBIR1 is widely conserved across species and a common co-receptor of receptor-like proteins involved in immunity (Liebrand et al., 2014; van der Burgh et al., 2019).*

Selection of experimental controls: Design the control TurboID-construct based on the localization of your protein bait of interest. The proteins used in this study are localized either in the nucleus (StCDF1) or in the plasma membrane (NbSOBIR1). As a control, the fusion protein YFP-YFP-TurboID (Kim *et al.*, 2019; Kim *et al.*, 2023) was used. The YFP-YFP-TurboID located at both nucleus and cytoplasm, which has been previously reported by Kim *et al.* (2019).

Experimental test: Before starting the procedure of the potato PL-mass spectrometry (MS) protocol, we recommend testing the TurboID fusion constructs by transient expression in *N. benthamiana*, as it is an easy plant model to work with. Once it has been verified that the TurboID fusion constructs is able to biotinylate proximal proteins in the leaves of *N. benthamiana*, we suggest testing them by transient expression in the potato genotype of interest. Additionally, we suggest to co-express the labelled bait with a known interactor to confirm that this interactor is being biotinylated. The selected interactor protein should also be tagged with a different label than the bait protein, to allow its specific detection on western blots. In potato, it is advisable to infiltrate biotin and to collect leaf samples at different time points (e.g. at 1, 3 and 6 hours post biotin infiltration (hpi)), as well as including a sample without biotin treatment. Both *N. benthamiana* and potato tests can be performed with 2 g of leaf tissue following the same steps as for MS sample preparation. Check *test option* in protocol steps 13-43. Per test sample, only one PD10 column for desalting and 50 µL of streptavidin bead suspension is needed. After the last wash of beads with Radioimmunoprecipitation assay (RIPA) buffer (step 29), proteins are eluted with 80 µL 4x Laemmli Sample Buffer® (Bio-Rad) diluted in RIPA and checked on western blot with the appropriate antibodies (steps 32-43).

Identification of biotinylated proteins: After the pull down with streptavidin beads, the biotinylated proteins are pre-processed depending on the approach that is going to be used. In most cases, peptides are obtained from an on-bead digestion using trypsin. Peptides are subsequently separated by liquid chromatography (LC) prior to identification by MS. We do not describe these steps in detail as they differ for each MS facility.

1. Plasmid construction

The cloning is performed by amplifying the DNA sequence of the gene that encodes the protein of interest (POI), gel extraction or PCR product purification, Gateway cloning, transformation of *Escherichia coli*, and plasmid purification.

a. Design primers to build the plasmids for Gateway cloning.

NOTE: The stop codons of the DNA sequence of the genes were removed from the reverse oligonucleotide used for PCR. The PCR fragment is cloned in a pEG101-TurboID (TurboID) vector for C-terminal tagging with YFP::V5::TurboID::HA(Kim *et al.*, 2023). If the gene under investigation is known to have its protein binding domain at the C-terminal end, consider tagging the gene at the N-terminal end. Generating such a vector based on the ImpGWB series should be unproblematic.

NOTE: In this protocol we used primers with attB ends to perform a BP reaction to the Entry vector pDONR221 (attP). After BP reaction, the pDONR221 construct contains the gene flanked with attL sites that will allow the LR reaction to pEG101-TurboID (attR).

NOTE: The Destination vector used in this study was generated by Kim *et al.* (2019); (Kim *et al.*, 2023) with CaMV 35S promoter (p35S). To improve the biotinylation efficiency, it may be beneficial to consider changing the promoter in the Destination vector based on the POI's expression pattern, timing, and tissue. For example, replacing the p35S with a SUC2 promoter to study phloem specific PPIs. If the protein is naturally well expressed and accumulated in potato plants, consider the use of the native promotor.

b. Prepare the PCR reaction mix to generate a Gateway-compatible PCR product with attB ends.
c. Visualize the PCR products by performing 1% agarose gel electrophoresis. When there are bands in addition to the target-sized DNA fragments, perform gel purification of the desired fragment using the QIAquick Gel Extraction Kit, according to the manufacturer's instructions. Otherwise, perform a PCR product purification using Zymo DNA Clean & Concentrator Kit.
d. Perform a 'BP' reaction (Invitrogen™ Gateway™ BP Clonase™ II Enzyme mix) to facilitate recombination between the PCR product and the pDONR221 vector (Invitrogen™ Gateway™ pDONR™221 Vector), resulting in the creation of an Entry vector.
e. Perform *E. coli* transformation by using One Shot™ TOP10 Chemically Competent *E. coli* cells, according to manufacturer's instructions.
f. Pick three single colonies into LB medium containing 50 µg/mL Kanamycin, and culture overnight at 37ºC in the shaker at 200 rpm.
g. Purify plasmids from the transformed cells using the QIAprep Spin Miniprep Kit following the manufacturer's recommendation.
h. Verify the sequence of Entry vectors using the primers M13-Fw and M13-Rv for Sanger sequencing.
i. Allow recombination of the Entry vector from the last step with the Destination vector via an "LR" reaction (Invitrogen™ Gateway™ LR Clonase™ II Enzyme mix), to create an Expression vector. Perform an *E. coli* transformation and selection as described above (steps e through g). Verify the sequence of the Expression vector with the primers P35S-CaMV-Fw and YFP-Rv.
j. Store the Expression vector in MQ water or the QIAprep Spin Miniprep Kit elution buffer at −20 °C until further use.

Key resources table

REAGENT or RESOURCE	SOURCE	IDENTIFIER
Antibodies and conjugated proteins		
anti-rabbit IgG, HRP	Agrisera	AS09-602
BirA (mutated/TurboID)	Agrisera	AS20-4440
Streptavidin Protein, HRP	Thermofisher	21124
Anti-GFP, HRP	Invitrogen	A10260
Antibiotics		
Chloramphenicol (Cm)	Duchefa	4800-94-6
Carbenicillin (Cb)	Duchefa	56-75-7
Kanamycin (Kn)	Duchefa	25389-94-0
Tetracycline (Tet)	Duchefa	64-75-5
Rifampicin (Ra)	Duchefa	13292-46-1
Chemicals and commercial resources		
Acetosyringone (3′,5′-Dimethoxy-4′-hydroxyacetophenone)	Sigma Aldrich	D134406
MES MONOHYDRATE (2-(N-morpholino)-ethane sulfonic acid)	Duchefa Biochemie	145224-94-8
Murashige and Skoog medium including vitamins	Duchefa Biochemie	M0222
Murashige and Skoog medium basal mixture	Duchefa Biochemie	M0221
Thermo Scientific™ Pierce™ Streptavidin Magnetic Beads	Thermo Scientific	10615204
Disposable PD 10 Desalting Columns	Sigma Aldrich	GE17-0851-01
Trans-Blot Turbo Mini 0.2 µm PVDF Transfer Packs	Bio-Rad	1704156
10x Tris/Glycine/SDS	Bio-Rad	1610772
StartingBlock™ (TBS) Blocking Buffer	Thermo Scientific	37542
Precision Plus Protein™ WesternC™ Blotting Standards	Bio-Rad	1610376
4x Laemmli Sample Buffer	Bio-Rad	1610747
Biotin	Merck	B4639-100MG
Pierce™ Protease Inhibitor Tablets, EDTA-free	Thermo Scientific	A32965
MG-132, proteasome inhibitor	Sigma Aldrich	M7449-1ML
SuperSignal West Dura Substrate	ThermoFisher	34076
Experimental models: Organisms/strains		
AGL1 (Cb^R, Cm^R)	Petti *et al.* (2009)	N/A
C58C1 (Te^R, Ra^R)	N/A	N/A
Constructs		
pEG101--YFP::V5::TurboID::HA (Kn^R)	Kim *et al.* (2019); (Kim *et al.*, 2023)	N/A
YFP-YFP::V5::TurboID::HA (Kn^R)	Kim *et al.* (2019); (Kim *et al.*, 2023)	N/A
NbSOBIR1-YFP::V5::TurboID::HA (Kn^R)	This paper	N/A
StCDF1-YFP::V5::TurboID::HA (Kn^R)	This paper	N/A
Oligonucleotides		
M13-Fw: GTAAAACGACGGCCAG	This paper	N/A
M13-Rv: CAGGAAACAGCTATGAC	This paper	N/A
P35S-CaMV-Fw: CTATCCTTCGCAAGACCCTTC	This paper	N/A

YFP-Rv: AAGAAGATGGTGCGCTCCTG	This paper	N/A
Other		
Screw cap tube, 15 ml, (LxØ): 120 x 17 mm, PP, with print (V-shaped 15 mL tubes)	Sarstedt	62.554.502
Eppendorf® Protein LoBind tubes 2ml (2 mL LoBind tubes)	Eppendorf	EP0030108132-100EA
Eppendorf® Safe-Lock Tubes 1,5 mL	Eppendorf	0030120086
Gene Pulser/MicroPulser Electroporation Cuvettes, 0.1 cm gap	Bio-rad	1652089
MicroPulser Electroporator	Bio-rad	1652100

Materials and equipment

- Chloramphenicol (Cm) 50 mg/mL: dissolve 500 mg of Cm in 10 mL of ethyl alcohol pure. Store at -20 °C in 1 mL aliquots. Dilute stock to 25 µL/mL in specified culture media.
- Carbenicillin (Cb) 50 mg/mL: dissolve 500 mg of Cb in 10 mL of milliQ water and filter sterilize through 0,2 µm filter. Store at -20 °C in 1 mL aliquots. Dilute stock to 50 µL/mL in specified culture media.
- Kanamycin (Kn) 50 mg/mL: dissolve 500 mg of Cm in 10 mL of milliQ water and filter sterilize through 0,2 µm filter. Store at -20 °C in 1 mL aliquots. Dilute stock to 50 µL/mL in specified culture media.
- Tetracycline (Te) 15 mg/mL: dissolve 150 mg of Cm in 10 mL of methanol. Store at -20 °C in 1 mL aliquots. Dilute stock to 15 µL/mL in specified culture media.
- Rifampicin (Ra) 50 mg/mL: dissolve 500 mg of Cm in 10 mL of DMSO. Store at -20 °C in 1 mL aliquots. Dilute stock to 50 µL/mL in specified culture media.
- Streptavidin Protein, HRP 1 mg/mL: add 2 mL of milliQ water to the tube that contains 2 mg of protein. Store at -20 °C in 50 µL aliquots.
- Acetosyringone (4-Hydroxy3,5-dimethoxyacetophenone) 200 mM: dissolve 196 mg of acetosyringone in 5mL of DMSO. Store at -20 °C in 0.5 mL aliquots. Dilute stock to 200 µM in the specified culture media.
  NOTE: Store at -20 °C in 0,5 mL aliquots.
- **MES solution 1:** (2-(N-morpholino)-ethane sulfonic acid) 1 M, pH 5,6: dissolve 4,265 g of MES in 20 mL of milliQ water, adjust with NaOH to pH 5,6.
  NOTE: MES is difficult to dissolve. First add 10 mL of milliQ, adjust with NaOH to pH 5,6 and then adjust the final volume to 20 mL. Filter sterilize through 0,2 µm filter. Store at -20 °C in 2 mL aliquots.
- **MES solution 2:** (2-(N-morpholino)-ethane sulfonic acid) 10 mM, pH 8: dissolve 32 mg of MES in 15 mL of milliQ water, adjust with NaOH to pH 8.
  NOTE: 10mM MES for dissolving biotin should be prepared before use. Keep MES in the dark by covering the bottle or tube with aluminum foil.
- MG-132 10 mM: MG-132 (M7449-1ML) is a ready-made solution at 10 mM in DMSO. Dilute to 40 µM in specified buffer.
- **Biotin** 10 µM: dissolve 0,37 mg of biotin in 150 mL of MES solution 2 (10 mM).
  NOTE: Prepare fresh on the day of use. This volume (150 mL) is calculated for a set of 15 plants, using 3 leaves per plant and a surface area of each of the leaves of about

30 cm^2. MCD-321 has leaves with a surface area of 30 cm^2 approximately each and CE3027 has leaves of approximately 15 cm^2 each.

OPTIONAL: Add proteasome inhibitor MG-132 40 µM to biotin 10 µM solution to reduce the degradation of ubiquitin-conjugated proteins before collection of samples.

MS20 plant propagation media	
Reagent	**Final concentration**
Murashige and Skoog medium including vitamins	4,4 g/L
Sucrose	20 g/L
Adjust to pH 5,8 with 1 M NaOH	
Micro agar	8 g/L
Autoclave at 121ºC for 20 min	

NOTE: Pour media immediately after autoclaving. Keep MS20 agar for max. 6 months at room temperature. Grow plants in MS20 for max. 6 months.

LB (Lysogeny broth) media	
Reagent	**Final concentration**
Tryptone	10 g/L
Yeast extract	5 g/L
NaCl	10 g/L
Autoclave at 121 ºC for 20 min	

NOTE: Keep LB media for max. 1 year at room temperature.

YEB (yeast extract beef) media	
Reagent	**Final concentration**
beef extract	5 g/L
bacteriological peptone	5 g/L
Sucrose	5 g/L
yeast extract	1 g/L
$MgSO_4 \cdot 7H_2O$	0.492 g/L
Autoclave at 121 ºC for 20 min	

NOTE: Keep YEB media for max. 1 year at room temperature.

MMA buffer	
Reagent	**Final concentration**
Sucrose	20 g/L
Murashige and Skoog basal salts	5 g/L
MES	1,95 g/L
Adjust to pH 5,6 with 1M NaOH	
Acetosyringone	200 µM

NOTE: Make fresh in ddH_2O or milliQ on the day of use.

RIPA (Radioimmunoprecipitation assay) buffer	
Reagent	**Final concentration**

Tris-HCl pH 7.6	25 mM
NaCl	150 mM
Sodium deoxycholate	1% (w/v)
SDS	0,1% (w/v)
NP-40	1% (v/v)

NOTE: RIPA can be stored at 4 °C for a month without protease and proteasome inhibitors. Add 1 tablet of protease inhibitor cocktail and MG-132 (40 µM) per 50 mL of RIPA the day of use when specified in the protocol.

NP-40 free RIPA buffer	
Reagent	**Final concentration**
Tris-HCl, pH 7.6	25 mM
NaCl	150 mM
Sodium deoxycholate	1% (w/v)
SDS	0,1% (w/v)

NOTE: NP-40 free RIPA can be stored at 4 °C for a month without protease and proteasome inhibitors. Add 1 tablet of protease inhibitor cocktail per 50 mL of NP-40 free RIPA the day of use when specified in the protocol.

TBS 10X	
Reagent	**Final concentration**
Tris-HCl pH 7.5	20 mM
NaCl	150 mM

NOTE: TBS 10X can be stored at 4 °C for 3 months. Make TBS 1X with ddH_2O on the day of use and add 0,1% Tween20 to make TBS-T. TBS-T 1X can be stored at 4 °C for 1 month.

Step-by-step method details

Propagating plant material

Timing: 30-35 days

1. Grow fresh cuttings of potato plants on MS20 *in vitro* at 24 °C in a climate chamber, under long day conditions (16 h/8 h day/night), for 2 weeks.
2. Grow for 1 week in 4x4cm square pots containing sterilized potting soil, in climate-regulated greenhouse compartments, within a temperature range of 18–22 °C and under natural light conditions.
3. Transfer to 12x12 cm square pots or to 14 cm diameter round pots and grow for 3-5 weeks under the same conditions.

NOTE: Some potato genotypes grow better in round pots. Check TROUBLESHOOTING – Problem 2.

NOTE: Number of plants to grow depends on setting of the experiment. Samples for MS are sent in triplicate for statistical analysis. One replicate consist of a set of

three plants and per plant, 3-5 leaves are infiltrated with the construct. Therefore, 9 plants in total per set of TurboID construct (3x3).

Agrobacterium tumefaciens preparation and agroinfiltration

Timing: 1-2 weeks

4. Transform 100 ng of the plasmids containing the TurboID fusion constructs to 20 µL of electro-competent *Agrobacterium tumefaciens* (in 1.5 mL Eppendorf tube). Pipette *Agrobacterium* cells with DNA into a prechilled 0.2 cm electroporation cuvette. Pulse cells at 1.4 kV with MicroPulser Electroporator. Add 0.25 mL of YEB (or LB) media to the cuvette, mix, and immediately transfer cells into a clean 1.5 mL Eppendorf tube. Grow for 2 hours in 0.5 mL of LB at 28 °C and 200 rpm. Plate 20-50 µL on LB agar plates (diameter 90 mm) with the appropriate antibiotics.

   NOTE: In this protocol, YFP-TurboID and SOBIR1-TurboID constructs were transformed into *Agrobacterium* strain C58C1 and CDF1-TurboID into AGL1. The antibiotics for C58C1 are Ra and Te, and for AGL1 are Cm and Cb. In addition, Kn antibiotic is added for selection of *Agrobacterium* colonies transformed with TurboID construct. Working concentrations are specified in “Material and equipment”.
   NOTE: *A. tumefaciens* transformation by electroporation has high efficiency and usually produces 30-60 colonies using this set-up. Longer incubation times (up to 4 hours) in LB will increase efficiency.
   OPTIONAL: Test different *A. tumefaciens* strains to check the accumulation of the fusion protein of interest upon transient expression. Check TROUBLESHOOTING – Problem 1 & 5.

5. Pick a single transformed *A. tumefaciens* colony and transfer to 10mL of LB media with the appropriate antibiotics and incubate for 2 days with continuous shaking at 200 rpm at 28 °C.
6. Transfer the cultures to a 250 mL flask containing YEB media with the appropriate antibiotics and supplemented with acetosyringone (final concentration 200 µM) and MES solution 1 (final concentration 10 mM) and incubate while shaking for 1 day at 28 °C, at 200 rpm.
7. Collect the cells by centrifugation at 3,000 x g for 10 min.
8. Resuspend the pelleted cells in freshly prepared MMA buffer to an OD_{600} of 0.3-0.4. For co-infiltration of two constructs, mix the *A. tumefaciens* cultures in a 1:1 ratio.

   NOTE: 30-50 mL of *A. tumefaciens* culture is usually enough for infiltrating 3-5 leaves per set of triplicates. Potato leaf size varies a lot and different genotypes have different structure, such as trichome density etc., which results in different requirements for *A. tumefaciens* infiltrate. On average, 1ml is sufficient for 1 potato leaf.

9. Incubate the *A. tumefaciens* suspensions in MMA for 1-2 hours at room temperature without rolling or shaking before infiltration.
10. Fully infiltrate 3-5 leaves of each potato plant with the suspension from the lower side of the leaves with a 1 mL needleless syringe.

    OPTIONAL: Water the potato plants 1-2 hours before agroinfiltration to facilitate the infiltration of the suspension, as the stomata will open. Make a scratch on the lower epidermis of the leaves to be infiltrated with a needle or scalpel to facilitate the infiltration. Check TROUBLESHOOTING – Problem 3.

    NOTE: Choose young, healthy, and just fully expanded leaves for the agroinfiltrations.
    NOTE: We recommend to change gloves between each set of constructs to avoid possible contamination between different constructs.

    NOTE: Infiltrated plants are maintained in the greenhouse within a temperature range of 18–22 °C and under natural light conditions till samples are collected.

Leaf sample collection

Timing: 2 days

OPTIONAL: Test with and without the addition of biotin. Check TROUBLESHOOTING – Problem 4.

OPTIONAL: Infiltrate a freshly prepared solution of 10 µM biotin in 10 mM MES pH 8, after 36-48 hpi, and collect leaf samples at 1-3 hpi after the infiltration of biotin.

OPTIONAL: To reduce the degradation of ubiquitin-conjugated proteins, additional MG-132 can be supply together with biotin solution (MG-132 40 µM to biotin 10 µM solution).

NOTE: The concentration and incubation time of biotin treatment was determined based on previous studies in *Arabidopsis* and *N. benthamiana*(Kim *et al.*, 2019; Kim *et al.*, 2023) (Zhang, Yongliang *et al.*, 2019).

11. After 36-48 hpi, cut the leaves off, remove the petiole and middle vein from the base with scissors. Place in a 50 mL tube with V-shaped bottom and immediately place into liquid nitrogen.

    NOTE: We recommend cleaning the scissors used for removing the petiole and middle vein with ethanol 70% between different treatments.
    PAUSE POINT: Keep leaves at -80 °C, either the intact leaves or ground, in tubes.

12. Grind samples in liquid nitrogen using a mortar and pestle to a fine powder and weigh.

NOTE: Make sure that the triplicates are all approximately of the same weight; 3-5 g ± 0.5g.

Protein extraction

Timing: 2-3 hours

13. Add 2 mL of RIPA buffer, supplemented with protease inhibitor cocktail and MG-132, per gram of ground leaf.

    NOTE: MG-132 is a proteome inhibitor and blocks the activity of proteasomes. It targets protein degradation differently from the protease inhibitor. For some proteins, such as DELLA(Wang *et al.*, 2009), MG-132 is crucial for its stability. Therefore, we recommended to supply MG-132 in with RIPA buffer.

14. Keep samples on ice, while vortex-mixing for 15 min. (vortex-mixing each sample, while keeping samples cold by placing the samples on ice during the rest time).
15. Pellet the debris by centrifugation at maximum speed (RCF: 17,000 x g) for 30 min at 4 °C. Make sure that the supernatant is clear, without remaining particles.
16. Transfer the supernatant to a pre-cooled V-shaped 15mL tube and adjust all samples to 10 mL with RIPA buffer, supplemented with protease inhibitor cocktail and MG132.

    NOTE: LoBind tubes are preferred for all steps.
    NOTE: The total volume of the samples should be around 10mL.
    NOTE: Each *Cytiva Life Sciences* PD-10 desalting column can only hold 2.5 mL per column. Per sample, approx. 10 mL of isolated protein solution is obtained, so 4 columns are needed.

Removal of free biotin from the protein extracts with *Cytiva Life Sciences* PD-10 desalting columns

Timing: 1-2 hours

NOTE: The following steps should be performed in 4 °C room.

17. Equilibration of the PD-10 desalting columns.
    a. Place the column in the provided rack and place a container below to collect the flow-through.
    b. Remove the top cap.
    c. Cut the sealed end and allow the storage solution to drain away.

d. Wash the column 3x with 4mL of RIPA without protease inhibitor cocktail and without MG132.
e. Wash the column 1x with 4mL of RIPA with protease inhibitor cocktail and with MG132.

18. Add 2.5 mL of the protein extract to the equilibrated PD-10 desalting column and discard the flow-through.
19. Transfer the columns to another rack, containing V-shaped 50 mL tubes.
20. Elute the columns with 3,5 mL of RIPA, supplemented with protease inhibitor cocktail and MG132.
21. Combine the eluates from each triplicate in one tube.

Pull down of the biotinylated proteins with *Thermo Scientific Pierce* Streptavidin Magnetic Beads

Timing: 3 hours

NOTE: The following steps should be performed at 4 °C
NOTE: In parallel, perform a test for checking the protein extract on a western blot.

22. Equilibration of the streptavidin beads.
    a. Resuspend the beads by pipetting and stirring before use.
    b. Pipette 200 µL of streptavidin beads (50% slurry) per sample in a 2 mL LoBind tube.

NOTE: For the test sample, use 100 µL of streptavidin beads per sample (50% slurry).
NOTE: To estimate the total volume of beads necessary to process all the samples, including an extra volume of 5% to account for pipetting errors, follow this calculation:
Total volume of beads = (Number of samples × Volume of beads per sample) + (5% of total volume of beads).
For example, if there are 5 samples, and each sample requires 200 µL of beads:
Total volume of beads = (5 × 200 µL) + (0.05 × (5 × 200 µL)) = 1050 µL.

    c. Place the tube into a magnetic stand for 3 min to collect the beads.
    d. Discard the supernatant.
    e. Wash the beads 3x with 1 mL of RIPA, supplemented with protease inhibitor cocktail and MG-132. For each washing step, add the buffer and mix by inversion until the beads are completely resuspended, and let the tube stand for 3 min in the magnetic rack, after which the supernatant is discarded.

23. After the last wash add 100 µL of RIPA per sample, supplemented with protease inhibitor cocktail, to the equilibrated beads and transfer the 100 µL resuspended beads to each of the V-shaped 15 mL tubes containing the desalted protein extracts.

    NOTE: For the test sample, add 50 µL of RIPA per sample, supplemented with protease inhibitor cocktail.

24. Incubate the samples in a rotator for 1 hour at 4 °C, at 10 rpm.

    NOTE: The incubation can be extended up to 12h (overnight) with continuous gentle shaking (10 rpm) at 4 °C.

25. Wash the beads.
    a. Place the tubes into a magnetic stand for 3 min to collect the beads.
    b. Discard the supernatants.

    NOTE: The supernatants can be collected (20-50 µL) and stored at -20 °C for testing the binding efficiency at a later timepoint.

26. Add 1 mL of NP40-free RIPA, supplemented with protease inhibitor cocktail, and mix by inversion of the tubes.
27. Transfer the mixture to a 2 mL LoBind tube.
28. Place the tubes into a magnetic stand for 3 min to collect the beads.
29. Wash the beads 3x with 1 mL of NP40-free RIPA, supplemented with protease inhibitor cocktail. Follow the same procedure as indicated in step **25** to wash the beads.
30. The samples are now ready for MS pre-processing. Go to **step 44**.
31. The sample test can be processed for western blot following **step 32**.

PAUSE POINT: The enriched biotinylated proteins can be stored at -20 °C for months before further processing for MS.

Identification of biotinylated proteins by western blotting

Timing: 4-5 hours

NOTE: This step is only performed for the protein samples that will NOT be processed for MS

32. Resuspend the streptavidin beads to which the biotinylated proteins are bound in 60 µL of RIPA.
33. Add 20 µL of 4x Laemmli Sample Buffer® (Bio-rad), previously mixed 1:9 with β-mercaptoethanol as the manufacturer's recommendation.
34. Incubate in a shaker at 95 °C for 10 min, at 300 rpm.

35. Place the tubes on ice for 2 min and spin the beads down at top speed in a microcentrifuge.
36. Load 25 µL of the supernatant on an SDS-PAGE gel. To avoid pipetting the beads, leave the tubes in the magnetic rack, Load 5 µL of the ladder Precision Plus Protein™ WesternC™ Blotting Standards.
37. Run the gel in an electrophoresis cell with 1x Tris/Glycine/SDS buffer.
38. Transfer the proteins to a Trans-Blot Turbo Mini 0.2 µm PVDF membrane in the Trans-Blot Turbo system at 25 V at 1,3 A for 7 min.
39. Block the membrane with 10 mL of StartingBlock (TBS) Blocking Buffer, supplemented with 0,5% (v/v) of Tween20 for 30 min.

NOTE: The standard blocking buffer, which consists of 5% of fat-free milk powder in 1x TBS-T, contains biotin that potentially interferes with the incubation of the blot with the streptavidin-HRP protein and subsequent detection steps. As an alternative, use BSA at a concentration of 3% in 1x TBS-T, or a commercial (biotin-free) blocking buffer as described in this protocol.

40. Add the appropriate antibody to the blocking buffer and incubate for 1 hour at RT or follow the manufacturer's instructions.
    a. Use a BirA (mutated/TurboID) antibody diluted 1:5000 in StartingBlock (TBS) Blocking Buffer to determine the accumulation of the Turbo-ID fusion protein *in planta.*
    b. Use a Streptavidin-HRP protein diluted 1:50000 in StartingBlock (TBS) Blocking Buffer to check for the presence of biotinylated proteins purified from the pull down using the streptavidin beads.
    c. Use an α-HA, α-GFP or α-V5 antibody to detect the accumulation of fusion proteins carrying these tags *in planta.* In this protocol, we used α-GFP diluted 1:1000 in StartingBlock (TBS) Blocking Buffer.
    d. Use appropriate antibody(ies) when checking for the presence of additional differently labelled interactor(s) after the pull down e. g. to verify the biotinylation of a tagged known interactor.

    NOTE: The dilutions of antibodies are based on specifications for Western blotting detection substrate used. In this protocol, we used SuperSignal West Dura.

41. If a secondary antibody is needed, as is the case for the BirA (mutated/TurboID) antibodies, wash the membrane 3 times with TBS-T buffer and dilute the conjugated secondary antibody. In this protocol, we used α-rabbit IgG, HRP diluted 1:10000 in TBS-T buffer. Incubate with the secondary antibody for 1 hour.
42. Wash the membrane 3 times with TBS-T buffer.
43. Develop the blot with the ECL substrate of choice (**Figure 1**).

Identification of the biotinylated proteins by mass spectrometry

Timing: 1-4 weeks

44. Send the samples from **step 30** to the MS facility.

NOTE: It might be required to store the sample in a specific buffer at a determined temperature before the samples are pre-processed for MS.

NOTE: We sent our samples to MS facility in Biochemistry Department at WUR for LC-MS analysis.

NOTE: MS facility in Biochemistry Department at WUR pre-process the samples to perform LC-MS(van Mourik *et al.*, 2023). The pre-processing involves cysteine reduction, tryptic digestion, and clean-up of the peptides. These steps can vary depending on the facility service.

45. Use the appropriate software for statistical analysis of the results from the LC-MS.

46. Select the proteins of interest for further studies.

Expected outcomes

To evaluate the efficacy of the transient TurboID-based proximity-dependent labelling method in *S. tuberosum*, several criteria can be assessed. First, the fused POI should be detected in transformed leaves. In this protocol, the POI is fused with YFP and TurboID. The YPF tag allows performing a confocal study to check the subcellular localization of POI. For instance, StCDF1 is known to accumulate in the nucleus (Goralogia, Greg S *et al.*, 2017), while NbSOBIR1 is found at the plasma membrane(Li, YH *et al.*, 2021)-(Postma *et al.*, 2016). Potential candidate interactors could be also filtered out by the localization of POI after statistical filtering. Secondly, the tagged POI should be produced and accumulate in potato leaves and be able to biotinylate proximal proteins. Abundance of POI-YFP-TurboID can be checked in WB using YFP and TurboID antibodies in step 43. Our previous observations suggest that overexpressing tagged protein in potato always leads to the issue of the tag being cleaved off. The POI-YFP-TurboID can be degraded and leads to no full-size POI-YFP-TurboID present from immunoblot (IB), but only partials (**Figure 1**). The absence of the full-size band in IB does not necessarily mean no accumulation or experimental failure. **Figure 2A** provides an overview of the proximity labelling MS results for StCDF1-YFP-TbID. Our analysis reveals the identification of more than 10 proteins located within the nucleus based on the MS dataset, showing positive enrichment in StCDF1 samples (**Figure 2B**). Notably, among these proteins are StCDF1 itself, as well as another well-known interactor, StFKF1 . Moreover, by comparing the MS results between applying extra biotin and without, it is obvious that there are 2 nucleus located proteins that were enriched only when extra biotin was supplied. However, the extra biotin application also increased the total amount of labelled proteins (**Figure 2A**).

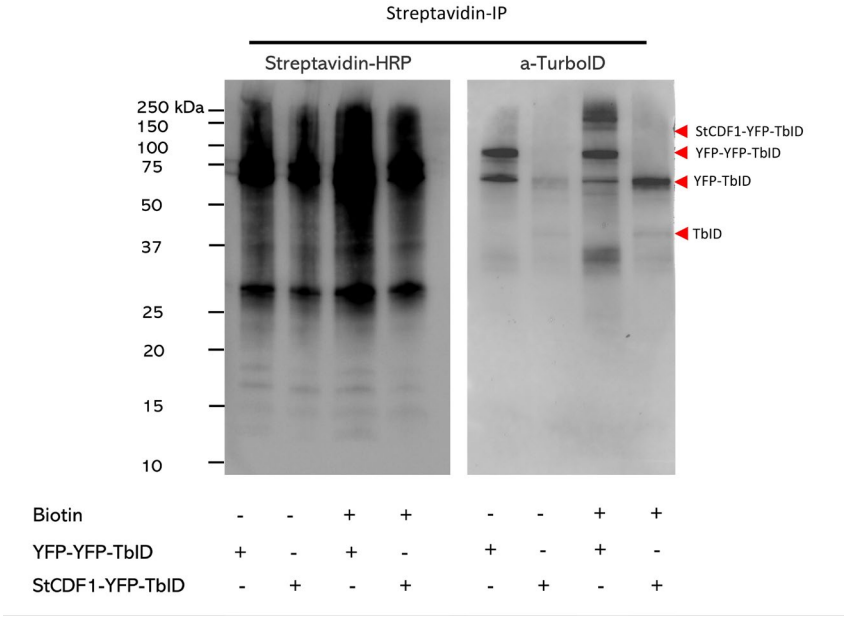

Figure 1: **Immunoblot analysis of protein extracts obtained in step 43.**
Immunoblot (IB) analysis following streptavidin affinity purification of potato (CE3027) leaf material transiently transfected with StCDF1-YFP-TurboID and YFP-YFP-TurboID, which was infiltrated with 10 µM of exogenous biotin 2 hours before harvest, as well as an untreated control sample. Biotinylated proteins were immunoprecipitated by Streptavidin-HRP (left). StCDF1-YFP-TurboID and YFP-YFP-TurboID was immunoprecipitated by anti-TurboID antibody (right). The red arrows represent target proteins. Expected sizes of StCDF1-YFP-TurboID and YFP-YFP-TurboID proteins are 122.4 and 99.6 kDa, respectively. In addition to full length or partial bait protein, YFP (27 kDa) and TurboID (35 kDa) free tags should be also visualized by using corresponding antibodies. In this context, partial proteins due to degradation could also be present in the WB. Partial proteins are: YFP-V5 (27 kDa), YFP-V5-TurboID (63 kDa), V5-TurboID (36 kDa), V5-TurboID-HA (37 kDa) and TurboID-HA (36 kDa).

Western blotting can also be used to determine the efficiency of the enrichment of the biotinylated proteins, including the protein of interest (POI) that is used as a bait fused to the TurboID enzyme, and control proteins fused to TurboID, such as YFP, GFP or GUS. The specificity of the labelling with biotin can be demonstrated using Streptavidin-HRP. The intensity of the signals can be used to estimate the labelling efficiency, which should be relatively high when the fusion protein accumulates in sufficient amounts *in planta*. It is worth noting that a low protein level of the bait can also be desirable in other plant systems such as *N. benthamiana*, as using a proper negative control will help avoiding background labelling. However, we find that tagged protein yield in potato transient transformation experiments is generally lower. Furthermore, we need to consider that potato tends to cleave the tagged protein. Consequently, the enrichment of biotinylated proximal proteins from low protein level POI-YFP-TurboID is rather poor in potato transient experiments. Therefore, getting a good production of POI-YFP-TurboID in potato is a key step for a successful TurboID-based PL approach.

Finally, the MS output comprises a plot of intensity that enables the identification of the biotinylated proteins in the sample. Intensities of proteins identified in the transiently expressed POI-TurboID samples are compared to the samples carrying the negative TurboID controls. Proteins that are significantly enriched in the POI-containing sample, when compared to the negative control, can be considered putative interactors of the POI. The identification of these proteins as interactors can be further validated by other methods, e. g. *in vivo* interaction assays such as yeast two-hybrid, *in vitro* assays such as co-immunoprecipitation or silencing studies (VIGS, CRISPR) followed by screening of the response (change in phenotype, loss-of-function phenotype). Moreover, the biological relevance of the putative interactors for POI functioning can be assessed by gene ontology analysis, which can reveal the biological processes or pathways in which they are involved.

Overall, the expected outcome of the transient TurboID-based proximity-dependent labelling method is a comprehensive and specific characterization of the protein interactome of the POI in *S. tuberosum*. This method has the potential to uncover novel interactors and protein complexes, thereby shedding light on the biological functions and mechanisms of action of the POI.

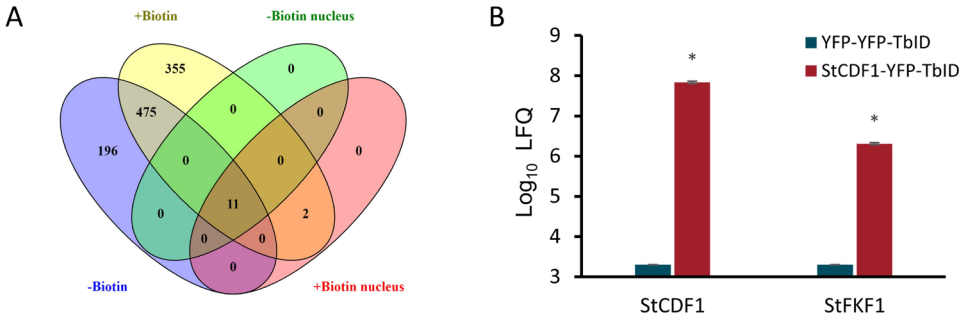

Figure 2: **Overview of mass spectrometry results of StCDF1-YFP-TbID.**
A. The Venn diagram illustrates the overlaps of enriched proteins in StCDF1 samples among protein sets under different treatments, including with and without extra biotin supply, with extra biotin supply and nucleus located, and without extra biotin supply and nucleus located proteins. **B.** Protein enrichment of StCDF1 and StFKF1 was analyzed in YFP-YFP-TbID and StCDF1-YFP-TbID samples (with extra biotin treatment) using mass spectrometry (MS). The data is presented as the mean of logarithm-based label-free quantification (LFQ) values ± standard error (n = 3). Statistical significance was determined using a Student's t-test (*P < 0.05). Notably, both proteins were not detected in the YFP-YFP-TbID samples. To address this, missing values were imputed using imputation methods based on the normal distribution.

Limitations

There are several limitations to this transient TurboID proximity-dependent labelling protocol for identifying PPIs in *S. tuberosum*. First, the approach of transient expression by agroinfiltration limits the experimental tissue to only leaves of potato. For detecting certain tissue-specific PPIs, stable transformed plants should be considered. Second, with the same amount of input leaf material and the same PL approach, the protein yield from potato leaf material is generally lower than that from *N. benthamiana*. For the MS analysis, this lower

protein yield will not pose a major problem. However, this low protein yield could cause some difficulties concerning the western blots, for example in detecting the POI which has been fused with the TurboID enzyme. Longer exposure times for the blots, combined with using high sensitivity ECL and/or decreasing antibody dilutions should be considered to solve this problem. Third, it is important to keep in mind that this PL method allows covalent labelling with biotin of any proteins that are in the proximity of the bait protein of interest at a particular moment. *In vivo* analysis still needs to be performed to verify an actual direct or indirect interaction between the two proteins (Zhang, Y *et al.*, 2020). Moreover, the labelling radius of TurboID is estimated to be around 35 nm and the labelling ability depends on the available lysines in the proximal proteins and the availability of biotin (Kim *et al.*, 2014; Branon *et al.*, 2018; May *et al.*, 2020; Sanchez & Feldman, 2021).

Troubleshooting

Problem 1:

The potato genotype of interest is not amenable to *A. tumefaciens* infiltration, or the bait protein does not accumulate in the selected potato genotype.

Potential solution

- Reduce the OD_{600} of the *A. tumefaciens* cell suspension to 0.3 or lower.
- Screen several genotypes from the same species.
- Screen additional *A. tumefaciens* strains that have a lower virulence.
- Consider stable transformation of the potato genotype of interest.

Problem 2:

The potato genotype fails to produce sufficient leaves and exhibits poor growth after four weeks of growth in the pots.

Potential solution

- Optimize the different growth conditions for the various potato genotypes by considering their individual preferences, such as their preference for a greenhouse with natural light or artificial light.
- Change the type of pots. Some genotypes prefer a different pot size or shape compared to others.

Problem 3:

The potato genotype is difficult to perform an infiltration with the *A. tumefaciens* suspension on.

Potential solution

- Water the plants 2 hours before infiltration or spray the leaves with water mist immediately before infiltration.
- Use a needle, scalpel or P-10 pipette tips to create small wounds on the abaxial surface of the leaves before infiltration.

Problem 4:

Low overall biotinylation signal as revealed by Western blotting (WB) (step 43)

Potential solution

There may be multiple causes of a low biotinylation signal, including:

- The endogenous biotin content of the potato leaves is not high enough for efficient labelling. Provide extra biotin (10 µM biotin, 10 mM MES, pH 8) at 1-3h before harvesting.
- The gene encoding the TurboID fusion protein is poorly expressed. To improve the level of gene expression, modifying the promoter should be considered. In addition, codon optimizing of the open reading frame encoding the POI and TurboID could also help to improve the expression levels.
- The POI fused with the TurboID enzyme is accumulating poorly. Consider changing the site at which the TurboID is fused to the POI. The C-terminal end of StCDF1 is responsible for its stability(Kloosterman, Bjorn *et al.*, 2013), and fusing TurboID to the C-terminal end of StCDF1 will inhibit its degradation and thereby enhance the labelling ability.
- Consider mutating any degradation signals or motifs in the POI. For example, using the StCDF1.2 allele (increased protein stability due to missing binding site for StFKF1(Kloosterman, Bjorn *et al.*, 2013)) rather the full length wild type StCDF1 (1.1). However, keep in mind that mutating this binding motif will affect the final MS result. The interactor which mediating the degradation, such as StFKF1 will not appear in StCDF1.2 proximity labelling MS results.

Problem 5:

Unbalanced expression by the negative control-expressing plasmids and POI-expressing plasmids.

Potential solution

- Transform plasmids to different strains of *A. tumefaciens*.

Note: In this study, both negative control plasmids were transformed to the C58C1 strain of *A. tumefaciens*, and the POI-expressing plasmids were transformed to AGL1. For the same *A. tumefaciens* strain, the negative control plasmid generally resulted in a higher expression than the POI-expressing plasmid. Therefore, C58C1, which results in lower protein accumulation levels, was selected to be used for both negative controls. When compared to C58C1, the AGL1 strain can help to promote higher expression levels of the POI-containing plasmids, but also possibly induces more cell death in some potato genotypes.

Problem 6:

A protein that has previously been found to interact with the POI is not present in the dataset generated by the LC-MS experiments.

Potential solution

- The absence of a known protein interactor does not necessarily mean that the protocol is not appropriate. For tissue-specific PPIs, stable transformation should be performed, and only the target tissue be harvested. If the expression of potential interactors follows the circadian rhythm, adjust the sample harvesting time.

Problem 7:

Background noise due to endogenous biotinylated proteins, unrelated to the presence of the POI fused to TurboID.

Potential solution

- Including a second control: using POI fused only with YFP and without TurboID enzyme.

Problem 8:

The LC-MS analysis of the sample for which the POI fused to TurboID was expressed, produced limited results, with only a small number of biotinylated proteins showing significant enrichment compared to the negative control sample.

Potential solution

- Perform targeted protein isolation based on POI localization.
- Add proteasome inhibitor (MG-132).

Resource availability

Lead contacts

Further information and requests for resources and reagents should be directed to and will be fulfilled by the lead contacts, Vivianne Vleeshouwers (vivianne.vleeshouwers@wur.nl) and Christian W.B. Bachem (christian.bachem@wur.nl).

Materials availability

Potato genotypes and described plasmids are available upon request from the lead contacts.

Data and code availability

All relevant data are available from the lead contacts upon request. There are no restrictions on data availability.

Acknowledgments

This work was supported by European Union's HORIZON 2020 Research programme under Grant Agreement no. 766048 “PROTECTA”, Wageningen University and Research (VGAAV)(T.M.F). L.S. is supported by the China Scholarship Council (No. 201807720077) and S.L.V. is supported by the Peruvian Council for Science, Technology and Technological Innovation (CONCYTEC) and its executive unit FONDECYT. We acknowledge Aardevo and Solynta for funding part of this research. We also like to thank Zhi-Yong Wang from the Department of Plant Biology (Carnegie Institution for Science, Stanford) to share the TurboID-containing vector.

Author contributions

Conceptualization, T.M.F. and L.S.; experiment, T.M.F. and L.S.; methodology, T.M.F., L.S. and S.L.V.; writing original draft, T.M.F. and L.S.; review & editing, M.J., V.V. and C.W.B.

Declaration of interests

The authors declare no competing interests.

Chapter 5

Uncovering the Molecular Partners and Mechanism of StCDF1 in Transcriptional Regulation in Potato

Li Shi[1,2], Sjef Boeren[3], Richard G.F. Visser[1], Christian W.B. Bachem[1]

[1]Plant Breeding, Wageningen University & Research, 6708PB, Wageningen, The Netherlands.
[2]Gradute School Experimental Plant Sciences, Wageningen University & Research, 6708PB, Wageningen, The Netherlands.
[3]Laboratory of Biochemistry, Wageningen University & Research, Wageningen, PO Box 386, Wageningen, 6700 AJ, The Netherlands.

Abstract

CYCLING DOF FACTOR1 (*StCDF1*) is genetically linked to several agronomically important traits, such as tuberization, senescence, and responses to abiotic and biotic stress. As a central regulator, StCDF1 plays a crucial role in various aspects of potato plant development. Previous molecular studies have demonstrated its multifaceted involvement in regulating different pathways. For instance, StCDF1 regulates the onset of tuberization, dependent on day length, by repressing the expression of *CONSTANS-Like 1* (*StCOL1*) and *SELF-PRUNING 5G* (*StSP5G*). Additionally, recent research has shown that StCDF1 can activate a distinct set of downstream genes. However, the exact molecular mechanisms underlying different regulatory functions remain largely unknown. To shed light on the regulatory mechanism of StCDF1, we utilized TurboID (TbID)-based proximity labelling (PL) in this study to identify StCDF1's protein interactors. Our findings revealed over 10 potential interactors of StCDF1, including 4 transcription factors belonging to the bHLH, bZIP, and homeobox transcription factor families. Moreover, we generated transgenic lines overexpressing a mutated form of StCDF1, specifically targeting the DOF DNA binding domain and co-repressor binding domain. Our observations indicate that StCDF1 may bind to different interactors to either repress or activate downstream targets. These discoveries provide valuable insights into the diverse traits regulated by StCDF1 during plant development.

Introduction

Potato (*Solanum tuberosum*) is the largest non-grain food crop grown across diverse regions in the world (FAO, 2019), and is valued for its high nutritional content, versatility, and adaptability (Çalışkan *et al.*, 2023). The tuber, which is the storage organ of potato, is a great source of carbohydrates and other essential nutrients. As a result, potatoes play a crucial role in global food security and livelihoods (Devaux *et al.*, 2014). Notably, potatoes originated in the Andes and evolved short-day dependance for tuber formation. Cultivated varieties of potatoes are derived from Chilean landraces, which are better adapted to long-day conditions (Ewing & Struik, 1992; Spooner *et al.*, 2005; Navarro *et al.*, 2011). This adaptability has made potatoes a popular crop all around the world.

A major-effect quantitative trait locus for potato plant maturity and initiation of tuber development was found and functionally linked to a DOF family gene (DNA-binding with one finger) coding for a transcription factor named *CYCLING DOF FACTOR1* (*StCDF1*) (Kloosterman, B. *et al.*, 2013). In *Arabidopsis*, it was reported that the C-terminal end of the AtCDF1 protein binds to both GIGANTEA (GI) and FLAVIN-BINDING KELCH REPEAT F-BOX PROTEIN 1 (FKF1) (Sawa *et al.*, 2007). This binding destabilizes the CDF1 protein in the late afternoon. Given its diurnal post-translational regulation, this gene has been identified as a key regulator of photoperiod-dependent flowering (Imaizumi *et al.*, 2005; Sawa *et al.*, 2007). In potato, this interaction between StGI, StFKF1 and the wild-type StCDF1(StCDF1.1) was tested and confirmed by performing yeast two hybrid (Kloosterman, B. *et al.*, 2013). Allelic variation at the 3′ end of the *StCDF1* gene results in truncated variants (*StCDF1.2* and *StCDF1.3*), which abolishes the interaction with StFKF1. Consequently, the StCDF1.2 and StCDF1.3 protein levels remain constant throughout the day as they are unaffected by this post-translational degradation under long day condition (Kloosterman, B. *et al.*, 2013). Our previous work has shown that, similar to *Arabidopsis*, StCDF1 directly binds to the *CONSTANS-Like 1* (*StCOL1*) promotor region and represses its expression to mediate tuberization (Kloosterman, B. *et al.*, 2013; Ramírez Gonzales *et al.*, 2021). In potato, StCOL1 negatively regulates tuberization by directly upregulating the expression of a potato homologue of *FLOWERING LOCUS T* (*FT*), called *SELF-PRUNING 5G* (*StSP5G*). Furthermore, StSP5G downregulates the expression of *SELF-PRUNING 6G* (*StSP6A*), which has been demonstrated to act as the mobile ‘tuberigen’ signal that initiates tuberization. Therefore, *StCDF1* plays an important role in regulating photoperiod-dependent tuberization by indirectly promoting expression of *StSP6A* (Navarro *et al.*, 2011; Abelenda *et al.*, 2014).

A mechanism of CDF-dependent repression of gene expression was reported by Goralogia, Greg S *et al.* (2017). To repress downstream target genes, such as *AtCO*. AtCDF1 recruits the well-known co-repressor, TOPLESS (TPL). TOPLESS/TOPLESS-RELATED (TPL/TPRs) belong to a major class of transcriptional co-repressors known as the Gro/Tup1 proteins (Causier *et al.*, 2012b; Wang *et al.*, 2013). Other than TPL itself, 5 other members were found in *Arabidopsis* : TPR1,TPR2,TPR3,TPR4 (Causier *et al.*, 2012b). Previous studies showed that TPL and TPRs are widely involved in regulating hormone signalling, plant immunity, flowering, stress responses, etc. (Plant *et al.*, 2021). Studies in potato have demonstrated that repression of *StCO1&2* by StCDF1, strongly influences the timing of tuberization onset (Kloosterman, B.

et al., 2013; Ramírez Gonzales *et al.*, 2021). However, it remains unclear whether one or more TPL/TPRs are involved in this regulation in potato.

Recently, Gonzales (2022) reported that StCDF1 not only acts as repressor but also has a function in activating downstream genes, like *Nitrate Transporter 1.7* (*StNRT1.7*). This activation function was also found in some of the CDF family members in *Arabidopsis*. AtCDF4 was found to upregulate endogenous ABA levels by directly activating *AtNCED2* and *AtNCED3* expression (Xu *et al.*, 2020). Furthermore, Gao *et al.* (2022) reported that AtCDF2 physically interacts with AtPIF4 through its DNA binding domain (dof domain) and together activated downstream targets, such as *AtYucca8*. These novel findings suggest that CDF family members have diverse functions in regulating plant development in multiple aspects. However, it remains unclear how StCDF1s activation function is implemented in potato.

As highlighted in various studies and previous chapters, StCDF1 plays a crucial role in regulating multiple pathways such as abiotic stress response, senescence, tuberization onset, nitrate metabolism, and more (Kloosterman, B. *et al.*, 2013; Tai *et al.*, 2018; Ramírez Gonzales *et al.*, 2021). Understanding the regulatory mechanisms of StCDF1 is essential to optimize potato plants to adapt to changing climates and ensure a stable yield. CDF1 functions as a transcription factor, and much of the research has focused on investigating its downstream regulatory network. There has been relatively little investigation into the protein-protein interactions (PPIs) involving StCDF1, particularly in the native environment of potato. For investigating PPIs in plants, several methods have been used like yeast two hybrid (Y2H), Co-immunoprecipitation (Co-IP), and immunoprecipitation or affinity purification combined with mass spectrometry (IP-MS/ AP-MS). Among these methods, Y2H has the advantages of being low in financial costs and easy to perform, but this method has a high labour cost, high false posistive rate and is limited to a non-native environment. Recently, TurboID, an engineered biotin ligase-based proximity labelling (PL) method, has been used to investigate PPIs in several model species (Kim *et al.*, 2019; Arora *et al.*, 2020; Zhang, Y *et al.*, 2020). However, it has not yet been utilized to identify the proximate interactor of a transcription factor in crop plants, like potato.

In the previous Chapter, we established a protocol to apply TurboID based PL in potato. In this study, we utilized this protocol to identify the proximate interactors of StCDF1 in potato. StCDF1.1 was fused with YFP and TurboID to biotinylate interacting proteins. Using control samples and stringent data filtering, we were able to identify 10 nuclear-located proximate candidates of StCDF1, including 2 members of the TPL/TPRs family. Abolishing the binding activity of StCDF1 to these co-repressor (TPL/TPRs) promotes a delayed senescence progression phenotype and enhances the final yield by 50%. Our findings suggest that StCDF1 has other regulatory mechanisms besides repressing downstream genes expression. This novel mechanism may have implications for breeding for improved yield.

Results

TurboID-based biotin labeling in *S. tuberosum*.

We used TurboID to identify the proximal interacting proteins of StCDF1 (Zhang, Yongliang *et al.*, 2019). In this experiment, we inserted the full-length *StCDF1.1* into the destination vector (Kim *et al.*, 2019) by Gateway cloning. The resulting expression vector is *p35S::StCDF1.1-YFP-V5-TurboID* (StCDF1.1-YFP-TbID). The *p35S::YFP-YFP-V5-TurboID* (YFP-YFP-TbID) vector was chosen as negative control (Kim *et al.*, 2019) (Fig. 1A).

To test whether the StCDF1.1-YFP-TbID vector was being expressed, translated and transported into the nucleus, confocal microscopic analysis was performed. The results confirmed that StCDF1.1-YFP-TbID and YFP-YFP-TbID are localized in the nucleus consistent with previously reported AtCDF1 localization (Fig. 1B)(Goralogia, Greg S *et al.*, 2017). Although it has been reported that applying exogenous biotin enhances TbID-mediated biotinylation *in planta* (Feng *et al.*, 2023), it is unclear whether potato leaf material requires extra biotin for sufficient labeling. Therefore, we compared the biotinylation of StCDF1.1-YFP-TbID and YFP-YFP-TbID with and without applying exogenous biotin (10uM) by immunoblots. The biotinylation seemed to be stronger in samples with extra biotin treatment, especially the level of biotinylation of TbID fused protein (**Chapter 4,** Figure 1).

Although a large amount of biotin signal was observed in both StCDF1.1-YFP-TbID samples (with and without extra biotin application), the full-length protein product of StCDF1.1-YFP-TbID was not detected on immunoblots (**Chapter 4,** Figure 1). To determine whether StCDF1.1-YFP-TbID is produced and functional, we performed protein affinity purification and mass spectrometry (MS) analysis on samples of YFP-YFP-TbID and StCDF1.1-YFP-TbID, both with and without extra biotin application. To filter the data for StCDF1.1 proximate candidates, a minimum threshold of two peptide spectrum matches (PSM) and statistical analysis were applied. The result indicates that with and without exogenous biotin treatment, StCDF1.1 was successfully biotinylated and detected by MS, as well as YFP and TurboID (Fig. 1C&D). Without additional biotin, only 1 statistically significant candidate was identified as a nuclear-localized interactor of StCDF1. However, with the addition of extra biotin, this number increased to 155 candidates. Although this result is not conclusive in terms of the benefits of exogenous biotin treatment for TbID-based PL in potato, it does suggest that this application can expand the pool of potential interactors of StCDF1.

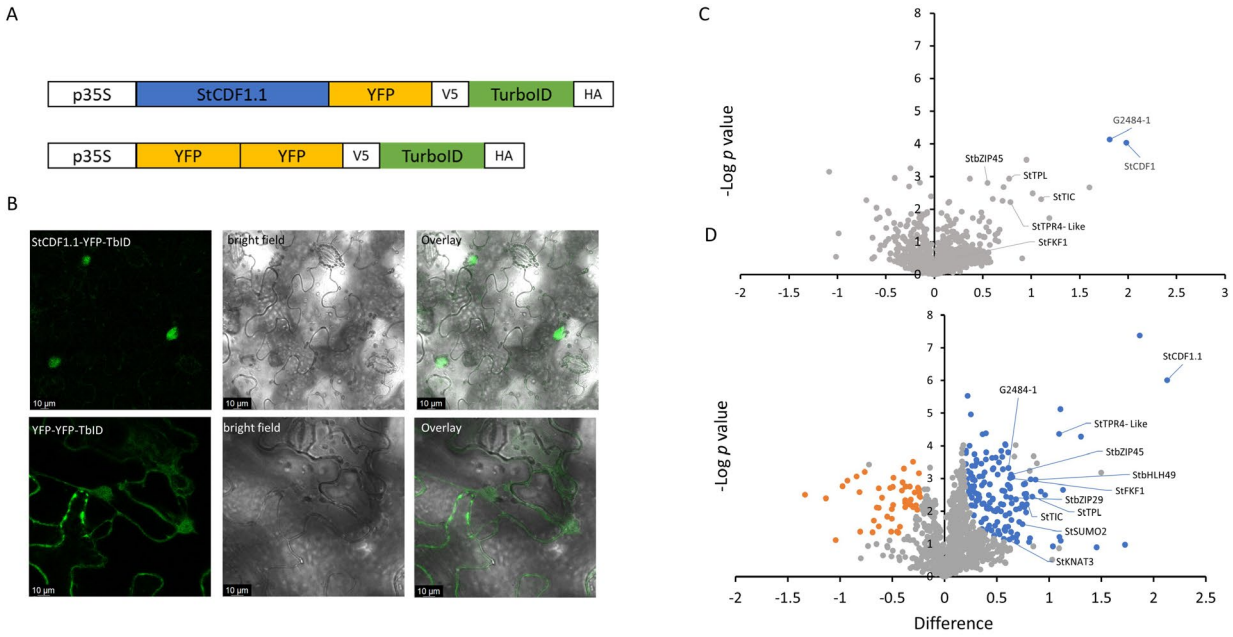

Figure 1. TurboID-based biotin labeling in *S. tuberosum*.
A. Schematic representation of the constructs used for TurboID -based PL. **B.** Confocal fluorescence scanning of StCDF1.1-YFP-TbID and YFP-YFP-TbID. Constructs were transformed into Agrobacterium, then transiently transfected into tobacco (*Nicotiana benthamiana*) leaves. 2 days after infiltration, the leaves were subjected to Carl Zeiss 710 confocal laser scanning microscopy for fluorescence detection. Scale bars: 10 µm. **C.** Volcano plots depicting candidates of StCDF1.1 and their enrichments identified by MS by comparing YFP-YFP-TbID without exogenous biotin treatment. Proteins significantly enriched in StCDF1.1-YFP-TbID samples are shown in blue. Proteins represented by grey dots did not exhibit significant differences in enrichment between StCDF1.1-YFP-TbID and YFP-YFP-TbID. p-value < 0.05. **D.** (C) with 10µM of exogenous biotin treatment.

Identification of StCDF1 interacting proteins

Three biological replicates with extra biotin treatment for StCDF1.1-YFP-TbID and YFP-YFP-TbID were sampled and processed as described in Materials and Methods for subsequent LC-MS/MS analysis. In total, over 1700 proteins were identified by LC-MS analysis and 155 showed significant positive enrichment in StCDF1.1-YFP-TbID samples compared to YFP-YFP-TbID samples (Supplementary Table 1). However, after filtering with subcellular localization, in total 10 statistically significant candidates of StCDF1.1 were found (Fig. 1D, Table.1). As expected, in addition to StCDF1, other proteins known to be interacting with StCDF1 were found, including: the corepressor StTPL/TPRs and clock output protein StFKF1. The presence of these proteins suggests high confidence in the candidates identified by TbID-based PL.

Table 1 The list of proximate candidates of StCDF1.1.

Candidate name	Gene ID	Uniprot ID (Major)	Description
StTPR4- Like	Soltu.DM.07G003470.1	M1D1Q9	WD-repeat protein
StbHLH49	Soltu.DM.01G008020.1	M1AH39	CIB1 LIKE PROTEIN 1
StTPL	Soltu.DM.03G031570.1	M1B3Z5	TOPLESS
StTIC	Soltu.DM.09G024160.1	M1D4M5	Time for coffee
StSUMO2	Soltu.DM.12G023430.1	M1B397	SMALL UBIQUITIN-LIKE MODIFIER (SUMO)
StbZIP45	Soltu.DM.11G019010.1	M1AK43	BZIP transcription factor
StbZIP29	Soltu.DM.01G050330.1	M0ZN09	BZIP transcription factor
StFKF1	Soltu.DM.01G000490.1	M1BRQ0	Circadian clock-associated FKF1
StG2484-1	Soltu.DM.08G024770.1	M1A111	Agenet domain containing protein
StKNAT3	Soltu.DM.08G009980.1	M1B9S2	Class II knotted-like homeobox protein

Full list of candidates identified by MS (Fig. 1E; filtered by statistical analysis and PSM numbers) for both StCDF1.1-YFP-TbID and YFP-YFP-TbID (with exogenous biotin treatment) including gene name, gene ID and description.

StGI protein was expected to interact with StCDF1.1 together with StFKF1 (Kloosterman, B. *et al.*, 2013). However, the StGI peptide was not detected in either the StCDF1 samples with biotin treatment or without. To confirm the identified candidates, we investigated the expression patterns of *StCDF1*, *StG2484-1*, *StbZIP45*, *StTIC*, *StGI*, and *StFKF1* under long-day conditions in CE3027 (background plant used for PL) (Fig. 2). Zeitgeber Time (ZT) was used to indicate the light period, with ZT0 being the start of the light period and each subsequent hour represented by the next sequential number (e.g., ZT1 represents one hour after the start of the light period). We observed that StCDF1 expression peaked at the beginning of the light period (ZT0) and gradually decreased until ZT6, with a small peak just before the end of the light period (ZT15). The expression patterns of StG2484-1 and StbZIP45 suggest that the potential interaction likely occurred during the early part of the light period (ZT0-ZT6). Our results are consistent with previous reports indicating that blue light-mediated StCDF1 degradation via binding to FKF1 occurs during the latter part of the light period. Surprisingly, *StTIC* has a very similar expression pattern to *StGI* and *StFKF1*, which peaks at ZT9. This suggests that *StTIC* might be a novel player involved in light regulation of StCDF1.

Furthermore, the PL samples were harvested in between ZT7-9. The capturing of potential interactors which are expressed at different periods of the day suggests the PL results do not just reveal the interactions that occur at the instant of harvesting but also interactions that occur for at least some time before harvesting.

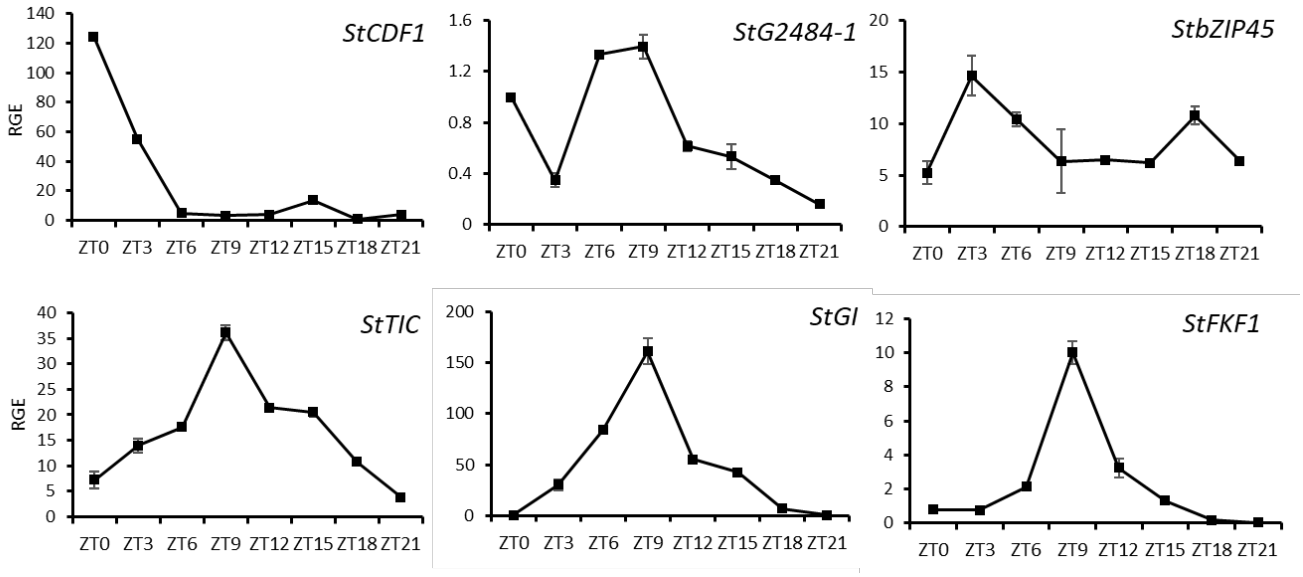

Figure 2. Expression analysis of StCDF1.1 proximate candidates and StCDF1.1 in CE3027. Expression of selected StCDF1.1 interacting candidates, mRNA levels were measured in long-day control conditions. Leaf samples were harvest at 32 DAP. ZT: Zeitgeber time. Error bars: mean± SE with n = 3 replicates.

StCDF1 represses downstream genes expression by interacting with TOPLESS

The repressing function of StCDF1 plays a major role in regulating the expression of downstream targets, like *StCOL* (Kloosterman, B. *et al.*, 2013). However, StCDF1 cannot carry out this repression function alone and requires the assistance of a co-repressor. 10 potential interactors of StCDF1 were identified using PL, with two of them being members of the TPL/TPRs family. Whereas *Arabidopsis* has 5 TPL/TPRs encoding genes, henceforth named AtTPL/TPRs, 6 loci were identified in the *S. tuberosum* genome, corresponding to the following accessions in Potato Genomics Resource database (Hirsch *et al.*, 2014) : *StTPL*: Soltu.DM.03G031570, *StTPR1-Like*: Soltu.DM.08G010780, *StTPR2*: Soltu.DM.08G021760, *StTPR3*: Soltu.DM.01G039780, *StTPR4*: Soltu.DM.03G030810.1 and *StTPR4-Like*: Soltu.DM.07G003470. To understand the co-repressor preference of StCDF1, we analyzed the phylogenetic relationships of TPL/TPRs proteins in Arabidopsis, tomato, and potato (Fig. 3A). We found that StTPL1-LIKE was distinct from the rest of the family, and we consider this to be an annotation error that we excluded from our subsequent analysis. The tree topology revealed that the *Arabidopsis* genes *AtTPL* and *AtTPR1* formed a distinct cluster separated from other *AtTPRs*, possibly due to a singular duplication event. This could explain why there is no *StTPR1* but only *StTPL* present in the potato genome. Conversely, a duplication event exclusive to *Solanum* was found in TPR4, with both the potato and tomato genomes containing one copy each of StTPR4 and StTPR4-Like.

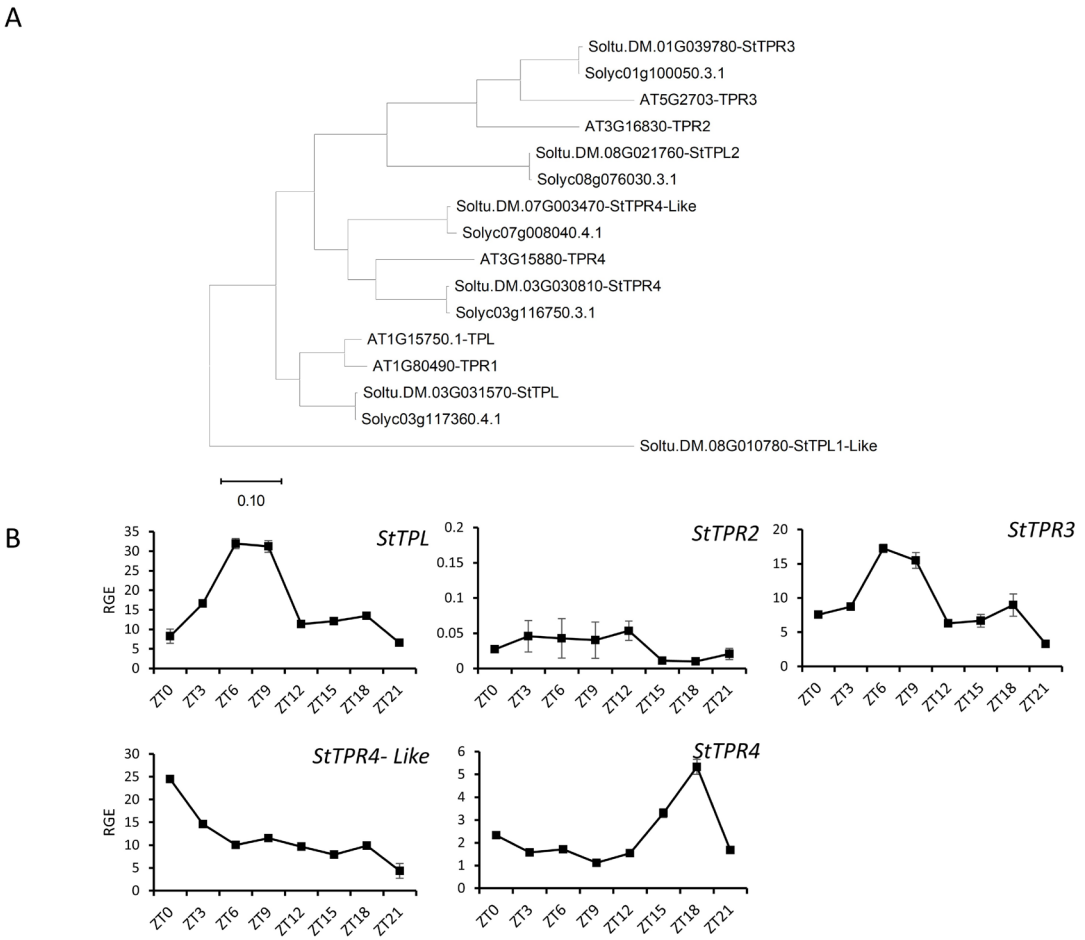

Figure 3. StCDF1 represses downstream genes expression by interacting with TOPLESS. **A.** Phylogenetic relationship of Arabidopsis, tomato and potato TPL and TPR proteins. 6 orthologs were found in both *Solanaceae* species. In potato, they were named as follows: *StTPL,StTPR1-Like, StTPR2, StTPR3, StTPR4 and StTPR4-Like.* **B.** Expression of selected *StTPL/TPRs.* Same samples as **Fig.2**. ZT: Zeitgeber time. Error bars: mean ± SE with n = 3 replicates.

TPL/TPR proteins are known to be critical components of circadian clock regulation (Plant *et al.*, 2021), but their expression patterns throughout the day have not been previously demonstrated. In this study, we investigated the 24-hour time course of all five potato TPL/TPR members and discovered that *StTPL*, *StTPR3*, and *StTPR4-Like* are upregulated during the early light period (ZT0-ZT6), while *StTPR4* is predominantly expressed during the night and *StTPR2* shows low expression throughout the full 24 hours. Notably, the expression pattern of *StTPR4-Like* closely resembles that of *StCDF1*, suggesting that these two genes may be co-regulated by the same circadian clock genes. It is worth mentioning that StTPR3 peptides were detected in MS and comparatively enriched in StCDF1.1-YFP-TbID samples (Supplementary Table 1), although the difference was not statistically significant. Therefore, we propose that the repression function of StCDF1 is dependent on recruiting StTPL, StTPR3 and StTPR4-Like at dawn.

Opposite effects, equal outcomes: StCDF1 repression function manipulation boosts yield by 50%

Protein-protein interactions often require specific motif recognition. Goralogia, Greg S *et al.* (2017) previously described the physical interaction between CDF1 and TPL, which revealed a short conserved sequence (IKLFG) at the N-terminal ends of AtCDFs and almost all CDF-related DOF transcription factors. This IKLFG motif, known to bind to TPL, is highly conserved among CDF-like DOF proteins found throughout land plants, including StCDF1 in potato (Goralogia, Greg S *et al.*, 2017). Finding StTPL/TPRs in the StCDF1 PL result provides additional confirmation that this interaction is common across plant species (Goralogia, Greg S *et al.*, 2017; Renau-Morata *et al.*, 2020). Interestingly, recent evidence suggests that StCDF1 might have an activation function in regulating the expression of downstream genes (Gonzales, 2022). To test whether this activation function relies on binding to TPL, we designed the following experiments. First, we synthesized three variants of StCDF1.2: one with mutations to the TPL binding domain (*StCDF1.2^{Coed} ΔTPL*), one with mutations to the DNA binding domain (*StCDF1.2^{Coed} Δdof*), and one without any mutations (*StCDF1.2^{Coed}*), which served as a control (**Chapter 2**). Codon optimization was applied to all three variants to eliminate post-transcriptional regulation or RNA-RNA interaction with *StFLORE* transcript (Ramírez Gonzales *et al.*, 2021). We selected *StCDF1.2* as the backbone for all variants to enhance protein stability by preventing ubiquitination mediated by binding to FKF1. Then, we overexpressed these variants using the 35S CaMV promoter in the CE3027 (StCDF1.1 homozygous) background.

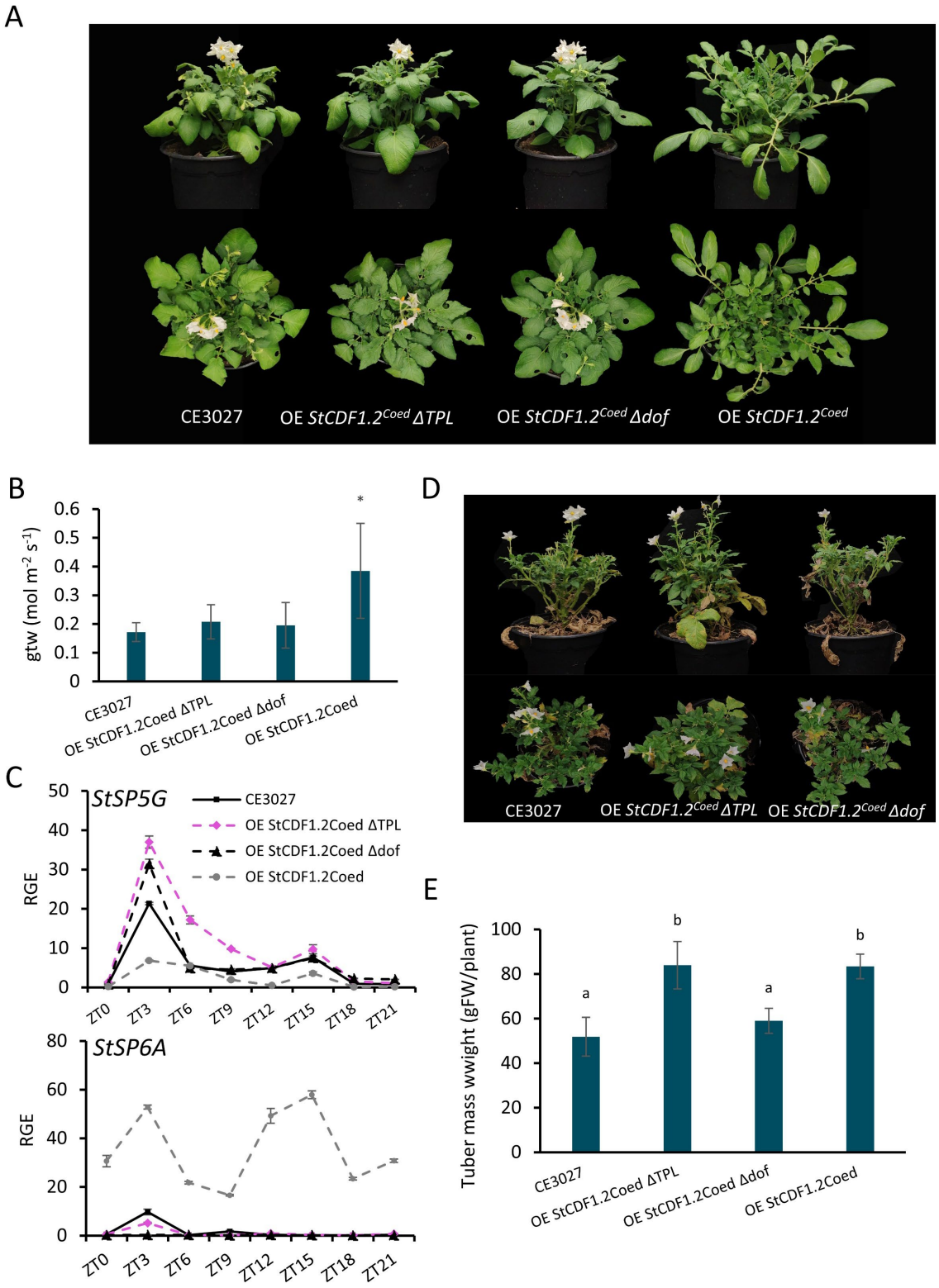

Figure 4. StCDF1 repression function manipulation boosts yield by 50%.

A. Phenotype of CE3027 (late maturing, homozygous for StCDF1.1), OE *StCDF1.2*^{Coed} *ΔTPL*, OE *StCDF1.2*^{Coed} *Δdof* and OE *StCDF1.2* ^{Coed} transgenics, at 32 DAP. **B.** Measurement of transpiration using total conductance (gtw) at 32 DAP(ZT3). Error bars: means ± SE, with n = 9 replicates. Letters indicate groups that are statistically significantly different from each other (t-test, *p < 0.05). **C.** Gene expression analysis of CE3027 wild type and OE *StCDF1.2*^{Coed} *ΔTPL*, OE *StCDF1.2*^{Coed} *Δdof* and OE *StCDF1.2* ^{Coed} transgenics. Expression of tuberization

related genes: *StSP5G* and *StSP6A*, mRNA levels were measured in long-day control conditions. Leaf samples were harvest at 32 DAP. ZT: Zeitgeber time. Error bars: mean ± SE with n = 3 replicates. **D.** Phenotypes of CE3027, OE *StCDF1.2^{Coed} ΔTPL* and OE *StCDF1.2^{Coed} Δdof* transgenics at 95 DAP. **E.** Measurement of tuber mass weight at final harvest (95DAP). Error bars: means ± SE, with n = 5 replicates. Letters indicate groups that are statistically significantly different from each other (t-test, *p < 0.05).

Unlike OE *StCDF1.2^{Coed}* transgenics, the over expression of *StCDF1.2^{Coed} ΔTPL* and *StCDF1.2^{Coed} Δdof* transgenics exhibit nearly identical plant morphologies, including plant height, flowering time, and other characteristics (Fig. 4A). Further examination of physiological parameters such as transpiration (gtw) revealed no significant differences between OE *StCDF1.2^{Coed} ΔTPL*, OE *StCDF1.2^{Coed} Δdof* and CE3027 (Fig. 4B). Additionally, tuberization onset occurs at the same time in the OE *StCDF1.2^{Coed} ΔTPL* and OE *StCDF1.2^{Coed} Δdof* transgenics as in CE3027, while OE *StCDF1.2^{Coed}* transgenics exhibit an earlier onset by 2 weeks. To confirm the tuberization phenotype we examined the expression pattern of *StSP6A* and *StSP5G* in these transgenics and CE3027 (Fig. 4C). As expected, both OE *StCDF1.2^{Coed} ΔTPL* and OE *StCDF1.2^{Coed} Δdof* transgenics exhibit a very similar pattern of expression of StSP5G and StSP6A compared to CE3027, while OE *StCDF1.2^{Coed}* transgenics show repression of *StSP5G* expression and increased *StSP6A* expression. Based on our analysis of the expression patterns of downstream genes of *StCDF1*, we have determined that the repression function of StCDF1 has been successfully abolished by creating mutations in either the TPL binding domain or the DNA binding domain (dof). Furthermore, the distinct phenotypic differences observed among these three transgenics suggest that the repressing function controls the majority of downstream regulations and the corresponding phenotypes.

Consistent with our previous observation **(Chapter 2)**, overexpression of *StCDF1.2^{Coed}* in CE3027 significantly shortened the life cycle. However, overexpression of the other two *StCDF1.2* variants did not significantly affect the life cycle length. Strikingly, a delayed senescence progression phenotype was found in the OE *StCDF1.2^{Coed} ΔTPL* transgenics during the later stage of development, but not in the OE *StCDF1.2^{Coed} Δdof* transgenics (Fig. 4D). Furthermore, over 50% of yield increase was achieved by overexpressing *StCDF1.2^{Coed} ΔTPL* and *StCDF1.2^{Coed}*, but not *StCDF1.2^{Coed} Δdof* (Fig. 4E). It has been reported that overexpressing *StCDF1.2* in a late-tuberizing background, such as CE3027, leads to an increase in yield, which was concluded to be due to the promotion of early tuberization (Kloosterman, B. *et al.*, 2013). However, the tuberization onset remains late in OE *StCDF1.2^{Coed} ΔTPL* transgenics as in its background CE3027 but achieved around the same amount of yield increase as OE *StCDF1.2^{Coed}* transgenics. Overall, out of all the transgenics tested, only the OE *StCDF1.2^{Coed} Δdof* transgenics line showed minimal phenotypic variation compared to the background CE3027. Previously, we showed that both the TPL and DNA binding (dof) domains are critical for StCDF1's repression function. Here, we present additional evidence suggesting that the dof domain of StCDF1 exerts more downstream regulatory effects than its TPL binding domain. By abolishing the binding ability of StCDF1 to TPL/TPRs, we revealed the hidden function of StCDF1 in regulating senescence progression, which may contribute to the increase in final yield.

We observed a distinct phenotype of OE *StCDF1.2*^{Coed} *ΔTPL* transgenics on senescence progression and increased yield. It remains unclear whether these phenotypes result from overexpressing *StCDF1.2*^{Coed} *ΔTPL*, which may have strengthened the activation function. To test whether *StCDF1.2*^{Coed} *ΔTPL* has an activation function, we selected a downstream candidate genes *StNCED3-2* and *StNCED4* to test in this experiment (Gonzales, 2022)(**Chapter 3**). Previous studies have reported that CDF4 can directly and positively regulate *NCED3* in *Arabidopsis* (Xu *et al.*, 2020). We followed the expression of the potato *StNCED3-2* and *StNCED4* throughout the day in these transgenics and CE3027. Both *StNCED3-2* and *StNCED4* expression was repressed in OE *StCDF1.2*^{Coed} transgenics (Fig. 5). Interestingly, *StNCED3* expression was strongly upregulated in OE *StCDF1.2*^{Coed} *ΔTPL* transgenics, especially at the beginning of the night break (ZT15) (Fig. 5). Moreover, no induction nor repression was found in OE *StCDF1.2*^{Coed} *Δdof* transgenics. These findings provide both phenotypic and molecular evidences that StCDF1 has a separate regulation mechanism independent of repressing downstream gene expression by recruiting co-repressors.

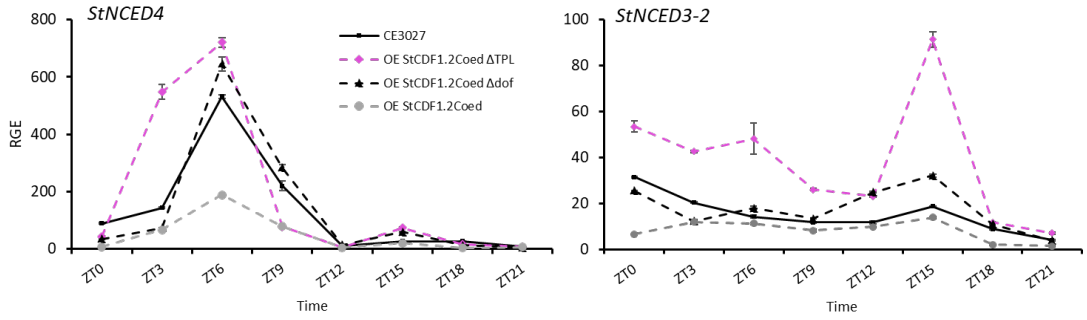

Figure 5. StCDF1 repression function manipulation affect downstream gene expression differently. Expression of *StNECD3-2* and *StNCED4* in the same samples as Fig.4(C). Error bars: mean ± SE with n = 3 replicates.

Discussion

The regulation of potato plant development through the photoperiodic pathway is a complex process that relies on a sequential and interdependent expression of many genes, both at the transcriptional and post-transcriptional levels. Our previous work found that allelic variations of StCDF1 influence many important agronomic traits, including tuberization onset, abiotic stress tolerance, and disease resistance, among others (Visker, 2005; Kloosterman, B. *et al.*, 2013; Ramírez Gonzales *et al.*, 2021; Hoopes, G *et al.*, 2022). StCDF1, as an upstream transcriptional regulator, acts as a central hub in the regulation of diverse traits related to potato plant development. Therefore, it is important to build understanding of the molecular mechanisms of StCDF1 in regulating different pathways independently and cooperatively.

The most well-known molecular mechanism of CDF1 is the repression of downstream gene expression *via* recruiting the co-repressor TPL (Goralogia, Greg S *et al.*, 2017). In this study, we confirmed this interaction in the native *in vivo* conditions of potato by performing proximity

labeling (PL) to screen all the proximal interactors of StCDF1. Our results suggest that during the early period of the day, StCDF1 is likely to employ StTPL, StTPR3, and StTPR4-Like to suppress the expression of downstream genes in leaves. Beside these three members of TPL/TPR, our expression analyses suggest that *StTPR2* has very low expression throughout the day in leaf material and *StTPR4* is primarily expressed during the dark period, so it is likely that they have functions in different tissues or during different periods of time. Interestingly, a previous study has reported that the TPR2 ortholog in tomato (SlTPR2) is exclusively recruited by a member of the Ethylene response factors (SlERF.F12) in regulating fruit ripening (Deng *et al.*, 2022). These results provide important insights into the spatiotemporal distribution and function of different TPL/TPR members in various pathways, contributing to a better understanding of their roles in potato plant development.

In this study, we also confirm our previous finding that StFKF1 interacts with StCDF1.1. However, we did not find GI in the PL results of StCDF1.1. Considering that StFKF1 has a similar expression pattern to StGI, and StFKF1 was successfully labeled and retrieved by MS, we could eliminate the possibility of unpreferred harvesting time or unpreferred choice of background genotype. As has been discussed in many PL experiments, missing one or several known interactors of the protein of interest in PL is a common issue (Sanchez & Feldman, 2021; Feng *et al.*, 2023). Interestingly, we uncovered a novel proximal interactor of StCDF1, namely StTIC. Notably, StTIC is involved in regulating the circadian clock and is positioned upstream of GI, functioning in close proximity to the central oscillator (Hall *et al.*, 2003; Ding *et al.*, 2007; Wang *et al.*, 2022). Although TIC is a non-transcription factor, it has been shown to affect downstream genes in both transcriptional and post-translational levels (Wang *et al.*, 2022). However, there is limited understanding of these molecular mechanisms. A recent *Arabidopsis* study showed that TIC physically interacts with TPL to jointly repress the expression of downstream genes, including *PhyA* (Wang *et al.*, 2022). Interestingly, the potato ortholog of *PhyA* has been reported to be a direct downstream gene of StCDF1 in potato (Gonzales, 2022). In this study, we found both StTIC and StTPL/TPRs in the StCDF1.1 PL-MS results. StTIC and StCDF1 have distinct types of TPL interacting domains, StTIC contains an Ethylene-responsive element binding factor-associated Amphiphilic Repression (EAR) motif, while StCDF1 has the non-EAR TPL recruitment motifs ([R/K]LFGV)(Goralogia, Greg S *et al.*, 2017; Leydon *et al.*, 2020; Renau-Morata *et al.*, 2020; Wang *et al.*, 2022). As a result, these proteins are likely to bind to different positions on TPL (Leydon *et al.*, 2020), which suggests that there is no competition between StTIC and StCDF1 for binding to StTPL/TPRs. Revealing whether these three proteins form a complex and together regulate downstream genes express requires further experiments.

In addition to the light-dependent protein degradation mediated by FKF1, our study also identified a member of the SUMO protein family as a proximal interactor of StCDF1.1, using PL-MS analysis. In *Arabidopsis*, it has been shown that AtCDF2 can be SUMOylated by AtSUMO3, and this posttranslational modification was found to have a negative impact on protein abundance (Budhiraja *et al.*, 2009; Elrouby *et al.*, 2013). Our results suggest that StCDF1.1 is likely to undergo a similar posttranslational modification by interacting with StSUMO2. More experiments need to be carried out to study the StCDF1.1 SUMOylation and its regulatory consequences.

Previous studies have suggested that CDFs not only act as repressors but can also activate downstream gene expression directly (Xu *et al.*, 2020; Gao *et al.*, 2022; Gonzales, 2022). In this study, we generated overexpression lines of OE *StCDF1.2*^{Coed} *ΔTPL*, OE *StCDF1.2*^{Coed} *Δdof* and OE *StCDF1.2*^{Coed} to investigate the mechanism of the StCDF1 activation function. Our data revealed that the DOF DNA binding domain is required for both repressing and activating downstream gene expression. Abolishing the TPL binding site of StCDF1 inhibited its repressive function and enhanced its activation effect. However, the expression pattern analysis of *StSP6A*, *StSP5G*, and *StNCED3* in all transgenics and their background (CE3027) indicated that not all downstream genes of StCDF1 could be regulated in both ways. This selective activation suggests that StCDF1 might require the assistance of another protein with DNA binding ability to activate specific downstream genes. Recently, Gao *et al.* (2022) described a mechanism wherein AtCDF2 and PHYTOCHROME-INTERACTING FACTOR 4 (AtPIF4) interact to form a protein complex and together promote downstream gene expression, such as *AtYUCCA8*. However, StPIF4 was not detected in StCDF1.1 PL-MS in this study. In addition, one basic helix–loop–helix transcription factor (StbHLH49) and two basic leucine-zipper transcription factors (StbZIP29 and StbZIP45) were found to be labeled by StCDF1.1-YFP-TbID. To identify which of these candidates are a co-activator of StCDF1, more evidence is required from future research.

As described in previous Chapters, StCDF1 regulates senescence in multiple aspects: senescence onset, senescence progression and total life cycle. Here, we provide further evidence that that StCDF1 can specifically regulate senescence progression without affecting onset or total life cycle. The delayed senescence progression associated with over 50% tuber mass weight increase was found in OE *StCDF1.2*^{Coed} *ΔTPL*. However, OE *StCDF1.2*^{Coed} transgenics also exhibited tuber mass weight increase by 50%, but the total life cycle was greatly shortened. These findings suggest that StCDF1 has a nuanced role in regulating senescence and can be targeted to selectively modulate specific aspects of the process.

Materials and Methods

Constructs for TurboID based PL, TbID-based PL in potato and Immunoblotting

The step by step protocol for generating constructs for TurboID, preforming TurboID based PI in potato and testing PL efficiency with immunoblotting is described in **Chapter 4.**

Proteomics data analysis

The sample preparation for LC–MS/MS was essentially performed as described in (van Mourik *et al.*, 2023). The IP eluate was diluted four times with 50 mM ammonium bicarbonate (Fluka), followed by cysteine residues reduction with 7.5 mM DTT (Fluka) and carbamidomethylation with 15 mM iodoacetamide (GE Healthcare). Proteins were digested with 0.75 µg of trypsin (Trypsin Gold, Mass Spectrometry Grade; Promega) overnight at room temperature. The next day, the trypsin was inactivated by supplying 10%TFA until pH < 4. All samples were filtered through homemade double C8-Filters into a 0.5ml low binding epp tube. The beads were washed with 100 ul 50% AcNi/50% 1ml/l HCOOH in water and filter/eluted the sup into the

same ep. The samples were dried down to 10µl using SpeedVac to remove all acetonitrile. The final volume was brought back to 50 µl with 1ml/l HCOOH in water.

Samples were measured by nLC-MS/MS with a Proxeon EASY nLC1000 and a Exploris 480 mass spectrometer as previously described (Feng *et al.*, 2022). LC-MS data analysis (false discovery rates were set to 0.01 on peptide and protein levels) and additional result filtering (minimally 2 peptides are necessary for protein identification of which at least one is unique and at least one is unmodified) were performed as described previously(Smaczniak *et al.*, 2012; Wendrich *et al.*, 2017) . To analyze the relative abundance of proteins, their normalized label-free quantification (LFQ) intensities were compared (Cox 2014). nLC-MSMS system quality was checked with PTXQC (Bielow *et al.*, 2016) using the MaxQuant result files.

Label-free quantification (LFQ) values from the 'proteinGroups.txt' output file of the MaxQuant were taken (Cox *et al.*, 2014)or further analysis in Perseus (version 1.6.15.0) (Tyanova et al., 2016).

Plant Materials and Growth Conditions

The wild-type diploid potato genotype CE3027 (homozygous for StCDF1.1/1.1) was used as background plant for generating transgenics. CE3130 carried two copies of truncated StCDF1 alleles (StCDF1.2/13). Both genotypes are offspring of C (USW5337.3) X E (VPH4 77.2102.37)(Celis-Gamboa, 2002; Kloosterman, B. *et al.*, 2013). The different version Condon edited *StCDF1.2* were synthesized (sequences alignment in Supplementary Figure 1) by Genscript and cloned into into the pENTR™/D-TOPO vector (Invitrogen™; K240020) and then PK7GW2 by LR reaction (Invitrogen™; 11791020). Then, performed Agrobacterium-mediated gene transformation to introduce the destination vector into the late-tuberizing and senescence background potato, CE3027. For each construct, two transgenic lines (OE *StCDF1.2* ^{Coed} 1#& 2#, OE *StCDF1.2* ^{Coed} *ΔTPL* 6#& 9#, and OE *StCDF1.2* ^{Coed} *Δdof* 9#& 11#,) from independent transformation even were used in this study.

All potato plant used in this experiment were maintained in *vitro* on MS20 at 24 °C under long day condition (16h light and 8h dark). Two week old tissue culture plants were transferred into 19cm pot with soil. The plants grown in a climate chamber, under control conditions of 16 h light (22 °C) and 8 h dark (18 °C)(LD, long day condition).

RNA sampling, isolation and quantitative PCR

The leaf material sampling for RNA was harvest with plant which have been grown in soil for 4 weeks. The RNA was isolated using MagMAX™ Plant RNA Isolation Kit (A33899) with the KingFisher™ Flex Purification System (5400610). The iScript™ cDNA Synthesis Kit was used for cDNA synthesis, following the manufactory instruction . *StELF3e* was used as a house keeping control, and primers for qPCR are listed in Supplemental Table 2.

Transpiration measurement

The parameters of transpiration were measured by LI-600 porometer/fluorometer (https://www.licor.com/env/products/LI-600) at ZT3, following the manufacturer's guidelines. For each plant line, 12 measuring were performed.

Phylogenetic Analysis

The complete protein sequences for phylogenetic analysis were retrieved from Spud DB potato genomic resource (http://spuddb.uga.edu/), The Arabidopsis Information Resource (TAIR, https://www.arabidopsis.org/) and Solanaceae Genomics Network (https://solgenomics.net/)(Supplementary Table 3). The protein sequences were aligned using the ClusterW method, and then phylogenetic analysis was performed by applying the Maximum Likelihood method with the default settings in MEGA11.

Confocal microscopy

The leaf of 4 week old *Nicotiana benthamiana* were infiltrated with a final concentration of 0.3 OD600 *Agrobacterium* with YFP-YFP-TbID and StCDF1-YFP-TbID separately. After 48h, leaf tissues were mounted on slides and imaged on an SP8 confocal microscope (Leica Microsystems, Heerbrugg, Germany).

Acknowledgements

This research is supported by Solynta and Aardevo. L.S. is supported by China Scholarship Council (No. 201807720077). We acknowledge the Wageningen University & Research, Unifarm greenhouse and Klima employees for their help with the maintenance of the plants.

Author Contributions

LS and CB designed the research. LS performed a large part of the experiments and analysed data. LS drafted the manuscript. LS, CB and RGFV revised the manuscript. All authors read and approved the final manuscript.

Supplementary Material

The following Supplementary materials are available to be download from the "Supplementary materials PhD thesis_ Shi(2023).zip" file, and thus only legends are shown below.

Supplementary Table 1. Statistical source data for Figure 1D&E.

Supplementary Table 2. Specific primer pairs for qRT-PCR reaction.

Supplementary Table 3. TPL/TPR homologues in 3 plant species.

Supplementary Data 1. The MS proteomics data in this experiment.

Supplementary Figure 1. Condon edited *StCDF1.2* sequences alignment.

Chapter 6

General Discussion

General Discussion

The life cycle of plants is the succession of phases from germination to death. After germination, plants enter a vegetative growth phase, rapidly increasing in photosynthetic capacity, size, and mass (Huijser & Schmid, 2011). This phase is vital for their eventual reproductive success. The transition to the reproductive phase marks a critical point in the life cycle, enabling plants to flower and produce fruits or seeds (Huijser & Schmid, 2011). Simultaneously, senescence occurs, leading to the relocation of nutrients from vegetative organs to reproductive organs (Miryeganeh, 2021). Each of these phases relies on the other and supports the central aim of reproduction. Understanding each phase is crucial, especially for crop plants involved in food production.

In the life cycle of plants, nearly all cells, tissues and organs undergo a process of senescence and eventual mortality. Throughout the senescence process, plants integrate a variety of internal and external signals, along with information regarding their developmental stage, via complex regulatory pathways (Guo *et al.*, 2021). Environmental signals, such as increased temperature and limited water availability, can induce stress responses in plants, which can subsequently lead to premature senescence and a reduction in yield (Sasi *et al.*, 2022). The senescence process can be associated not only with abiotic stress but also with biotic stress. Pathogen infections can trigger programmed cell death, which share molecular pathways with senescence processes (Zhang *et al.*, 2021). In addition to external stresses, the signaling of plant senescence is also influenced by various internal factors such as circadian rhythm, source-sink relationship, hormonal signaling, nutrient availability, etc. (Thomas, 2013; Guo *et al.*, 2021; Sasi *et al.*, 2022). Undoubtedly, leaf senescence significantly impacts agronomy of plants, such as yield, biomass, and nutritional composition. Manipulating leaf senescence is of great importance in plant breeding programs due to its profound influence on plant productivity.

Potato (*Solanum tuberosum* L.) is a widely cultivated non-grain staple food crop (FAO, 2019) and is renowned globally for its use in cooking popular dishes. In addition, it serves as a valuable raw material for industrial applications such as starch production, animal feed, and biofuel production (Semeijn & Buwalda, 2018; Natarajan *et al.*, 2019; Awogbemi *et al.*, 2022). The tuber yield production is influenced by diverse traits. Tuberization onset timing and senescence are two tightly linked traits, which together affect final yield.

The senescence and tuberization onset respond to seasonal cues, including temperature variations and day length. These cues play a crucial role in initiating growth cycles and inducing dormancy in many herbaceous perennials. The potato, often seen as an annual crop, possesses an intriguing botanical characteristic: it is actually a herbaceous perennial. Additionally, the equatorial Andes, the native region of potatoes, experiences minimal pronounced seasonal changes. This raises intriguing questions about how potatoes have evolved to perceive and respond to these potentially subtle environmental cues.

In the research described in this thesis, I investigated the tight link between tuberization onset and leaf maturity by exploring the molecular function of the StCDF1 (*CYCLING DOF FACTOR 1*) locus, which is a clock regulator and has been genetically linked to both traits.

StCDF1 regulates different aspects in the senescence process

Leaf senescence is a highly regulated and complex process. During this process, nutrients are released from senescent leaves and subsequently mobilized to support the growth of other leaves, developing seeds, or storage tissues (Thomas, 2013; Schippers *et al.*, 2015). The efficient mining and recycling of nutrients during senescence are crucial for achieving high yields in crops, such as potato.

Similar to other leaf developmental stages, senescence can also be dissected into different aspects. Smart (1994) outlines a framework for leaf senescence, which involves several phases. The process starts with the recognition of internal and external cues, followed by a genetic switch activation. Subsequently, carbohydrates and lipids are broken down, proteins and nucleic acids degrade, and essential nutrients are reallocated. Accumulation of free radicals leads to oxidative stress, culminating in leaf necrosis and death. Externally, the leaf undergoes a color change from green to brown.

To investigate gene expression changes throughout these different senescence stages, various experimental approaches have been employed, including microarray analysis, mRNA sequencing, Northern blot analysis, and differential screening through subtractive hybridization techniques (Lim *et al.*, 2003; Sasi *et al.*, 2022). This comprehensive analysis has revealed that during plant leaf senescence, coordinated waves of gene expression occur, with different senescence-related genes being activated and deactivated at specific stages of the process (Smart, 1994; Buchanan-Wollaston, 1997; Sasi *et al.*, 2022). These coordinated waves drive the progression of leaf senescence towards its ultimate endpoint: death. Despite the identification of a large number of genes involved in different stages of senescence through high-throughput sequencing technologies, the mechanisms underlying the coordinated regulation among these genes remain unclear.

The *StCDF1* locus was functionally linked to leaf maturity/senescence in many previous genetic and molecular studies (Visker, 2005; Kloosterman, B. *et al.*, 2013). Previous observations suggest the truncated StCDF1 alleles (StCDF1.2/1.3) induced early tuberization onset but shortened life cycle (Kloosterman, B. *et al.*, 2013). This thesis offers a comprehensive examination of the effects of the *StCDF1.2* allele on various aspects of senescence through detailed observations (**Chapter 2**). Our findings reveal that plants carrying the *StCDF1.2* allele show both delayed onset of senescence and accelerated progression, resulting in a shortened life cycle. Furthermore, our research highlights an additional discovery: StCDF1 also has the ability to independently regulate the progression of senescence, distinct from its effects on senescence onset and the overall life cycle (**Chapter 5**). These intriguing findings suggest that different senescence aspects can be regulated by the same transcription factor, even in opposite ways.

In **Chapter 2**, we identified a direct downstream target of StCDF1, namely *StORE1S02* (*ORESARA1*), which is a senescence regulator specifically regulating senescence onset in potato. Moreover, we uncovered the role of StORE1S02 in positively regulating sugar transportation during senescence by activating expression of *StSWEET11* and *StSWEET15/SAG29*. Interestingly, our previous work demonstrated the mobile “tubergen”,

namely StSP6A, which physically interacts with StSWEET11 to promote symplasmic transport of sucrose and tuber formation (Abelenda *et al.*, 2019). Hereby, we provide molecular evidence that StCDF1 regulates tuberization not only by indirectly promoting the expression of *StSP6A*, but also indirectly influences expression of sugar transporters, such as *StSWEET11* and *StSWEET15/SAG29*.

Potatoes, being tuber crops, heavily rely on the efficient transport of carbohydrates from leaves to stolons to achieve optimal yields (Dahal *et al.*, 2019). While it has been demonstrated in various other crops that delayed senescence enhances yield (Lira, Bruno S *et al.*, 2017; Joshi *et al.*, 2019; Li *et al.*, 2022), applying the same principle to potatoes may not yield the same results due to the concurrent processes of sugar relocation and senescence onset. When *StORE1S02* expression was knocked down in an early tuberizing/ short life cycle background, it resulted in extended life cycle accompanied by sugar accumulation in the leaves. Despite the delayed senescence observed, it is important to note that this did not result in an improvement in the final yield (**Chapter 2**). One factor that hindered the overall productivity was the high sugar accumulation in the leaves, which may in turn inhibit photosynthesis (Kühn *et al.*, 1996). As a consequence, the extended lifespan of the leaves, caused by blocked sugar transportation, failed to generate optimal carbohydrate yields. Therefore, a strategic mindset is crucial when breeding potatoes for extended life cycles and delayed senescence, with a specific focus on targeting the right pathways.

The pathways involved in regulating senescence are complicated. In many *Arabidopsis* studies, many flowering related genes were found to also have an impact on senescence, such as *GI* (*GIGENTEA*), *KHZ1&2* (*CCCH zinc-finger and K-homolog1&2*), *HDA6* (*histone acetyltransferases and histone deacetylases 6*), *PIFs* (*PHYTOCHROME INTERACTING FACTORs*), etc. (Wu *et al.*, 2008; Kumar *et al.*, 2012; Yan *et al.*, 2017; Kim *et al.*, 2020; Li, Na *et al.*, 2021; Sasi *et al.*, 2022). However, this interconnection between reproduction and senescence is largely unknown. The role of StCDF1 in senescence initiation is intriguing, particularly its influence on sugar transportation. Moreover, StCDF1 plays a crucial role in promoting the reproductive process of tuberization, which depends on the efficient transport of sugars from source to sink (Abelenda *et al.*, 2019). These molecular connections provide valuable insights into the concurrent phenotypes observed in both senescence and tuberization, both of which are regulated by StCDF1. In commercial breeding programs, selecting high-yield potential potato varieties often involves prioritizing the combination of early tuberization and a long lifecycle. For selecting early tuberizing genotypes, the truncated *StCDF1* alleles were primarily inadvertently selected in breeding programs. Carrying truncated *StCDF1* alleles can subsequently influence the sugar signaling pathway involved in senescence regulation. Although this link is tight, we believe that it is not impossible to prolong the life cycle/stay-green in early tuberizing genotype to obtain better yield.

Increasing the crops' photosynthesis period and breeding for functional stay-green have been prominent objectives in crop improvement over the past decades(Thomas & Howarth, 2000; Vadez *et al.*, 2013; Thomas & Ougham, 2014). Thomas and Howarth (2000) described several ways for plants to stay green: Type A stay-green refers to the ability of plants to maintain a steady level of chlorophyll and photosynthesis until just before the grains reach physiological

maturity, after which there is a sudden decline. On the other hand, type B stay-green is characterized by a gradual senescence process, where the decline in chlorophyll content and photosynthetic rate occurs at a slower pace. For cosmetic or non-functional stay-green, such as in the case of dried or frozen green leaves or simply inhibiting the degradation of chlorophyll, the plants maintain their green color and chlorophyll activity, but experience a reduction or complete loss of photosynthetic capacity. The delayed senescence progression and the corresponding increase in yield observed in OE *StCDF1.2*^{Coed} *ΔTPL* transgenic plants (**Chapter 5**) can be classified as Type B, representing functional stay-green. However, the stay-green phenotype in *StORE1S02* knock down transgenics is a non-functional stay-green, due to the reduced photosynthesis by high sugar accumulation in leaf. It is evident that functional stay-green traits are more favorable in crop breeding compared to mere 'cosmetic' stay-green characteristics.

The extensive molecular studies conducted on model plants such as *Arabidopsis* have revealed numerous genes involved in regulating senescence (Lim *et al.*, 2003; Rauf *et al.*, 2013; Zhao *et al.*, 2016). Furthermore, the emergence of CRISPR-Cas has revolutionized the process of targeted mutagenesis, making it increasingly convenient and efficient for precise genetic alterations (Arora & Narula, 2017). However, using these reverse genetic approaches to break the tight link between tuberization and senescence is still difficult. As mentioned earlier, many of these genes also play crucial roles in other important developmental processes. Moreover, assessing the impact of senescence-related gene homologues on crop yield based solely on model plant studies is challenging due to differences in reproduction. For instance, in *Arabidopsis*, mutations in the sgr (Stay-Green Related) gene, responsible for encoding the chlorophyll-degrading enzyme Mg^{++} dechelatase, result in a stay-green phenotype (Park *et al.*, 2007; Gregersen *et al.*, 2013; Shin *et al.*, 2020). However, the rice ossgr mutants, which also exhibit a stay-green phenotype, did not retain their photosynthetic capacity during the grain-filling stage and did not confer a yield advantage (Jiang *et al.*, 2007). This indicates that the ossgr mutants lack functional stay-green characteristics, highlighting the need for further investigation into the effects of gene homologues in crop plants (Jiang *et al.*, 2007; Shin *et al.*, 2020). Testing the homologues of these senescence-related genes through molecular approaches to determine if they confer functional stay-green in potatoes without affecting tuberization would be a time-consuming and labor-intensive process. As a result, pursuing this approach for breeding may not be practical. In contrast, classic genetic approaches remain highly effective in identifying the functional genetic loci that regulate targeted senescence-related traits while maintaining harmony with other important agronomic traits.

By integrating existing knowledge with the insights gained from this thesis, we propose the following strategies to assist in the breeding of potato with a longer life cycle and early tuberization. 1) Identifying new genetic loci by excluding the StCDF1 effect; 2) Screening for functional stay-green. Given that allelic variations in StCDF1 have a significant impact on senescence-related traits, we recommend the following approaches: firstly, utilizing a population with homologous loci on StCDF1 or secondly, classifying subpopulations based on StCDF1 loci for mapping senescence-related traits. Employing these methods will greatly increase the likelihood of identifying novel genetic loci, which are involved in regulating senescence. Furthermore, screening for functional stay-green should be pursued. By utilizing

advanced field phenotyping tools like field explorers (like those available in NPEC), we can instantly assess the photosynthesis status of entire plants. This enables us to effectively differentiate between functional and non-functional stay-green.

StCDF1 acts as a central hub and regulator

The circadian rhythm is an endogenous biological clock that regulates various physiological processes in plants, including growth, development, metabolism, and responses to environmental cues (Kim *et al.*, 2017; Venkat & Muneer, 2022). The rhythm of the day-night cycle imparts valuable temporal information about environmental changes to plants, effectively imprinting it within their life processes (Kim *et al.*, 2017). CDF1 is one of the well-known clock-regulated factors that regulate photoperiodic flowering in *Arabidopsis*. The expression level of CDF1 exhibits oscillations that follow a circadian rhythm (Shim & Imaizumi, 2015). Furthermore, the stability of the CDF1 protein is also regulated by the circadian system through physical interactions with GI (GIGANTEA) and FKF1 (and FLAVIN-BINDING KELCH REPEAT F-BOX PROTEIN 1) proteins (Imaizumi *et al.*, 2005; Sawa *et al.*, 2007). The CDF1-GI-FKF1 protein complex is formed in the afternoon under long-day conditions, with FKF1 playing a crucial role in the degradation of CDF1 proteins. This post-translational regulation of CDF1 has an essential impact on the flowering pathway in *Arabidopsis* (Sawa et al., 2007). By degrading CDF1, the repression of CO (CONSTANS) and FT (FLOWERING LOCUS T) expression is relieved. CO and FT are important genes involved in the floral pathway, which controls the transition from vegetative growth to flowering in plants. The removal of CDF1-mediated repression allows the activation of CO and FT gene expression. This activation initiates a cascade of events in the flowering pathway, ultimately leading to the induction of flowering (Sawa *et al.*, 2007).

In potato, StCDF1 was found to be linked to maturity in many previous studies (Visker, 2005; Kloosterman, B. *et al.*, 2013; Massa *et al.*, 2018). This maturity includes both the above ground leaf maturity (senescence) and the underground maturity (tuberization onset)(Kloosterman, B. *et al.*, 2013). The molecular mechanism of StCDF1 in regulating tuberization has been unraveled, and it exhibits significant parallels to the flowering pathway in *Arabidopsis* (Sawa *et al.*, 2007; Kloosterman, B. *et al.*, 2013). In **Chapter 2**, we proposed that StCDF1 has distinct roles in regulating various aspects of senescence. It is worth noting that both tuberization and senescence are critical developmental processes that involve complex molecular regulations. Many pathways have been discovered to exert influence on senescence, such as those responding to light conditions, circadian rhythm, phytohormones, nutrition, and environmental conditions. Within this thesis, we have reported that StCDF1 regulates the onset of senescence by directly repressing the expression of *StORE1S02* (**Chapter 2**). Interestingly, both potato and *Arabidopsis* studies have demonstrated that ABA treatment can activate the expression of ORE1 (Arabidopsis Hormone Database; http://ahd.cbi.pku.edu.cn; Solanaceae Genomics Resource; http://spuddb.uga.edu/;). Abscisic acid, is among the most crucial phytohormones involved in regulating plant development and responses to environmental changes (Adams *et al.*, 2018; Belbin & Dodd, 2018). It has been observed that ABA plays a positive role in inducing senescence (Zhao *et al.*, 2016). In **Chapter 3**, we found that StCDF1 negatively regulates ABA biosynthesis by suppressing the expression of rate-limiting enzymes in ABA biosynthesis,

namely *StNCEDs* (9-cis-epoxycarotenoid dioxygenase). Therefore, the reduced ABA content observed in overexpressing *StCDF1.2* transgenics could also contribute to the suppression of *StORE1S02* expression. This suggests that StCDF1 exerts a negative influence on *StORE1S02* expression through both direct and indirect mechanisms. Besides, ABA affects leaf senescence in comprehensive ways. Thus, the effect of StCDF1 on senescence can result from direct transcriptional regulation and also the secondary effect *via* the ABA signaling pathway.

Beyond just senescence, ABA has a more profound and diverse influence on plant development. Many previous studies show that the rhythmic production of ABA is under influence of several essential clock genes, such as: LHY, CCA, PRRs, TOC, etc. (Adams *et al.*, 2018; Belbin & Dodd, 2018; Pizzio, 2022). Interestingly, CDF4 in *Arabidopsis* was previously found to positively regulate ABA biosynthesis via upregulating *NCED2* and *NCED3* expression (Xu *et al.*, 2020). However, our results show that StCDF1 plays a negative role in this regulation in potato (**Chapter 3**). This contrast is intriguing and raises the question how this opposite regulation occurs.

The repression function of CDF1 has been reported by Goralogia, Greg S *et al.* (2017). By recruiting well characterized co-repressor, namely TOPLESS, CDF1 together with TPL binds to the promoter of CO to repress its expression and this leads to delayed flowering in *Arabidopsis*. StCDF1 shows similar repression of *StCOL*s' expression in regulating tuberization in potato (Kloosterman, B. *et al.*, 2013). By performing proximity labeling for StCDF1 and generating transgenic plants overexpressing *StCDF1.2*^{Coed} with abolished TPL binding site, we further confirmed that the physical interaction with TPL is essential for StCDF1's repressing function. In contrast to early tuberizing transgenic plants overexpressing *StCDF1.2*^{Coed}, the tuberization process is delayed in transgenic plants overexpressing *StCDF1.2*^{Coed} *ΔTPL*, resembling a late tuberizing background (**Chapter 5**). This delay is attributed to the failure of StCDF1.2^{Coed} ΔTPL to repress the expression of *StSP5G*. Surprisingly, the *StNCED3* expression was strongly upregulated only in overexpressing *StCDF1.2*^{Coed} *ΔTPL* transgenics at dusk but not in OE *StCDF1.2*^{Coed} transgenics, *StCDF1.2*^{Coed} *Δdof* or the untransformed control plants. Our observations agree with Xu *et al.* (2020) that the activation function of *StCDF1* does not require to binding to TPL. The trans-activation activity assays of CDF4 shows that the approximately 70 amino acids following the Dof DNA binding domain play a crucial role in the activation process (Xu *et al.*, 2020). It is possible that CDF physically interacts with other transcription factors at this site, to activate downstream gene expression. In **Chapter 5**, we employed TurboID-based proximity labeling to identify interactors of StCDF1. We found over 10 interactors of StCDF1, which includes 4 transcription factors belonging to the bHLH, bZIP, and homeobox transcription factor families. To further validate these interactors and unravel the underlying molecular mechanism, additional experiments need to be conducted.

It is intriguing to observe that StCDF1 exhibits the ability to both repress and activate the expression of the same downstream gene, depending on different mechanisms. ABA, widely acknowledged for its vital role in abiotic stress responses, is a prominent hormone in this regard. StCDF1 possesses the capability to regulate the level of ABA by potentially activating

or repressing it through its influence on the expression of the key ABA biosynthesis gene, *StNCED3*. This concept raises an intriguing possibility: can we breed plants that have the ability to dynamically regulate ABA biosynthesis in response to environmental conditions? Understanding this molecular mechanism opens up exciting opportunities for breeding these "smart" plants.

In various plant systems, ABA exhibits beneficial effects on plant responses to different abiotic stresses, whether through external application or manipulation of its internal levels (Sah *et al.*, 2016). In this study, we observed increased heat tolerance with a reduced ABA level in the leaf in *StCDF1.2*^{Coed} overexpressing transgenics. The same type of heat tolerance and reduced ABA level can also be achieved by carrying the early alleles of StCDF1. Our observations agree with previous studies that the early maturing potato genotypes exhibit better heat tolerance (Zhang, G *et al.*, 2020). Interestingly, the overexpressing *StCDF1.2*^{Coed} transgenics show great heat tolerance, while they were previously reported to be sensitive to drought stress. Ramírez Gonzales *et al.* (2021) reported that StCDF1 has a negative effect on potato drought tolerance. The hypothesis is that StCDF1 suppresses its antisense long non-coding RNA, known as *StFLORE*, which in turn leads to increased water loss under drought stress by interfering with stomata closure. In this thesis, we uncovered a novel function of StCDF1 in regulating ABA biosynthesis and confirmed that this negative impact on ABA production was reflected in increased stomata conductance in *StCDF1.2*^{Coed} overexpressing transgenics. Our findings support previous observations that the early alleles of StCDF1 (StCDF1.2/1.3) have a negative effect on drought stress response. The connection between StCDF1 and ABA biosynthesis suggests there exists significant potential to link StCDF1 with numerous other ABA-dependent signaling pathways.

It has been previously reported that the loci of StCDF1 were mapped for yield in different field trials involving various populations and years (Visker, 2005; Anithakumari *et al.*, 2012). StCDF1 plays a multifaceted role in regulating diverse traits with a potential effect on yield, such as tuberization, senescence, response to abiotic stresses, nitrate metabolism, and biotic resistance (Kloosterman, B. *et al.*, 2013; Tai *et al.*, 2018; Ramírez Gonzales *et al.*, 2021; Gonzales, 2022). The intricate and highly coordinated regulation of StCDF1 brings these diverse pathways together, acting as a central hub that ultimately influences the final potato yield. Furthermore, the pivotal position of StCDF1 in integrating these pathways highlights its importance in understanding the overall yield determination mechanism.

How does using advanced technologies to study central regulators benefit breeding?

Over the past decade, molecular biotechnology has made remarkable advancements and achieved significant progress. With the launch of genome-edited food made with CRISPR–Cas9 technology on the open market for the first time in Japan (Waltz, 2022), this cutting-edge technology is finally directly applied to plant breeding outside academic studies. Besides genome editing, a multitude of molecular approaches have been developed and applied to investigate the molecular functions of plant genes. These innovative techniques are frequently employed in model plant systems, such as *Arabidopsis* or *N. benthamiana*, allowing researchers to explore the molecular regulatory mechanisms extensively. In **Chapter 4**, we adapted an advanced molecular technology, namely TurboID based proximity labeling, into a

potato system. By employing this approach, we successfully verified the co-repressors of StCDF1: StTPL, StTPR3 and StTPR4- Like (**Chapter 5**) and uncovered several novel interactors of StCDF1. Furthermore, in the same chapter, we employed the domain swap technique to gain deeper insights into the distinct effects of different functional domains of StCDF1. By swapping specific domains of StCDF1, we were able to elucidate their individual contributions and unravel the intricate molecular mechanisms underlying the protein's functionality (**Chapter 5**). StCDF1, being a central regulator, is involved in various regulatory pathways. By elucidating the interacting partners of StCDF1, we can enhance our understanding of its regulatory mechanism and predict its functions in unexplored regulatory networks. In this thesis, we found that StCDF1 mediated several pathways in ways that differ from those of CDFs in *Arabidopsis*. Therefore, detailed understanding of the molecular mechanisms in specific crop plants cannot be entirely substituted by researching model plants.

In **Chapter 5**, we also presented that over 50% yield increase was achieved by overexpressing *StCDF1.2*^{Coed} *ΔTPL* transgenic plants compared to untransformed control plant. This significant improvement in yield not only provides valuable insights into the regulation mechanism of StCDF1 but also holds great potential for breeding purposes. However, it is important to note that the natural *StCDF1 ΔTPL* variant has not been reported or found in currently available open datasets (Solanaceae Genomics Resource; http://spuddb.uga.edu/). Given that the TPL binding domain is highly conserved across CDF proteins in different species, discovering a natural *StCDF1 ΔTPL* variant poses challenges (Renau-Morata *et al.*, 2020). Genome editing offers a promising approach to create this variant in a more time-efficient manner. Furthermore, by combining genome editing with hybrid breeding techniques, we can expedite and streamline breeding programs. Together, the utilization of advanced molecular techniques, such as domain swapping, enables comprehensive molecular investigations of central regulators like StCDF1. This approach has led to the creation of a novel artificial variant of StCDF1, which holds significant promise for enhancing final yield. Moreover, the integration of genome editing and hybrid breeding represents an ideal combination to accelerate and enhance breeding efforts.

In potato breeding programs, the process of mapping genetic loci for abiotic stress tolerance in field conditions entails significant costs in terms of time and labor. This is primarily due to the intricate nature of plant stress adaptation and the unpredictable influence of environmental factors. StCDF1 has been identified and mapped for its role in regulating drought stress responses and is also speculated to be involved in regulating other abiotic stress responses. In **Chapter 3**, we conducted an experiment wherein both overexpressing StCDF1.2 transgenic lines and untransformed control plants were subjected to heat stress. This investigation revealed a novel function of StCDF1 in regulating heat tolerance. Consequently, the StCDF1 loci can be utilized for selecting for heat tolerance in potato breeding programs. Once transgenic plants are generated, it becomes comparatively easier to conduct experiments under controlled conditions with specific stressors. Screening different stresses using these transgenic plants not only aids researchers in understanding the interplay between various stress responses but also provides valuable information on the novel functions of these loci for breeding selection programs.

References

References

Abelenda JA, Bergonzi S, Oortwijn M, Sonnewald S, Du M, Visser RG, Sonnewald U, Bachem CW. 2019. Source-sink regulation is mediated by interaction of an FT homolog with a SWEET protein in potato. *Current Biology* **29**(7): 1178-1186. e1176.

Abelenda JA, Cruz-Oró E, Franco-Zorrilla JM, Prat S. 2016. Potato StCONSTANS-like1 suppresses storage organ formation by directly activating the FT-like StSP5G repressor. *Current Biology* **26**(7): 872-881.

Abelenda JA, Navarro C, Prat S. 2014. Flowering and tuberization: a tale of two nightshades. *Trends in Plant Science* **19**(2): 115-122.

Adams S, Grundy J, Veflingstad SR, Dyer NP, Hannah MA, Ott S, Carré IA. 2018. Circadian control of abscisic acid biosynthesis and signalling pathways revealed by genome-wide analysis of LHY binding targets. *New Phytologist* **220**(3): 893-907.

Alvarez JM, Schinke A-L, Brooks MD, Pasquino A, Leonelli L, Varala K, Safi A, Krouk G, Krapp A, Coruzzi GM. 2020. Transient genome-wide interactions of the master transcription factor NLP7 initiate a rapid nitrogen-response cascade. *Nature communications* **11**(1): 1157.

Anithakumari A, Nataraja KN, Visser RG, van der Linden CG. 2012. Genetic dissection of drought tolerance and recovery potential by quantitative trait locus mapping of a diploid potato population. *Molecular Breeding* **30**: 1413-1429.

Arora D, Abel NB, Liu C, Van Damme P, Yperman K, Eeckhout D, Vu LD, Wang J, Tornkvist A, Impens F. 2020. Establishment of proximity-dependent biotinylation approaches in different plant model systems. *Plant Cell* **32**(11): 3388-3407.

Arora L, Narula A. 2017. Gene editing and crop improvement using CRISPR-Cas9 system. *Frontiers in Plant Science* **8**: 1932.

Asim M, Zhang Y, Sun Y, Guo M, Khan R, Wang XL, Hussain Q, Shi Y. 2022. Leaf senescence attributes: the novel and emerging role of sugars as signaling molecules and the overlap of sugars and hormones signaling nodes. *Critical Reviews in Biotechnology*: 1-19.

Awogbemi O, Kallon DVV, Owoputi AO. 2022. Biofuel generation from potato peel waste: current state and prospects. *Recycling* **7**(2): 23.

Belbin FE, Dodd AN. 2018. ABA signalling is regulated by the circadian clock component LHY. *New Phytologist* **220**(3): 661-663.

Bielow C, Mastrobuoni G, Kempa S. 2016. Proteomics quality control: quality control software for MaxQuant results. *Journal of proteome research* **15**(3): 777-787.

Branon TC, Bosch JA, Sanchez AD, Udeshi ND, Svinkina T, Carr SA, Feldman JL, Perrimon N, Ting AY. 2018. Efficient proximity labeling in living cells and organisms with TurboID. *Nature biotechnology* **36**(9): 880-887.

Buchanan-Wollaston V. 1997. The molecular biology of leaf senescence. *Journal of Experimental Botany* **48**(2): 181-199.

Buckley TN, Farquhar GD, Mott KA. 1999. Carbon-water balance and patchy stomatal conductance. *Oecologia* **118**: 132-143.

Budhiraja R, Hermkes R, Muller S, Schmidt J, Colby T, Panigrahi K, Coupland G, Bachmair A. 2009. Substrates related to chromatin and to RNA-dependent processes are modified by Arabidopsis SUMO isoforms that differ in a conserved residue with influence on desumoylation. *Plant Physiology* **149**(3): 1529-1540.

Çalışkan ME, Yousaf MF, Yavuz C, Zia MAB, Çalışkan S 2023. History, production, current trends, and future prospects. *Potato Production Worldwide*: Elsevier, 1-18.

Campbell R, Ducreux L, Cowan G, Young V, Chinoko G, Chitedze G, Kwendani S, Chiipanthenga M, Bita CE, Mwenye O. 2023. Allelic variants of a potato HEAT SHOCK COGNATE 70 gene confer improved tuber yield under a wide range of environmental conditions. *Food and Energy Security* **12**(1): e377.

Causier B, Ashworth M, Guo W, Davies B. 2012a. The TOPLESS interactome: a framework for gene repression in Arabidopsis. *Plant Physiology* **158**(1): 423-438.

Causier B, Lloyd J, Stevens L, Davies B. 2012b. TOPLESS co-repressor interactions and their evolutionary conservation in plants. *Plant signaling & behavior* **7**(3): 325-328.

Celis-Gamboa BC. 2002. *The life cycle of the potato (Solanum tuberosum L.): from crop physiology to genetics*: Wageningen University and Research.

Chen H, Ahmad M, Rim Y, Lucas WJ, Kim JY. 2013. Evolutionary and molecular analysis of D of transcription factors identified a conserved motif for intercellular protein trafficking. *New Phytologist* **198**(4): 1250-1260.

Clot CR, Wang X, Koopman J, Navarro AT, Bucher J, Visser RG, Finkers R, van Eck HJ. 2023. High-Density Linkage Map Constructed from a Skim Sequenced Diploid Potato Population Reveals Transmission Distortion and QTLs for Tuber Yield and Pollen Shed. *Potato Research*: 1-25.

Corrales A-R, Nebauer SG, Carrillo L, Fernández-Nohales P, Marqués J, Renau-Morata B, Granell A, Pollmann S, Vicente-Carbajosa J, Molina R-V. 2014. Characterization of tomato Cycling Dof Factors reveals conserved and new functions in the control of flowering time and abiotic stress responses. *Journal of Experimental Botany* **65**(4): 995-1012.

Corrales AR, Carrillo L, Lasierra P, Nebauer SG, Dominguez-Figueroa J, Renau-Morata B, Pollmann S, Granell A, Molina RV, Vicente-Carbajosa J. 2017. Multifaceted role of cycling DOF factor 3 (CDF3) in the regulation of flowering time and abiotic stress responses in Arabidopsis. *Plant, cell & environment* **40**(5): 748-764.

Cox J, Hein MY, Luber CA, Paron I, Nagaraj N, Mann M. 2014. Accurate proteome-wide label-free quantification by delayed normalization and maximal peptide ratio extraction, termed MaxLFQ. *Molecular & cellular proteomics* **13**(9): 2513-2526.
Dahal K, Li X-Q, Tai H, Creelman A, Bizimungu B. 2019. Improving potato stress tolerance and tuber yield under a climate change scenario–a current overview. *Frontiers in Plant Science* **10**: 563.
Demirel U 2023. Environmental requirements of potato and abiotic stress factors. *Potato Production Worldwide*: Elsevier, 71-86.
Deng H, Chen Y, Liu Z, Liu Z, Shu P, Wang R, Hao Y, Su D, Pirrello J, Liu Y. 2022. SlERF. F12 modulates the transition to ripening in tomato fruit by recruiting the co-repressor TOPLESS and histone deacetylases to repress key ripening genes. *The Plant Cell* **34**(4): 1250-1272.
Deva CR, Urban MO, Challinor AJ, Falloon P, Svitákova L. 2020. Enhanced leaf cooling is a pathway to heat tolerance in common bean. *Frontiers in plant science* **11**: 19.
Devaux A, Kromann P, Ortiz O. 2014. Potatoes for sustainable global food security. *Potato Research* **57**: 185-199.
Ding Z, Millar AJ, Davis AM, Davis SJ. 2007. TIME FOR COFFEE encodes a nuclear regulator in the Arabidopsis thaliana circadian clock. *The Plant Cell* **19**(5): 1522-1536.
Domazakis E, Wouters D, Visser RGF, Kamoun S, Joosten M, Vleeshouwers V. 2018. The ELR-SOBIR1 Complex Functions as a Two-Component Receptor-Like Kinase to Mount Defense Against Phytophthora infestans. *Mol Plant Microbe Interact* **31**(8): 795-802.
Durian G, Sedaghatmehr M, Matallana-Ramirez LP, Schilling SM, Schaepe S, Guerra T, Herde M, Witte C-P, Mueller-Roeber B, Schulze WX. 2020. Calcium-dependent protein kinase CPK1 controls cell death by in vivo phosphorylation of senescence master regulator ORE1. *The Plant Cell* **32**(5): 1610-1625.
Elrouby N, Bonequi MV, Porri A, Coupland G. 2013. Identification of Arabidopsis SUMO-interacting proteins that regulate chromatin activity and developmental transitions. *Proceedings of the National Academy of Sciences* **110**(49): 19956-19961.
Endo A, Sawada Y, Takahashi H, Okamoto M, Ikegami K, Koiwai H, Seo M, Toyomasu T, Mitsuhashi W, Shinozaki K. 2008. Drought induction of Arabidopsis 9-cis-epoxycarotenoid dioxygenase occurs in vascular parenchyma cells. *Plant Physiology* **147**(4): 1984-1993.
Ewing E. 1981. Heat stress and the tuberization stimulus. *American Potato Journal* **58**(1): 31-49.
Ewing E, Struik P. 1992. Tuber formation in potato: induction, initiation, and growth. *Horticultural reviews* **14**: 89-198.
Fahad S, Bajwa AA, Nazir U, Anjum SA, Farooq A, Zohaib A, Sadia S, Nasim W, Adkins S, Saud S. 2017. Crop production under drought and heat stress: plant responses and management options. *Frontiers in Plant Science*: 1147.
FAO 2019. FAOSTAT.
FAOSTAT 2021.
Feng C, Roitinger E, Hudecz O, Cuacos M, Lorenz J, Schubert V, Wang B, Wang R, Mechtler K, Heckmann S. 2023. TurboID-based proteomic profiling of meiotic chromosome axes in Arabidopsis thaliana. *Nature Plants*: 1-15.
Feng Y, Bui TPN, Stams AJ, Boeren S, Sánchez-Andrea I, de Vos WM. 2022. Comparative genomics and proteomics of Eubacterium maltosivorans: functional identification of trimethylamine methyltransferases and bacterial microcompartments in a human intestinal bacterium with a versatile lifestyle. *Environmental Microbiology* **24**(1): 517-534.
Fornara F, de Montaigu A, Sánchez-Villarreal A, Takahashi Y, Ver Loren van Themaat E, Huettel B, Davis SJ, Coupland G. 2015. The GI–CDF module of Arabidopsis affects freezing tolerance and growth as well as flowering. *The Plant Journal* **81**(5): 695-706.
Fornara F, Panigrahi KC, Gissot L, Sauerbrunn N, Rühl M, Jarillo JA, Coupland G. 2009. Arabidopsis DOF transcription factors act redundantly to reduce CONSTANS expression and are essential for a photoperiodic flowering response. *Developmental cell* **17**(1): 75-86.
Gao H, Song W, Severing E, Vayssières A, Huettel B, Franzen R, Richter R, Chai J, Coupland G. 2022. PIF4 enhances DNA binding of CDF2 to co-regulate target gene expression and promote Arabidopsis hypocotyl cell elongation. *Nature Plants* **8**(9): 1082-1093.
Gepstein S, Sabehi G, Carp M-J, Hajouj T, Nesher MFO, Yariv I, Dor C, Bassani M. 2003. Large-scale identification of leaf senescence-associated genes. *The Plant Journal* **36**(5): 629-642.
Gonzales LYRr. 2022. Linking plant development and tuberization: to key environmental inputs of light, water and nitrogen in potato.
Goralogia GS, Liu TK, Zhao L, Panipinto PM, Groover ED, Bains YS, Imaizumi T. 2017. CYCLING DOF FACTOR 1 represses transcription through the TOPLESS co-repressor to control photoperiodic flowering in Arabidopsis. *Plant J* **92**(2): 244-262.
Goralogia GS, Liu TK, Zhao L, Panipinto PM, Groover ED, Bains YS, Imaizumi T. 2017. CYCLING DOF FACTOR 1 represses transcription through the TOPLESS co-repressor to control photoperiodic flowering in Arabidopsis. *The Plant Journal* **92**(2): 244-262.
Gregersen PL, Culetic A, Boschian L, Krupinska K. 2013. Plant senescence and crop productivity. *Plant molecular biology* **82**: 603-622.
Gühl K, Holmer R, Xiao TT, Shen D, Wardhani TA, Geurts R, van Zeijl A, Kohlen W. 2021. The effect of exogenous nitrate on LCO signalling, cytokinin accumulation, and nodule initiation in Medicago truncatula. *Genes* **12**(7): 988.
Guiboileau A, Sormani R, Meyer C, Masclaux-Daubresse C. 2010. Senescence and death of plant organs: nutrient recycling and developmental regulation. *Comptes rendus biologies* **333**(4): 382-391.

Guo Y, Ren G, Zhang K, Li Z, Miao Y, Guo H. 2021. Leaf senescence: progression, regulation, and application. *Molecular Horticulture* **1**(1): 1-25.
Gupta S, Malviya N, Kushwaha H, Nasim J, Bisht NC, Singh V, Yadav D. 2015. Insights into structural and functional diversity of Dof (DNA binding with one finger) transcription factor. *Planta* **241**: 549-562.
Guzzo MC, Costamagna C, Salloum MS, Rotundo JL, Monteoliva MI, Luna CM. 2021. Morpho-physiological traits associated with drought responses in soybean. *Crop Science* **61**(1): 672-688.
Hall A, Bastow RM, Davis SJ, Hanano S, McWatters HG, Hibberd V, Doyle MR, Sung S, Halliday KJ, Amasino RM. 2003. The TIME FOR COFFEE gene maintains the amplitude and timing of Arabidopsis circadian clocks. *The Plant Cell* **15**(11): 2719-2729.
Hancock RD, Morris WL, Ducreux LJ, Morris JA, Usman M, Verrall SR, Fuller J, Simpson CG, Zhang R, Hedley PE. 2014. Physiological, biochemical and molecular responses of the potato (S olanum tuberosum L.) plant to moderately elevated temperature. *Plant, cell & environment* **37**(2): 439-450.
Hannapel DJ, Sharma P, Lin T, Banerjee AK. 2017. The multiple signals that control tuber formation. *Plant Physiology* **174**(2): 845-856.
Hawkes J. 1957. Potato breeding in Russia—July, 1956. *Euphytica* **6**: 38-44.
Henriques R, Wang H, Liu J, Boix M, Huang LF, Chua NH. 2017. The antiphasic regulatory module comprising CDF5 and its antisense RNA FLORE links the circadian clock to photoperiodic flowering. *New Phytologist* **216**(3): 854-867.
Hijmans RJ. 2003. The effect of climate change on global potato production. *American Journal of Potato Research* **80**: 271-279.
Hirsch CD, Hamilton JP, Childs KL, Cepela J, Crisovan E, Vaillancourt B, Hirsch CN, Habermann M, Neal B, Buell CR. 2014. Spud DB: A resource for mining sequences, genotypes, and phenotypes to accelerate potato breeding. *The Plant Genome* **7**(1): plantgenome2013.2012.0042.
Hoeberichts FA, van Doorn WG, Vorst O, Hall RD, van Wordragen MF. 2007. Sucrose prevents up-regulation of senescence-associated genes in carnation petals. *Journal of Experimental Botany* **58**(11): 2873-2885.
Hoopes G, Meng X, Hamilton JP, Achakkagari SR, Guesdes FdAF, Bolger ME, Coombs JJ, Esselink D, Kaiser NR, Kodde L. 2022. Phased, chromosome-scale genome assemblies of tetraploid potato reveal a complex genome, transcriptome, and predicted proteome landscape underpinning genetic diversity. *Molecular plant* **15**(3): 520-536.
Hoopes GM, Zarka D, Feke A, Acheson K, Hamilton JP, Douches D, Buell CR, Farré EM. 2022. Keeping time in the dark: Potato diel and circadian rhythmic gene expression reveals tissue-specific circadian clocks. *Plant Direct* **6**(7): e425.
Horacio P, Martinez-Noel G. 2013. Sucrose signaling in plants: a world yet to be explored. *Plant signaling & behavior* **8**(3): e23316.
Hörtensteiner S. 2009. Stay-green regulates chlorophyll and chlorophyll-binding protein degradation during senescence. *Trends in Plant Science* **14**(3): 155-162.
Huijser P, Schmid M. 2011. The control of developmental phase transitions in plants. *Development* **138**(19): 4117-4129.
Hurtado PX, Schnabel SK, Zaban A, Veteläinen M, Virtanen E, Eilers PHC, van Eeuwijk FA, Visser RGF, Maliepaard C. 2011. Dynamics of senescence-related QTLs in potato. *Euphytica* **183**(3): 289-302.
Imaizumi T, Schultz TF, Harmon FG, Ho LA, Kay SA. 2005. FKF1 F-box protein mediates cyclic degradation of a repressor of CONSTANS in Arabidopsis. *Science* **309**(5732): 293-297.
Jiang H, Li M, Liang N, Yan H, Wei Y, Xu X, Liu J, Xu Z, Chen F, Wu G. 2007. Molecular cloning and function analysis of the stay green gene in rice. *The Plant Journal* **52**(2): 197-209.
Jing S, Sun X, Yu L, Wang E, Cheng Z, Liu H, Jiang P, Qin J, Begum S, Song B. 2022a. Transcription factor StABI5-like 1 binding to the FLOWERING LOCUS T homologs promotes early maturity in potato. *Plant Physiology*.
Jing S, Sun X, Yu L, Wang E, Cheng Z, Liu H, Jiang P, Qin J, Begum S, Song B. 2022b. Transcription factor StABI5-like 1 binding to the FLOWERING LOCUS T homologs promotes early maturity in potato. *Plant Physiology* **189**(3): 1677-1693.
Joshi S, Choukimath A, Isenegger D, Panozzo J, Spangenberg G, Kant S. 2019. Improved wheat growth and yield by delayed leaf senescence using developmentally regulated expression of a cytokinin biosynthesis gene. *Frontiers in Plant Science* **10**: 1285.
Jumper J, Evans R, Pritzel A, Green T, Figurnov M, Ronneberger O, Tunyasuvunakool K, Bates R, Žídek A, Potapenko A. 2021. Highly accurate protein structure prediction with AlphaFold. *Nature* **596**(7873): 583-589.
Kadosh D, Struhl K. 1998. Targeted recruitment of the Sin3-Rpd3 histone deacetylase complex generates a highly localized domain of repressed chromatin in vivo. *Molecular and cellular biology* **18**(9): 5121-5127.
Kamranfar I, Xue GP, Tohge T, Sedaghatmehr M, Fernie AR, Balazadeh S, Mueller-Roeber B. 2018. Transcription factor RD 26 is a key regulator of metabolic reprogramming during dark-induced senescence. *New Phytologist* **218**(4): 1543-1557.
Khedher MB, Ewing EE. 1985. Growth analyses of eleven potato cultivars grown in the greenhouse under long photoperiods with and without heat stress. *American Potato Journal* **62**(10): 537-554.
Kim DI, KC B, Zhu W, Motamedchaboki K, Doye V, Roux KJ. 2014. Probing nuclear pore complex architecture with proximity-dependent biotinylation. *Proceedings of the National Academy of Sciences* **111**(24): E2453-E2461.
Kim H, Kim HJ, Vu QT, Jung S, McClung CR, Hong S, Nam HG. 2018. Circadian control of ORE1 by PRR9 positively regulates leaf senescence in Arabidopsis. *Proc Natl Acad Sci U S A* **115**(33): 8448-8453.

Kim H, Park SJ, Kim Y, Nam HG. 2020. Subcellular localization of GIGANTEA regulates the timing of leaf senescence and flowering in Arabidopsis. *Frontiers in Plant Science* **11**: 589707.
Kim JA, Kim H-S, Choi S-H, Jang J-Y, Jeong M-J, Lee SI. 2017. The importance of the circadian clock in regulating plant metabolism. *International journal of molecular sciences* **18**(12): 2680.
Kim JH, Woo HR, Kim J, Lim PO, Lee IC, Choi SH, Hwang D, Nam HG. 2009. Trifurcate feed-forward regulation of age-dependent cell death involving miR164 in Arabidopsis. *Science* **323**(5917): 1053-1057.
Kim T-W, Park CH, Hsu C-C, Kim Y-W, Ko Y-W, Zhang Z, Zhu J-Y, Hsiao Y-C, Branon T, Kaasik K. 2023. Mapping the signaling network of BIN2 kinase using TurboID-mediated biotin labeling and phosphoproteomics. *The Plant Cell* **35**(3): 975-993.
Kim T-W, Park CH, Hsu C-C, Zhu J-Y, Hsiao Y, Branon T, Xu S-L, Ting AY, Wang Z-Y. 2019. Application of TurboID-mediated proximity labeling for mapping a GSK3 kinase signaling network in Arabidopsis. *BioRxiv*: 636324.
Kleinwechter U, Gastelo M, Ritchie J, Nelson G, Asseng S. 2016. Simulating cultivar variations in potato yields for contrasting environments. *Agricultural Systems* **145**: 51-63.
Kloosterman B, Abelenda JA, Gomez Mdel M, Oortwijn M, de Boer JM, Kowitwanich K, Horvath BM, van Eck HJ, Smaczniak C, Prat S, et al. 2013. Naturally occurring allele diversity allows potato cultivation in northern latitudes. *Nature* **495**(7440): 246-250.
Kloosterman B, Abelenda JA, Gomez MdMC, Oortwijn M, de Boer JM, Kowitwanich K, Horvath BM, van Eck HJ, Smaczniak C, Prat S. 2013. Naturally occurring allele diversity allows potato cultivation in northern latitudes. *Nature* **495**(7440): 246-250.
Krogan NT, Hogan K, Long JA. 2012. APETALA2 negatively regulates multiple floral organ identity genes in Arabidopsis by recruiting the co-repressor TOPLESS and the histone deacetylase HDA19. *Development* **139**(22): 4180-4190.
Kühn C, Quick W, Schulz A, Riesmeier J, Sonnewald U, Frommer W. 1996. Companion cell-specific inhibition of the potato sucrose transporter SUT1. *Plant, cell & environment* **19**(10): 1115-1123.
Kumar SV, Lucyshyn D, Jaeger KE, Alós E, Alvey E, Harberd NP, Wigge PA. 2012. Transcription factor PIF4 controls the thermosensory activation of flowering. *Nature* **484**(7393): 242-245.
Larkindale J, Knight MR. 2002. Protection against heat stress-induced oxidative damage in Arabidopsis involves calcium, abscisic acid, ethylene, and salicylic acid. *Plant Physiology* **128**(2): 682-695.
Larsen DH, Marcelis LF, van Kempen D, Kohlen W, Nicole CC, Woltering EJ. 2023. Far-red light during cultivation improves postharvest chilling tolerance in basil. *Postharvest Biology and Technology* **198**: 112232.
Lee KH, Piao HL, Kim H-Y, Choi SM, Jiang F, Hartung W, Hwang I, Kwak JM, Lee I-J, Hwang I. 2006. Activation of glucosidase via stress-induced polymerization rapidly increases active pools of abscisic acid. *Cell* **126**(6): 1109-1120.
Lehretz GG, Sonnewald S, Hornyik C, Corral JM, Sonnewald U. 2019. Post-transcriptional regulation of FLOWERING LOCUS T modulates heat-dependent source-sink development in potato. *Current Biology* **29**(10): 1614-1624. e1613.
Lehretz GG, Sonnewald S, Lugassi N, Granot D, Sonnewald U. 2021. Future-proofing potato for drought and heat tolerance by overexpression of hexokinase and SP6A. *Frontiers in plant science* **11**: 614534.
Levy D. 1986. Genotypic variation in the response of potatoes (Solanum tuberosum L.) to high ambient temperatures and water deficit. *Field Crops Research* **15**(1): 85-96.
Levy D, Coleman WK, Veilleux RE. 2013. Adaptation of potato to water shortage: irrigation management and enhancement of tolerance to drought and salinity. *American Journal of Potato Research* **90**: 186-206.
Leydon AR, Wang W, Gala HP, Gilmour S, Juarez-Solis S, Zahler ML, Zemke JE, Zheng N, Nemhauser JL. 2020. Structure-function analysis of Arabidopsis TOPLESS reveals fundamental conservation of repression mechanisms across eukaryotes. *BioRxiv*: 2020.2003. 2004.976134.
Li G, Zhang C, Zhang G, Fu W, Feng B, Chen T, Peng S, Tao L, Fu G. 2020. Abscisic acid negatively modulates heat tolerance in rolled leaf rice by increasing leaf temperature and regulating energy homeostasis. *Rice* **13**: 1-16.
Li J, Wang Y, Wen G, Li G, Li Z, Zhang R, Ma S, Zhou J, Xie C. 2019. Mapping QTL underlying tuber starch content and plant maturity in tetraploid potato. *The Crop Journal* **7**(2): 261-272.
Li N, Bo C, Zhang Y, Wang L. 2021. PHYTOCHROME INTERACTING FACTORS PIF4 and PIF5 promote heat stress induced leaf senescence in Arabidopsis. *Journal of Experimental Botany* **72**(12): 4577-4589.
Li N, Euring D, Cha JY, Lin Z, Lu M, Huang L-J, Kim WY. 2021. Plant hormone-mediated regulation of heat tolerance in response to global climate change. *Frontiers in plant science* **11**: 627969.
Li R, Hu D, Ren H, Yang Q, Dong S, Zhang J, Zhao B, Liu P. 2022. How delaying post-silking senescence in lower leaves of maize plants increases carbon and nitrogen accumulation and grain yield. *The Crop Journal* **10**(3): 853-863.
Li W, Liu Y, Liu M, Zheng Q, Li B, Li Z, Li H. 2019. Sugar accumulation is associated with leaf senescence induced by long-term high light in wheat. *Plant Science* **287**: 110169.
Li YH, Ke TY, Shih WC, Liou RF, Wang CW. 2021. NbSOBIR1 Partitions Into Plasma Membrane Microdomains and Binds ER-Localized NbRLP1. *Front Plant Sci* **12**: 721548.
Liebrand TW, van den Burg HA, Joosten MH. 2014. Two for all: receptor-associated kinases SOBIR1 and BAK1. *Trends Plant Sci* **19**(2): 123-132.
Lightenthaler H. 1987. Chlorophylls and carotenoids: pigments of photosynthetic biomembranes. *Methods in enzymology* **148**: 350-382.
Lim PO, Woo HR, Nam HG. 2003. Molecular genetics of leaf senescence in Arabidopsis. *Trends in Plant Science* **8**(6): 272-278.

Lin X, Torres Ascurra YC, Fillianti H, Dethier L, de Rond L, Domazakis E, Aguilera-Galvez C, Kiros AY, Jacobsen E, Visser RGF, et al. 2022. Recognition of Pep-13/25 MAMPs of Phytophthora localizes to an RLK locus in Solanum microdontum. *Front Plant Sci* **13**: 1037030.

Lira BS, Gramegna G, Trench BA, Alves FR, Silva EM, Silva GF, Thirumalaikumar VP, Lupi AC, Demarco D, Purgatto E. 2017. Manipulation of a senescence-associated gene improves fleshy fruit yield. *Plant Physiology* **175**(1): 77-91.

Lira BS, Gramegna G, Trench BA, Alves FRR, Silva EM, Silva GFF, Thirumalaikumar VP, Lupi ACD, Demarco D, Purgatto E, et al. 2017. Manipulation of a Senescence-Associated Gene Improves Fleshy Fruit Yield. *Plant Physiol* **175**(1): 77-91.

Lohman KN, Gan S, John MC, Amasino RM. 1994. Molecular analysis of natural leaf senescence in Arabidopsis thaliana. *Physiologia Plantarum* **92**(2): 322-328.

López-Ráez JA, Kohlen W, Charnikhova T, Mulder P, Undas AK, Sergeant MJ, Verstappen F, Bugg TD, Thompson AJ, Ruyter-Spira C. 2010. Does abscisic acid affect strigolactone biosynthesis? *New Phytologist* **187**(2): 343-354.

Ma X, Zhang Y, Turečková V, Xue G-P, Fernie AR, Mueller-Roeber B, Balazadeh S. 2018. The NAC transcription factor SlNAP2 regulates leaf senescence and fruit yield in tomato. *Plant Physiology* **177**(3): 1286-1302.

Manrique-Carpintero NC, Coombs JJ, Cui Y, Veilleux RE, Buell CR, Douches D. 2015. Genetic map and QTL analysis of agronomic traits in a diploid potato population using single nucleotide polymorphism markers. *Crop Science* **55**(6): 2566-2579.

Marand AP, Jansky SH, Gage JL, Hamernik AJ, de Leon N, Jiang J. 2019. Residual Heterozygosity and Epistatic Interactions Underlie the Complex Genetic Architecture of Yield in Diploid Potato. *Genetics* **212**(1): 317-332.

Marinus J, Bodlaender K. 1975. Response of some potato varieties to temperature. *Potato Research* **18**(2): 189-204.

Massa AN, Manrique-Carpintero NC, Coombs J, Haynes KG, Bethke PC, Brandt TL, Gupta SK, Yencho GC, Novy RG, Douches DS. 2018. Linkage analysis and QTL mapping in a tetraploid russet mapping population of potato. *BMC genetics* **19**(1): 1-13.

Matallana-Ramirez LP, Rauf M, Farage-Barhom S, Dortay H, Xue G-P, Dröge-Laser W, Lers A, Balazadeh S, Mueller-Roeber B. 2013. NAC transcription factor ORE1 and senescence-induced BIFUNCTIONAL NUCLEASE1 (BFN1) constitute a regulatory cascade in Arabidopsis. *Molecular plant* **6**(5): 1438-1452.

Maul F, Sargent SA, Balaban MO, Baldwin EA, Huber DJ, Sims CA. 1998. Aroma volatile profiles from ripe tomatoes are influenced by physiological maturity at harvest: an application for electronic nose technology. *Journal of the American Society for Horticultural Science* **123**(6): 1094-1101.

May DG, Scott KL, Campos AR, Roux KJ. 2020. Comparative application of BioID and TurboID for protein-proximity biotinylation. *Cells* **9**(5): 1070.

Meade F, Hutten R, Wagener S, Prigge V, Dalton E, Kirk HG, Griffin D, Milbourne D. 2020. Detection of Novel QTLs for Late Blight Resistance Derived from the Wild Potato Species Solanum microdontum and Solanum pampasense. *Genes (Basel)* **11**(7).

Miryeganeh M. 2021. Senescence: the compromised time of death that plants may call on themselves. *Genes* **12**(2): 143.

Monneveux P, Ramírez DA, Pino M-T. 2013. Drought tolerance in potato (S. tuberosum L.): Can we learn from drought tolerance research in cereals? *Plant Science* **205**: 76-86.

Moore B, Zhou L, Rolland F, Hall Q, Cheng W-H, Liu Y-X, Hwang I, Jones T, Sheen J. 2003. Role of the Arabidopsis glucose sensor HXK1 in nutrient, light, and hormonal signaling. *Science* **300**(5617): 332-336.

Muhammad Aslam M, Waseem M, Jakada BH, Okal EJ, Lei Z, Saqib HSA, Yuan W, Xu W, Zhang Q. 2022. Mechanisms of abscisic acid-mediated drought stress responses in plants. *International journal of molecular sciences* **23**(3): 1084.

Murashige T, Skoog F. 1962. A revised medium for rapid growth and bio assays with tobacco tissue cultures. *Physiologia Plantarum* **15**(3): 473-497.

Natarajan N, Vasudevan M, Vivekk Velusamy V, Selvaraj M. 2019. Eco-friendly and edible waste cutlery for sustainable environment. *International Journal of Engineering and Advanced Technology* **9**(1s4).

Navarro C, Abelenda JA, Cruz-Oró E, Cuéllar CA, Tamaki S, Silva J, Shimamoto K, Prat S. 2011. Control of flowering and storage organ formation in potato by FLOWERING LOCUS T. *Nature* **478**(7367): 119-122.

Park JS, Park SJ, Kwon SY, Shin AY, Moon KB, Park JM, Cho HS, Park SU, Jeon JH, Kim HS, et al. 2022. Temporally distinct regulatory pathways coordinate thermo-responsive storage organ formation in potato. *Cell Rep* **38**(13): 110579.

Park S-Y, Yu J-W, Park J-S, Li J, Yoo S-C, Lee N-Y, Lee S-K, Jeong S-W, Seo HS, Koh H-J. 2007. The senescence-induced staygreen protein regulates chlorophyll degradation. *The Plant Cell* **19**(5): 1649-1664.

Petti C, Wendt T, Meade C, Mullins E. 2009. Evidence of genotype dependency within Agrobacterium tumefaciens in relation to the integration of vector backbone sequence in transgenic Phytophthora infestans-tolerant potato. *Journal of bioscience and bioengineering* **107**(3): 301-306.

Pizzio GA. 2022. Abscisic acid machinery is under circadian clock regulation at multiple levels. *Stresses* **2**(1): 65-78.

Plant AR, Larrieu A, Causier B. 2021. Repressor for hire! The vital roles of TOPLESS-mediated transcriptional repression in plants. *New Phytologist* **231**(3): 963-973.

Plantenga FD, Bergonzi S, Abelenda JA, Bachem CW, Visser RG, Heuvelink E, Marcelis LF. 2019a. The tuberization signal StSP6A represses flower bud development in potato. *Journal of Experimental Botany* **70**(3): 937-948.

Plantenga FD, Heuvelink E, Rienstra JA, Visser RG, Bachem CW, Marcelis LF. 2019b. Coincidence of potato CONSTANS (StCOL1) expression and light cannot explain night-break repression of tuberization. *Physiologia Plantarum* **167**(2): 250-263.

Postma J, Liebrand TW, Bi G, Evrard A, Bye RR, Mbengue M, Kuhn H, Joosten MH, Robatzek S. 2016. Avr4 promotes Cf-4 receptor-like protein association with the BAK1/SERK3 receptor-like kinase to initiate receptor endocytosis and plant immunity. *New Phytologist* **210**(2): 627-642.

Pourtau N, Jennings R, Pelzer E, Pallas J, Wingler A. 2006. Effect of sugar-induced senescence on gene expression and implications for the regulation of senescence in Arabidopsis. *Planta* **224**(3): 556-568.

Prat S. 2006. Seasonal control of tuberization in potato: conserved elements with the flowering response. *Annu. Rev. Plant Biol* **57**: 151-180.

Pulido A, Laufs P. 2010. Co-ordination of developmental processes by small RNAs during leaf development. *Journal of experimental botany* **61**(5): 1277-1291.

Qin X, Zeevaart JA. 2002. Overexpression of a 9-cis-epoxycarotenoid dioxygenase gene in Nicotiana plumbaginifolia increases abscisic acid and phaseic acid levels and enhances drought tolerance. *Plant Physiology* **128**(2): 544-551.

Qiu K, Li Z, Yang Z, Chen J, Wu S, Zhu X, Gao S, Gao J, Ren G, Kuai B, et al. 2015. EIN3 and ORE1 Accelerate Degreening during Ethylene-Mediated Leaf Senescence by Directly Activating Chlorophyll Catabolic Genes in Arabidopsis. *PLoS Genet* **11**(7): e1005399.

Rajametov SN, Yang EY, Cho MC, Chae SY, Jeong HB, Chae WB. 2021. Heat-tolerant hot pepper exhibits constant photosynthesis via increased transpiration rate, high proline content and fast recovery in heat stress condition. *Scientific Reports* **11**(1): 14328.

Ramirez Gonzales L, Shi L, Bergonzi SB, Oortwijn M, Franco-Zorrilla JM, Solano-Tavira R, Visser RGF, Abelenda JA, Bachem CWB. 2021. Potato CYCLING DOF FACTOR 1 and its lncRNA counterpart StFLORE link tuber development and drought response. *Plant J* **105**(4): 855-869.

Ramírez Gonzales L, Shi L, Bergonzi SB, Oortwijn M, Franco-Zorrilla JM, Solano-Tavira R, Visser RG, Abelenda JA, Bachem CW. 2021. Potato CYCLING DOF FACTOR 1 and its lncRNA counterpart StFLORE link tuber development and drought response. *The Plant Journal* **105**(4): 855-869.

Rauf M, Arif M, Dortay H, Matallana-Ramírez LP, Waters MT, Gil Nam H, Lim PO, Mueller-Roeber B, Balazadeh S. 2013. ORE1 balances leaf senescence against maintenance by antagonizing G2-like-mediated transcription. *EMBO reports* **14**(4): 382-388.

Raymundo R, Asseng S, Robertson R, Petsakos A, Hoogenboom G, Quiroz R, Hareau G, Wolf J. 2018. Climate change impact on global potato production. *European Journal of Agronomy* **100**: 87-98.

Renau-Morata B, Carrillo L, Dominguez-Figueroa J, Vicente-Carbajosa J, Molina RV, Nebauer SG, Medina J. 2020. CDF transcription factors: plant regulators to deal with extreme environmental conditions. *Journal of Experimental Botany* **71**(13): 3803-3815.

Renau-Morata B, Molina RV, Carrillo L, Cebolla-Cornejo J, Sánchez-Perales M, Pollmann S, Domínguez-Figueroa J, Corrales AR, Flexas J, Vicente-Carbajosa J. 2017. Ectopic expression of CDF3 genes in tomato enhances biomass production and yield under salinity stress conditions. *Frontiers in Plant Science* **8**: 660.

Sah SK, Reddy KR, Li J. 2016. Abscisic acid and abiotic stress tolerance in crop plants. *Frontiers in Plant Science* **7**: 571.

Sanchez AD, Feldman JL. 2021. A proximity labeling protocol to probe proximity interactions in C. elegans. *STAR protocols* **2**(4): 100986.

Sasi JM, Gupta S, Singh A, Kujur A, Agarwal M, Katiyar-Agarwal S. 2022. Know when and how to die: gaining insights into the molecular regulation of leaf senescence. *Physiology and Molecular Biology of Plants* **28**(8): 1515-1534.

Sawa M, Nusinow DA, Kay SA, Imaizumi T. 2007. FKF1 and GIGANTEA complex formation is required for day-length measurement in Arabidopsis. *Science* **318**(5848): 261-265.

Schippers JH, Schmidt R, Wagstaff C, Jing H-C. 2015. Living to die and dying to live: the survival strategy behind leaf senescence. *Plant Physiology* **169**(2): 914-930.

Semeijn C, Buwalda PL 2018. Potato starch. *Starch in Food*: Elsevier, 353-372.

Shim JS, Imaizumi T. 2015. Circadian clock and photoperiodic response in Arabidopsis: from seasonal flowering to redox homeostasis. *Biochemistry* **54**(2): 157-170.

Shin D, Lee S, Kim T-H, Lee J-H, Park J, Lee J, Lee JY, Cho L-H, Choi JY, Lee W. 2020. Natural variations at the Stay-Green gene promoter control lifespan and yield in rice cultivars. *Nature communications* **11**(1): 2819.

Smaczniak C, Li N, Boeren S, America T, Van Dongen W, Goerdayal SS, De Vries S, Angenent GC, Kaufmann K. 2012. Proteomics-based identification of low-abundance signaling and regulatory protein complexes in native plant tissues. *Nature protocols* **7**(12): 2144-2158.

Smart CM. 1994. Gene expression during leaf senescence. *New Phytologist* **126**(3): 419-448.

Spooner DM, McLean K, Ramsay G, Waugh R, Bryan GJ. 2005. A single domestication for potato based on multilocus amplified fragment length polymorphism genotyping. *Proceedings of the National Academy of Sciences* **102**(41): 14694-14699.

Stöckle CO, Nelson RL, Higgins S, Brunner J, Grove G, Boydston R, Whiting M, Kruger C. 2010. Assessment of climate change impact on Eastern Washington agriculture. *Climatic change* **102**: 77-102.

Struik PC 2007. Responses of the potato plant to temperature. *Potato biology and biotechnology*: Elsevier, 367-393.

Sussmilch FC, Brodribb TJ, McAdam SA. 2017. Up-regulation of NCED3 and ABA biosynthesis occur within minutes of a decrease in leaf turgor but AHK1 is not required. *Journal of Experimental Botany* **68**(11): 2913-2918.
Suzuki N, Bassil E, Hamilton JS, Inupakutika MA, Zandalinas SI, Tripathy D, Luo Y, Dion E, Fukui G, Kumazaki A. 2016. ABA is required for plant acclimation to a combination of salt and heat stress. *PLoS One* **11**(1): e0147625.
Tai HH, De Koeyer D, Sønderkær M, Hedegaard S, Lagüe M, Goyer C, Nolan L, Davidson C, Gardner K, Neilson J. 2018. Verticillium dahliae disease resistance and the regulatory pathway for maturity and tuberization in potato. *The Plant Genome* **11**(1): 170040.
Tanaka M, Kikuchi A, Kamada H. 2008. The Arabidopsis histone deacetylases HDA6 and HDA19 contribute to the repression of embryonic properties after germination. *Plant Physiology* **146**(1): 149-161.
Taoka K-i, Ohki I, Tsuji H, Furuita K, Hayashi K, Yanase T, Yamaguchi M, Nakashima C, Purwestri YA, Tamaki S. 2011. 14-3-3 proteins act as intracellular receptors for rice Hd3a florigen. *Nature* **476**(7360): 332-335.
TeKrony D, Egli D, Balles J, Pfeiffer T, Fellows R. 1979. Physiological maturity in soybean 1. *Agronomy Journal* **71**(5): 771-775.
Teo C-J, Takahashi K, Shimizu K, Shimamoto K, Taoka K-i. 2017. Potato tuber induction is regulated by interactions between components of a tuberigen complex. *Plant and Cell Physiology* **58**(2): 365-374.
Thomas H. 2013. Senescence, ageing and death of the whole plant. *New Phytologist* **197**(3): 696-711.
Thomas H, Howarth CJ. 2000. Five ways to stay green. *Journal of Experimental Botany* **51**(suppl_1): 329-337.
Thomas H, Ougham H. 2014. The stay-green trait. *Journal of Experimental Botany* **65**(14): 3889-3900.
Timlin D, Lutfor Rahman S, Baker J, Reddy V, Fleisher D, Quebedeaux B. 2006. Whole plant photosynthesis, development, and carbon partitioning in potato as a function of temperature. *Agronomy Journal* **98**(5): 1195-1203.
Tyanova S, Temu T, Sinitcyn P, Carlson A, Hein MY, Geiger T, Mann M, Cox J. 2016. The Perseus computational platform for comprehensive analysis of (prote) omics data. *Nature methods* **13**(9): 731-740.
Vadez V, Deshpande S, Kholova J, Ramu P, Hash CT. 2013. Molecular breeding for stay-green: Progress and challenges in sorghum. *Translational genomics for crop breeding: abiotic stress, yield and quality* **2**: 125-141.
van den Berg RG, Spooner DM. 1992. A reexamination of infraspecific taxa of a wild potato, Solanum microdontum (Solanum sect. Petota: Solanaceae). *Pl. Syst. Evol.* **182:239-252**.
van der Burgh AM, Postma J, Robatzek S, Joosten M. 2019. Kinase activity of SOBIR1 and BAK1 is required for immune signalling. *Mol Plant Pathol* **20**(3): 410-422.
Van der Plank J. 1946. Origin of the first European potatoes and their reaction to length of day. *Nature* **157**(3990): 503-505.
van Doorn WG. 2008. Is the onset of senescence in leaf cells of intact plants due to low or high sugar levels? *Journal of Experimental Botany* **59**(8): 1963-1972.
van Mourik H, Chen P, Smaczniak C, Boeren S, Kaufmann K, Bemer M, Angenent GC, Muino JM. 2023. Dual specificity and target gene selection by the MADS-domain protein FRUITFULL. *Nature Plants* **9**(3): 473-485.
Varadi M, Anyango S, Deshpande M, Nair S, Natassia C, Yordanova G, Yuan D, Stroe O, Wood G, Laydon A. 2022. AlphaFold Protein Structure Database: massively expanding the structural coverage of protein-sequence space with high-accuracy models. *Nucleic acids research* **50**(D1): D439-D444.
Varala K, Marshall-Colón A, Cirrone J, Brooks MD, Pasquino AV, Léran S, Mittal S, Rock TM, Edwards MB, Kim GJ. 2018. Temporal transcriptional logic of dynamic regulatory networks underlying nitrogen signaling and use in plants. *Proceedings of the National Academy of Sciences* **115**(25): 6494-6499.
Venkat A, Muneer S. 2022. Role of circadian rhythms in major plant metabolic and signaling pathways. *Frontiers in Plant Science* **13**: 836244.
Visker M. 2005. *Association between late blight resistance and foliage maturity type in potato: physiological and genetic studies*: Wageningen University and Research.
Visker M, Keizer L, Van Eck H, Jacobsen E, Colon L, Struik P. 2003. Can the QTL for late blight resistance on potato chromosome 5 be attributed to foliage maturity type? *Theoretical and Applied Genetics* **106**(2): 317-325.
Visser RGF, Hesseling-Meinders A, Jacobsen E, Nijdam H, Witholt B, Feenstra WJ. 1989. Expression and inheritance of inserted markers in binary vector carrying Agrobacterium rhizogenes transformed potato (Solanum tuberosum L.). *Theoretical and Applied Genetics* **78**(5): 705-714.
von Caemmerer S, Baker N 2007. The biology of transpiration. From guard cells to globe: American Society of Plant Biologists. 3-3.
Wallace D, Baudoin J, Beaver J, Coyne D, Halseth D, Masaya P, Munger H, Myers J, Silbernagel M, Yourstone K. 1993. Improving efficiency of breeding for higher crop yield. *Theoretical and Applied Genetics* **86**(1): 27-40.
Waltz E. 2022. GABA-enriched tomato is first CRISPR-edited food to enter market. *Nat. Biotechnol* **40**(1): 9-11.
Wang F, Zhu D, Huang X, Li S, Gong Y, Yao Q, Fu X, Fan L-M, Deng XW. 2009. Biochemical insights on degradation of Arabidopsis DELLA proteins gained from a cell-free assay system. *The Plant Cell* **21**(8): 2378-2390.
Wang G, Wang C, Lu G, Wang W, Mao G, Habben JE, Song C, Wang J, Chen J, Gao Y. 2020. Knockouts of a late flowering gene via CRISPR–Cas9 confer early maturity in rice at multiple field locations. *Plant molecular biology* **104**(1): 137-150.

Wang L, Kim J, Somers DE. 2013. Transcriptional corepressor TOPLESS complexes with pseudoresponse regulator proteins and histone deacetylases to regulate circadian transcription. *Proceedings of the National Academy of Sciences* **110**(2): 761-766.
Wang Y, Su C, Yu Y, He Y, Wei H, Li N, Li H, Duan J, Li B, Li J. 2022. TIME FOR COFFEE regulates phytochrome A-mediated hypocotyl growth through dawn-phased signaling. *The Plant Cell* **34**(8): 2907-2924.
Wendrich JR, Boeren S, Möller BK, Weijers D, De Rybel B. 2017. In vivo identification of plant protein complexes using IP-MS/MS. *Plant hormones: methods and protocols*: 147-158.
Wingler A. 2018. Transitioning to the next phase: the role of sugar signaling throughout the plant life cycle. *Plant Physiology* **176**(2): 1075-1084.
Woo HR, Kim JH, Nam HG, Lim PO. 2004. The delayed leaf senescence mutants of Arabidopsis, ore1, ore3, and ore9 are tolerant to oxidative stress. *Plant and Cell Physiology* **45**(7): 923-932.
Woo HR, Masclaux-Daubresse C, Lim PO 2018. Plant senescence: how plants know when and how to die: Oxford University Press UK. 715-718.
Wu K, Zhang L, Zhou C, Yu C-W, Chaikam V. 2008. HDA6 is required for jasmonate response, senescence and flowering in Arabidopsis. *Journal of Experimental Botany* **59**(2): 225-234.
Xu J, Dai H. 2016. Brassica napus Cycling Dof Factor1 (BnCDF1) is involved in flowering time and freezing tolerance. *Plant growth regulation* **80**(3): 315-322.
Xu P, Chen H, Cai W. 2020. Transcription factor CDF4 promotes leaf senescence and floral organ abscission by regulating abscisic acid and reactive oxygen species pathways in Arabidopsis. *EMBO reports* **21**(7): e48967.
Xujun W, Qingguo X, Zhijian Y. 2005. Advances of research on rice leaf senescence physiology. *Zhongguo Nong xue Tong bao= Chinese Agricultural Science Bulletin* **21**(3): 187-190,210.
Yan Z, Jia J, Yan X, Shi H, Han Y. 2017. Arabidopsis KHZ1 and KHZ2, two novel non-tandem CCCH zinc-finger and K-homolog domain proteins, have redundant roles in the regulation of flowering and senescence. *Plant molecular biology* **95**: 549-565.
Yang S, Fang G, Zhang A, Ruan B, Jiang H, Ding S, Liu C, Zhang Y, Jaha N, Hu P. 2020. Rice EARLY SENESCENCE 2, encoding an inositol polyphosphate kinase, is involved in leaf senescence. *BMC plant biology* **20**(1): 1-15.
Yang X, Wen Z, Zhang D, Li Z, Li D, Nagalakshmi U, Dinesh-Kumar SP, Zhang Y. 2021. Proximity labeling: an emerging tool for probing in planta molecular interactions. *Plant communications* **2**(2): 100137.
Yari Kamrani Y, Shomali A, Aliniaeifard S, Lastochkina O, Moosavi-Nezhad M, Hajinajaf N, Talar U. 2022. Regulatory role of circadian clocks on ABA production and signaling, stomatal responses, and water-use efficiency under water-deficit conditions. *Cells* **11**(7): 1154.
Yuan J, Murphy A, De Koeyer D, Lague M, Bizimungu B. 2016. Effectiveness of the field selection parameters on potato yield in Atlantic Canada. *Canadian Journal of Plant Science* **96**(4): 701-710.
Zaheer K, Akhtar MH. 2016. Potato production, usage, and nutrition—a review. *Critical reviews in food science and nutrition* **56**(5): 711-721.
Zandalinas SI, Rivero RM, Martínez V, Gómez-Cadenas A, Arbona V. 2016. Tolerance of citrus plants to the combination of high temperatures and drought is associated to the increase in transpiration modulated by a reduction in abscisic acid levels. *BMC plant biology* **16**: 1-16.
Zhang G, Tang R, Niu S, Si H, Yang Q, Bizimungu B, Regan S, Li X-Q. 2020. Effects of earliness on heat stress tolerance in fifty potato cultivars. *American Journal of Potato Research* **97**: 23-32.
Zhang X, Campbell R, Ducreux LJ, Morris J, Hedley PE, Mellado-Ortega E, Roberts AG, Stephens J, Bryan GJ, Torrance L. 2020. TERMINAL FLOWER-1/CENTRORADIALIS inhibits tuberisation via protein interaction with the tuberigen activation complex. *The Plant Journal* **103**(6): 2263-2278.
Zhang Y, Gao Y, Wang H-L, Kan C, Li Z, Yang X, Yin W, Xia X, Nam HG, Li Z. 2021. Verticillium dahliae secretory effector PevD1 induces leaf senescence by promoting ORE1-mediated ethylene biosynthesis. *Molecular plant* **14**(11): 1901-1917.
Zhang Y, Li Y, Yang X, Wen Z, Nagalakshmi U, Dinesh-Kumar SP. 2020. TurboID-based proximity labeling for in planta identification of protein-protein interaction networks. *JoVE (Journal of Visualized Experiments)*(159): e60728.
Zhang Y, Song G, Lal N, Nagalakshmi U, Li Y, Zheng W, Huang P, Branon T, Ting A, Walley J 2019. TurboID-based proximity labeling reveals that UBR7 is a regulator of N NLR immune receptor-mediated immunity. Nat Commun 10: 3252.
Zhang Y, Song G, Lal NK, Nagalakshmi U, Li Y, Zheng W, Huang P-j, Branon TC, Ting AY, Walley JW. 2019. TurboID-based proximity labeling reveals that UBR7 is a regulator of N NLR immune receptor-mediated immunity. *Nature communications* **10**(1): 3252.
Zhao Y, Chan Z, Gao J, Xing L, Cao M, Yu C, Hu Y, You J, Shi H, Zhu Y. 2016. ABA receptor PYL9 promotes drought resistance and leaf senescence. *Proceedings of the National Academy of Sciences* **113**(7): 1949-1954.
Zhaowei L, Qian Z, Fangmin C. 2020. Sugar starvation enhances leaf senescence and genes involved in sugar signaling pathways regulate early leaf senescence in mutant rice. *Rice Science* **27**(3): 201-214.
Zhu A, Li J, Fu W, Wang W, Tao L, Fu G, Chen T, Feng B. 2022. Abscisic Acid Improves Rice Thermo-Tolerance by Affecting Trehalose Metabolism. *International Journal of Molecular Sciences* **23**(18): 10615.
Zhu Z, Xu F, Zhang Y, Cheng YT, Wiermer M, Li X, Zhang Y. 2010. Arabidopsis resistance protein SNC1 activates immune responses through association with a transcriptional corepressor. *Proceedings of the National Academy of Sciences* **107**(31): 13960-13965.

Summary

Potato (*Solanum tuberosum* L.) is the most important non-grain crop in the world. Potato tubers are cooked in diverse ways in different cultures and it also has many industrial uses, including animal feed, biofuel production, etc. Achieving high tuber yield is a long-standing goal of potato breeding programs. At the same time, yield is known as one of the most complex traits because it is under the influence of diverse internal and external signals. In potato breeding programs, early tuberization and late senescence are considered two important characteristics for achieving high yield. In previous field studies, both above (senescence) and underground (tuberization onset) maturity together with the final yield were genetically linked to the StCDF1 locus in different populations, years and locations. **Chapter 1** introduced the current understanding of StCDF1's function in regulating tuberization onset in a photoperiod dependent manner. Other than tuberization onset and senescence, StCDF1 was speculated to be involved in regulating plants' response to abiotic stresses, such as heat and drought. We also summarized the current knowledge on StCDF1 molecular mechanism in regulating downstream target genes expression.

Although StCDF1 has been known to regulate potato plants senescence for a long time, the molecular mechanism remains elusive. In **Chapter 2**, a novel direct downstream target of StCDF1 was uncovered, namely *StORE1S02*. *StORE1S02* is a homologue of *ORESARA*, which has been identified as a positive regulator for leaf senescence in *Arabidopsis*. In our study, we found that StCDF1 directly binds to *StORE1S02*'s promoter to repress its expression. Interestingly, our observations suggest that StCDF1 negatively regulates senescence onset but promotes rapid senescence progression. The overexpressing *StORE1S02* transgenic plants exhibit early senescence onset but the total life cycle length was not affected. This phenotype supports our previous observations and provided a molecular basis for StCDF1 regulating senescence onset independently of other senescence aspects. Moreover, we found high sugar accumulation in the leaves of *StORE1S02* knock-down transgenic lines. At the same time, the expression of two sugar efflux transporters from the SWEET (Sugar Will Eventually be Exported Transporters) family, *StSWEET11* and *StSWEET15/SAG29*, were reduced in the same transgenics. Our findings suggest that StORE1S02 mediates senescence onset *via* regulating sugar transportation. Notably, StSWEET11 has been previously identified as a physical interactor of the "tubergen" StSP6A, facilitating symplastic sucrose transport and ultimately leading to tuber formation. Here, we provide molecular evidence highlighting the crucial role of the StSP6A-StSWEETs balance in tuber formation and development, with StCDF1 playing a key regulatory role in maintaining this balance. Our findings highlight the tight link connecting tuberization and senescence to the *StCDF1* locus. These findings deepen our understanding of the intricate biology underlying potato plant development and provide a foundation for further research on crop improvement and yield optimization.

In **Chapter 3**, we investigated the role of StCDF1 in regulating heat response in potato plants. The overexpression of *StCDF1*.2 resulted in enhanced heat tolerance, leading to a remarkable 16-47% increase in yield in transgenic plants compared to the non-transgenic control plants. Interestingly, we observed higher levels of transpiration specifically in the overexpressing *StCDF1.2* transgenic plants, but only under control conditions. Continuous overexpression of

StCDF1.2 or the presence of truncated *StCDF1* alleles (*StCDF1.2/1.3*) led to a significant upregulation of *StSP6A* expression, both during heat stress and under normal conditions. Despite a reduction in *StSP6A* expression following heat treatment, the expression levels remained 100 times higher than those of the late tuberizing genotype. These findings collectively suggest that StCDF1 positively regulates heat tolerance not only by mitigating heat-induced necrosis but also by maintaining strong induction of *StSP6A* expression to safeguard tuberization from heat interference. Thereby, we propose that the allelic *StCDF1* locus can be used in selecting heat tolerant genotypes in potato breeding programs.

The observed high transpiration in plants overexpressing *StCDF1.2* or carrying truncated *StCDF1* alleles aligns with our previous findings, which indicated that these plants are susceptible to drought stress. Further analysis of the previously generated DAP-seq data for StCDF1 revealed that the rate-limiting enzymes for abscisic acid (ABA) biosynthesis, specifically the *9-cis-epoxycarotenoid dioxygenases* (*StNCEDs*), are direct targets of StCDF1. To investigate this relationship further, we examined the expression patterns of *StNCED3* and *StNCED4* throughout the day in both the overexpressing *StCDF1.2* transgenics and their transformed control plants. Our results demonstrate that StCDF1 plays a vital role in regulating the expression of these key enzymes involved in abscisic acid (ABA) biosynthesis, following the circadian rhythm. Finally, the low ABA content was found in leaf tissue in overexpressing *StCDF1.2* transgenics and plants carrying truncated *StCDF1.2* alleles. Together, our results suggest StCDF1 has a negative impact on ABA biosynthesis.

In **Chapter 4**, a comprehensive protocol for conducting transient TurboID-based proximity labeling in potato leaf material is presented. This protocol offers a step-by-step guide, encompassing crucial details such as plasmid construction, preparation of plant materials, optimal growing conditions for plants, and sample processing procedures. The protocol acknowledges and thoroughly discusses the major challenges encountered during the experimental process, such as difficulties with infiltration, low protein yield, and protein degradation. Notably, the protocol was successfully tested using two proteins localized in the nucleus and plasma membrane, respectively. Furthermore, two distinct potato genotypes were employed to validate the efficacy of this protocol. The developed protocol serves as a valuable tool for diverse research purposes, particularly in the identification of Protein-Protein Interaction Networks within the potato system.

The TurboID based proximity labeling result of StCDF1 was presented and discussed in **Chapter 5**. In total, 10 interactors of StCDF1 were identified in this experiment, including the known interactors of StCDF1: StFKF1 (FLAVIN-BINDING KELCH REPEAT F-BOX PROTEIN 1) and StTPL. TOPLESS (StTPL) was speculated to be the co-repressor of StCDF1 in regulating photoperiod dependent tuberization. To further investigate the repressing function of StCDF1, we generated a construct overexpressing StCDF1.2 with a mutated TPL binding domain and transformed it into a late tuberizing potato genotype. The overexpressing *StCDF1.2*^{Coed} *ΔTPL* transgenic plants exhibited a late tuberizing phenotype which confirmed that the repressing function mediated by binding to StTPL is crucial to promote tuberization. Interestingly, we found that the overexpressing *StCDF1.2*^{Coed} *ΔTPL* transgenic plants show delayed senescence progression concurrent with over 50% yield increase. These phenotypes

were not found in transgenic plants overexpressing *StCDF1.2^{Coed} Δdof* and their transformed control plants. Moreover, we found that *StNCED3* expression was strongly upregulated in transgenics overexpressing *StCDF1.2^{Coed} ΔTPL*. This finding supports our previous analysis that StCDF1 may not only act as a repressor but also as an activator in regulating downstream gene transcription, with this activation not requiring binding to TPL. Together with novel interactors of StCDF1 identified by TurboID based proximity labeling, we propose the activation function of StCDF1 may depend on physical interaction with other transcription factors. To further verify which transcription factor(s) activate downstream target genes expression together with StCDF1, more experiments need to be conducted.

Chapter 6 summarizes and discusses the key results from previous chapters, relating them to published studies. It provides recommendations for the plant science community and commercial potato breeding programs, bridging the gap between research findings and practical applications.

Acknowledgements

My PhD journey is nearing the end. Through this period of time, I have received so much invaluable support from so many people. I would like to take this opportunity to express my gratitude to all those who have been with me throughout this journey.

First of all, I would like to thank my supervisor **Christian Bachem**. I still remember all the difficulties we had initiating this project due to funding and other issues. I can not thank you enough for trusting my ability and providing me this great opportunity. I am deeply grateful for your constant accessibility and inspiring guidance. Over the past 4.5 years, there have been many instances when our hypotheses encountered significant obstacles or reached dead ends, but with your patient guidance, I've never felt lost. Whenever I try different approaches or test random ideas, you often joke, “Li is doing typical Li’s things”. Thank you for granting me the freedom to pursue my interests while also guiding and ensuring I stay on the right path. I very much appreciate that you introduced me to your “potato networks” and promoted so many great collaborations. I remember after I told you I had submitted my thesis, you said: “Well done! it is impressive that you can finish your PhD in a relatively good time and without being mad at your supervisors”. Emm, that would be more believable if I say it myself, right? Yes, I am very lucky to have you as my supervisor. I joined your group in 2017, and during our very first meeting for my master's thesis, you sketched the StCDF1-mediated tuberization pathway with a pencil. Now, my PhD thesis has added some contributions to this very same map. You are a great researcher and supervisor, I have learned so much from you and will keep on learning from you.

Secondly, I want to thank my promoter **Richard Visser**. I sincerely appreciate all your helpful advice and rapid response to my questions and feedback to my manuscripts. I enjoyed all of our discussions, both academic and non-academic, it was always inspiring to hear different opinions on topics like how potato senescence developed or which sci-fi series was the best in 2019. I greatly appreciated your availability and support on this project.

My appreciation also goes to my collaborators from CRAG, who made remarkable contributions to my project. **Salome Prat**, I can’t thank you enough for your invaluable contribution in every discussion. Your distinctive ideas in designing molecular experiments are always so inspiring. The last time you visited Wageningen for the ADAPT meeting, it was so nice to finally meet you in person and I really enjoyed our discussion. I have learned so much from you and I truly appreciate your effort. **Maroof Ahmed Shaikh**, it is a great pleasure to work with you. Thank you so much for helping me to preform all transient assays and even cloning sometimes. You have the most detail-observant eyes, that is incredibly helpful in formatting for publication. Our research topic are very close to each other, which make us the best pals to talk about all of the newest findings. As always, good luck with everything!

I would like to extend my sincere appreciation to the exceptional staff of the company partners involved in this project: **Solynta** and **Aardevo**. Without your support and collaboration, none of this would have worked. Especially to **Michiel de Vries** and **Sybille Ursula Mittmann**, thank you so much for providing assistance and valuable suggestions in our consortium meetings and for the manuscripts.

During this project, I supervised three talented Msc students. To **Stella Provelengiou**, **Laura de Biolley** and **Wendi Zhao**, thank you for contributing to this research. **Stella**, you were my first MSc Student. In your thesis, you established the weekly phenotyping and sample harvesting system. I continued using this system through my PhD study. **Laura**, thank you for sampling a 24h time course twice with me! Your work is excellent and now this story has gone to publication. **Wendi**, I was so happy to have you in this project. You are hard working, attentive and patient. Phenotyping and sampling plants under heat was not easy, but you did an excellent job! It's been a pleasure working with each of you, and I believe you all have a bright future ahead. Thank you for your excellent contributions.

Also, I would like to express my gratitude to the PBR secretaries **Danielle van der Wee** and **Nicole Trefflich**, and EPS coordinators **Susan Urbanus** and **Juliane Teapal**. Thank you for your availability and handling of all administrative matters.

My gratitude further goes to both current and previous members of the Potato development group: **Marian Oortwijn**, **Sara Bergonzi**, **Lorena Ramirez Gonzales**, **Jose A Abelenda**, **Ernst-Jan Eggers**, **Csaba Papdi**, **Miru Du**, **Hongbo Li**, **Xulan Wang** and **Beiyu Tu**. I enjoyed all of the discussions at the Cookie meetings. The time we all went to the field together to harvest is very memorable! Our scientific discussions, coffee breaks, lunch breaks and shared activities have been some of the most enjoyable moments of my PhD journey. I appreciate all the help and support I have received. **Marian**, thank you for always being willing to provide help in and outside of the lab. You are always very warm hearted and kind. You are like a big sister to me. I really enjoyed our dinners together. **Sara**, it is my pleasure to work with you with the same population in the past 4 years. Many thanks for bringing tasty cake to cookie meetings and to the field. **Lorena**, you are my MSc thesis supervisor, I learned so much from you. Thanks for your patience and willingness to have discussions every time. **Abe**, thank you for suggesting me to try proximity labeling! It worked in the end and became two chapters in my thesis! **Ernst**, I enjoyed our conversations in the office and appreciated your help in all genetic analysis. **Csaba**, thank you for all the nice molecular tricks and nice discussions. **Miru**, thank you for all the support through my Master to Phd study period. **Hongbo**, thanks for helping me with the bioinformatic analysis. **Xulan**, thanks for all the nice talk/gossiping at the lunch breaks, water breaks and weekends. I appreciate that whenever I have questions related to field experiment or genetic analysis, you were always willing to help. Thank you for hosting all the party/game/food nights at your home, these are wonderful memories through this journey. **Beiyu**, thanks for the precious time we shared at the lunch breaks. Thanks for your trust in me for all the molecular tricks. I hope these tricks can make your lab life easier in the coming few years.

Thanks to all my fellow PhDs in PBR: **Tatiana Marti Ferrando (Tati)**, **Zihan Liu**, **Chengcheng Cai (CC)**, **Dong Zhang**, **Corentin Clot**, **Daniel Monino Lopez**, **Eleni Koseoglou**, **Jorge Aleman Baez**, **Celia Anton Sales**, **Antonino Crucitti**, **Marcella Bovio**, **Alejandro Therese Navarro**, **Pichaya Cheewapoonphon (Jaae)**, **Marietheres Kleuter (Mites)**, **Romanos Zois**, **William de Martines**, **Miguel Ramirez Gaona**, **Lampros Siskos**, **Sri Sunarti**, **Aviv Andriani**, **Yerisf Torres Ascurra**, **Xiaoxue Sun**, **Huayi Li**, **Xiao Lin**, **Wei Sun**, **Tianpeng Wang**, **Jingjing Mao**, **Xuexue Shen**, **Yi Wu**, **Ying Liu**, **Yingjie Li** and **Mengjing Sun**. With you all,

there are so many nice memories from in the lab and around the lunch table. I truly appreciate your company throughout this long journey. **Tati**, we started working together after we realized that both of us wanted to apply proximity labeling in potato. You are so organized and record every detail in every experiment. Thank you very much for rolling me around in the greenhouse when I had back pain, working together in the cold room and staying late in the lab. I wish you a fantastic future filled with wonderful experiences and exciting parties. **Zihan**, we met during master studying and became good friend till now. Thank you for all of the wonderful memories we shared together. I hope to see you graduate soon as well. **CC**, thank you for answering all my questions related to everything! You are like a CCpedia for formatting, generating figures, publication, etc. Your tips are always so helpful. I wish everything goes well with you in Beijing. **Corentin**, thank you for all the nice potato discussion. You and Xulan are like an external knowledge base for potato genetics to me. I appreciated your patience for explaining all genetic approaches and perspectives. **Jaae**, thanks for taking care of Bobo and Mumu with Beiyu. I hope all your future experiments go well.

To my **colleagues** at PBR, though I won't individually list everyone, I want to convey my heartfelt gratitude to each and every one of you. I enjoyed being a member of the Plant breeding group during my PhD project. Thank you for making me feel welcome and supported in this department. A special thanks goes to **Gerard van der Linden** for providing insight into plant abiotic stress response and sharing the magical recovery experience. **Guusje Bonnema**, thank you for promoting and organizing several nice team activities, which were such enjoyable experiences.

Thanks to other friends whom I met here in the Netherlands. **Si Qin (Sisi)**, **Ziyang Xiao**, **Yiyuan Ding (Dading)**, thank you for the wonderful memories we shared together, cooking, hanging out, playing video games and card games and more. **Sisi**, we met each other right after we just arrived in the Netherlands. Later, we found out we had already met in an old event in Beijing. Thank you for introducing me to protein experts in your group and being a great friend through this journey. **Ziyang**, you are always so creative and fun! I am so happy that you found the topic you like to work with. The talks with you were always accompanied with great laughs. **Dading**, thank you for recommending the wine and food tricks. I wish you have great success in your work. **Wen Huang**, **Yaohua You**, **Ying Su**, thank you for all the nice informative conversations. It was really nice to be able to consult with you and thank you all for sharing your experiences.

Ying Lin, **Xiaozhen Zhao**, **Mengting Shao**, **Shiqin Yan**, and **Jiaxin Wang**, I'm thankful for the connections we've maintained during this journey despite the physical distance between us. Our conversations and calls have been a great source of comfort. I will continue to cherish our friendship in the future, and I wish you all tremendous success in your respective endeavors, whether it be work or research.

I extend my gratitude to the **China Scholarship Council** for awarding me a grant to pursue my studies in Wageningen. Additionally, I appreciate the guidance and extensive knowledge shared by my bachelor supervisor, **Prof. Congfeng Song**, in the field of molecular biology, which has laid a robust foundation for my future PhD research.

感谢我最亲爱的父母，施明全，张瑶。从大学开始我就一直在外，回家陪伴你们的时间太少，感谢你们的支持与理解。感谢你们的言传身教，你们的求学经历激励着我去解决在博士课题中遇到的种种难题。感谢干亲家人，杨贤伟，袁丁和杨苏立。感谢你们对我们一家的照顾。希望你们身体健康，开心快乐，去做自己想做的事。感谢所有关心与支持的亲人朋友们。

Alexander, thank you for being a part of my life in the past 6 years. I am grateful for every minute we've spent together. I appreciate your tolerance when I get caught up in my 'crazy fast jumping' thoughts about potatoes, sometimes even during our holidays. I am looking forward to continuing our journey together with Bobo and Mumu.

About the author

Li Shi was born on Nov 29th 1994 in Beijing, China. She pursued her bachelor's degree in Plant Protection at Nanjing Agriculture University in Nanjing from 2012 to 2016. After graduation, she moved to Netherlands and started her MSc study in Plant Breeding in Wageningen University (WU). During her master's study, she conducted her major and minor thesis under the supervision of Dr. Christian Bachem at the Laboratory of Plant Breeding in WUR. In 2019, she received a fellowship from the China scholarship Council (CSC) to continue her research in potato development as a PhD student. This thesis presents the outcome of her PhD research entitled "Tubers and Time: Exploring the Intricate Link between Tuberization and Senescence", which was supervised by Prof. Dr. Richard G.F. Visser (promoter) and Dr. Christian Bachem (co-promoter, daily supervisor).

Education Statement of the Graduate School

Experimental Plant Sciences

Issued to: **Li Shi**
Date: **29 November 2023**
Group: **Plant Breeding**
University: **Wageningen University & Research**

1) Start-Up Phase	*date*	*cp*
► **First presentation of your project**		
No time to die: Uncoupling tuberization and senescence in potato	4 Oct 2021	1.5
► **Writing or rewriting a project proposal**		
Breeding for earliness and maturity in potato: Beama	Apr 2020	6.0
► **MSc courses**		
Subtotal Start-Up Phase		7.5

2) Scientific Exposure	*date*	*cp*
► **EPS PhD days**		
EPS PhD Days 'Get2Gether', Soest, NL	10-11 Feb 2020	0.6
EPS PhD Days 'Get2Gether', Online	1-2 Feb 2021	0.4
► **EPS theme symposia**		
EPS Theme 1 Symposium – Developmental Biology of Plants, Wageningen, NL	5 Feb 2020	0.3
EPS Theme 3 Symposium – Metabolism and Adaptation, Online	30 Oct 2020	0.2
EPS Theme 4 Symposium – Genome Biology, Online	11 Dec 2020	0.2
EPS Theme 1 Symposium – Developmental Biology of Plants, Wageningen, NL	14 Jun 2022	0.3
► **National platform meetings**		
Annual meeting 'Experimental Plant Sciences', Lunteren, NL	8-9 Apr 2019	0.6
Annual meeting 'Experimental Plant Sciences', Online	12-13 Apr 2021	0.5
Annual meeting 'Experimental Plant Sciences', Lunteren, NL	11-12 Apr 2022	0.6
► **Seminars (series), workshops and symposia**		
SLU & WUR Symposium: Plant Breeding and Biotechnology, Wageningen, NL	11-13 Jun 2019	0.9
6th Wageningen PhD symposium “Science with Impact”, Wageningen, NL	25 Oct 2019	0.3
Plantae Seminar: Sophia Stone and Sjon Hartman, Online	14 Apr 2021	0.2
Seed Valley Talks: How to beat the next plant virus pandemic, Online	20 May 2021	0.2
YoungWUR Workshop: Mind the gap before Your next research career step! How can Research Analytics help?	1 Jun 2021	0.1
4th EPSO Plant Science Seminar, Online	17 Jun 2021	0.2
5th EPSO Plant Science Seminar, Online	16 Sep 2021	0.2
EMBL-EBI Seminar: Applications and impacts of the BrAPI project on plant breeding, Online	26 Apr 2023	0.1
► **Seminar plus**		
► **International symposia and congresses**		
Conference "Potato futures: impact of hybrid varieties", Online	30 Oct 2020	0.3
SoI International Online Meeting 2020, Online	9-11 Nov 2020	0.6
21st EUCARPIA General Congress, Online	23-26 Aug 2021	0.8
ADAPT annual meeting 2022, Wageningen, NL	23-24 Jun 2022	0.6
SOLANACEAE2022 International Conference, Thessaloniki, GR	1-5 Nov 2022	1.3
► **Presentations**		
Talk: company consortium meeting	25 Apr 2019	1.0
Poster: 'No time to die: Uncoupling tuberization and senescence in potato'	13-15 dec 2021	1.0
Poster: 'Aging later but faster, how StCDF1 regulates senescence in *Solanum tuberosum*'	1-5 Nov 2022	1.0
► **Interviews**		
► **Excursions**		
EPS company visit to Averis Seeds, Valthermond, NL	7 Jun 2019	0.2
EPS company visit to Rijk Zwaan, Online	16 Jun 2021	0.2
Subtotal Scientific Exposure		12.9

3) In-Depth Studies	*date*	*cp*
► **Advanced scientific courses & workshops**		
EPS course: Gentle hands-on introduction to Python programming, Online	Mar-Apr 2021	0.9
eScience Center workshop: Data Carpentry with R, Online	18 Oct 2021	0.2
PE&RC course: Tidy data transformation and visualization with R, online	8-18 Jun 2021	1.2
EPS course: Transcription factors and transcriptional regulation, Wageningen, NL	13-15 dec 2021	1.0
► **Journal club**		
► **Individual research training**		
Protein work training in Laboratory of Phytopathology (WUR)	28-29 Apr 2021	0.6

Protein work training in Laboratory of Phytopathology (WUR)	8-9 Dec 2021	0.6
Subtotal In-Depth Studies		4.5

4) Personal Development	*date*	*cp*
► **General skill training courses**		
WGS workshop: Critical thinking and argumentation, Wageningen, NL	19 Sep 2019	0.3
EPS introduction course, Wageningen, NL	29 Oct 2019	0.3
Wageningen in'to Languages course: Basic Dutch 1, Wageningen, NL	2 Mar - 30 Jun 2020	1.5
EPS workshop: Becoming a mindful scientist, Online	10 Sep 2021	0.1
WGS course: Supervising BSc & MSc thesis students, Wageningen, NL	7-8 Oct 2021	0.6
WGS course: Adobe InDesign - from Dissertation Layout to Poster Design, Online	2-10 Nov 2021	0.6
WGS PhD Workshop Carousel, Wageningen, NL	12 May 2023	0.3
► **Organisation of scientific meetings, PhD courses or outreach activities**		
► **Membership of EPS PhD Council**		
Subtotal Personal Development		3.7

5) Teaching & Supervision Duties	*date*	*cp*
► **Courses**		
► **Supervision of BSc/MSc projects**		
Supersivion MSc major thesis "Solyntus - Familiarization with a new genotype"	Sep 2019 - Feb 2020	1.0
Supervision MSc major thesis "Functional analysis of *ORESARA1* and regulatory network study in *Solanum tuberosum*" its life cycle?	Sep 2021 - Mar 2022	1.0
Supersivion MSc major thesis "*StCDF1*'s function and effect under heat stress in *S. tuberosum*"	Jul 2022 - Jan 2023	1.0
Subtotal Teaching & Supervision Duties		3.0

TOTAL NUMBER OF CREDIT POINTS*	**31.6**

Herewith the Graduate School declares that the PhD candidate has complied with the educational requirements set by the Educational Committee of EPS with a minimum total of 30 ECTS credits.

** A credit represents a normative study load of 28 hours of study.*

The research described in this thesis was co-funded by Solynta and Aardevo.

Li Shi was sponsored by the China Scholarship Council under grant number 201807720077.

Financial support from Wageningen University for printing this thesis is gratefully acknowledged.

Cover design: Suli Yang

Layout design: Li Shi & Alexander van der Hall

Printing: RIDDERPRINT